Inflatable Antennas for Portable Direct Satellite Communication

Naomi Mathers

Bachelor of Engineering

School of Electrical and Computer Engineering

Science, Engineering and Technology Portfolio

RMIT University

Melbourne, Australia

February 2010

Declaration

I certify that except where due acknowledgement has been made, the work is that of the author alone; the work has not been submitted previously, in whole or in part, to qualify for any other academic award; the content of the thesis is the result of work which has been carried out since the official commencement date of the approved research program; any editorial work, paid or unpaid, carried out by a third party is acknowledged; and, ethics procedures and guidelines have been followed.

Naomi Mathers
8 February 2010

Acknowledgements

I would like to acknowledge the support of my family and friends. Without their encouragement and patience would not have been possible for me to undertake this project. I would like to thank Prof. Andrew Jennings from RMIT University supervising this project in its closing stages; his advice and experience were invaluable. I would like to thank Assoc. Prof. Lachlan Thompson and Dr. Kamran Ghorbani from RMIT University for their supervision during the early stages of this project. I would also like to acknowledge Dr. Ghorbani for the design of the microstrip patch that was used to feed the gossamer horn presented in this thesis. I would like to thank Mr. David Welch from RMIT University for manufacturing the microstrip patch and the rigid horns used in the testing. I would like to thank Mr Terry Rosewarne from RMIT University for manufacturing the composite parabolic reflector used as the comparison for the inflatable antenna. I would like to thank Dr. Christophe Granet from CSIRO's Electromagnetics and Antennas Group, for completing the CST Microwave Studio simulations presented in this thesis. Finally, I would like to thank Mr. John Wright from Visypak Australia for donating the material used to manufacture the antenna presented.

Contents

List of figures

List of Tables

Glossary of symbols

C	circumference of feed horn
d	primary reflector diameter
d_s	sub-reflector diameter
D	ideal antenna directivity
D_c	feed directivity
D_0	antenna directivity
E	modulus of elasticity
f	focal length of main reflector
f_c	applied compression stress
f_s	applied shear stress
F	frequency
$F_{C_{CR}}$	critical buckling stress for curved panel under compression stress only
$F_{S_{CR}}$	critical buckling stress for curved panel under shear stress only
G	gain
I	current
l	length of feed horn
N_x, N_y	Normal forces per unit length perpendicular to x and y directions
N_φ, N_θ	Membrane forces per unit length in the two meridian planes
p_{CRIT}	critical external pressure that would buckle a pressure vessel
P	single load
q	internal pressure
r	radius
R	resultant load
R	radius of feed horn
R_C	compression force
R_P	force due to internal pressure
R_S	shear buckling stress
s	quadratic phase factor
t	thickness
T	period
v	wave velocity of propagation

ε	efficiency
λ	wavelength
θ_0	antenna included angle
θ	horn flare angle
σ	conductivity
$\sigma_x, \sigma_y, \sigma_z$	normal components of stress parallel to x, y and z axes
μ	permeability
δ	skin depth

Abstract

Satellite-based communication system can provide access to voice, data, video and internet transmission that is independent of terrestrial infrastructure. This is particularly important in disaster response situations and military maneuvers where mobile personnel need to maintain direct contact with each other and the central control. One of the factors that currently limits the effectiveness and practicality of these systems is portability. These systems require lightweight equipment that can be quickly and easily deployed and operated in a variety of environments. Parabolic dish antennas are the only antennas capable of providing the high gain required for direct satellite communication but their size and weight severely limit their portability and hence their use for portable direct satellite communication. Inflatable structures have been used in the space environment to overcome the limitations of launch vehicle size and weight restrictions. They are constructed from thin film, or gossamer materials, and use internal pressure to maintain their shape. Inflatable structures are lightweight, have a low stowed volume and a high packing efficiency. It is proposed that this type of structure can be used to produce an inflatable parabolic dish antenna that can operate under terrestrial conditions to overcome the limits on portability for land-based communication. This thesis presents a design for a parabolic dish antenna and conical feed horn constructed entirely from polyester thin film. To further reduce the weight and stowed volume of the antenna the conical horn is fed by a microstrip patch. The performance of the components and their ability to operate under terrestrial conditions are assessed by comparing the results to those of an identical rigid system.

Introduction

Satellite-based communication systems provide access to voice, data, video and internet transmission that is independent of terrestrial infrastructure. The satellite communication network can be accessed either via a fixed ground station or directly from a portable terminal. Access to satellite-based communication which is independent of a ground station is particularly important in disaster response situations and military manoeuvres where mobile personnel need to maintain direct contact with each other and the central control [1, 2].

Satellite-based personal communications systems (SPCS) are an effective way to connect mobile personnel with a central support network in both military and disaster management situations [3]. SPCS use the network of orbiting satellites to make broadband communication possible when there is no infrastructure on the ground or the infrastructure has been damaged. One of the factors that currently limits the effectiveness and practicality of these systems is portability [1, 2]. To increase portability these systems require lightweight equipment that can be quickly and easily deployed and operated in a variety of environments. Parabolic dish antennas are the only antennas capable of providing the high gain required for direct satellite communication but their size and weight severely limit their portability and the effectiveness of the SPCS.

To increase the portability of SPCS, without sacrificing performance, it is desirable to replace the reflector and feed system with a lightweight, stowable alternative that matches the performance of a rigid antenna. Rigid deployable structures such as umbrella and petal reflectors have been used to reduce stowed volume but they offer only limited reduction in weight and have limited shape accuracy [4, 5].

Inflatable structures have been used in the space environment to overcome the limitations the launch vehicle places on the achievable size of the structure and its weight [6]. The launch of the Inflatable Antenna Experiment (IAE) demonstrated that an inflatable structure was capable of achieving the shape accuracy and dimensional stability required to perform as an antenna in the space environment [7]. It is proposed that inflatable structures technology can be used to produce an inflatable parabolic dish antenna that will

operate reliably under terrestrial conditions to overcome the limits on portability for land-based direct satellite communication.

This thesis presents the design of an inflatable antenna with gossamer feed horn fed by a microstrip patch. It will be shown how a combination of structural design, material selection and internal pressure can be used to produce a parabolic reflector and conical feed horn from thin film materials which can match the performance of a rigid antenna under the influence of gravity. It will then be shown how this approach can be used to produce a reusable antenna capable of direct satellite communication which is truly human portable. This will be achieved by:

1. Measuring the return loss and radiation pattern of a feed horn manufactured from thin film and fed by a microstrip patch which resonates at 12.5 GHz, and comparing it to the return loss and radiation pattern of a rigid Aluminium feed horn of the same design fed by the same microstrip patch.
2. Measuring the radiation pattern of a parabolic dish antenna fed by the above gossamer horn and comparing it to the radiation pattern of a rigid parabolic dish antenna of the same design fed by the same gossamer horn.
3. Measuring the weight and stowed volume of the gossamer and rigid antennas and comparing their portability.
4. Comparing the portability and performance of the inflatable antenna with existing alternatives.

This work was conducted between March 2002 and December 2005 and was first published in February 2003.

1. Background

1.1 Satellite-based Personal Communications Systems (SPCS)

Satellite-based Personal Communications Systems (SPCS) allow the user to directly access the global communications network. This network uses wireless based technologies, both terrestrial and satellite-based, to offer a seamless infrastructure that provides global personal connectivity and access to broadband wireless multimedia, communications and services, by anyone, from anywhere, at any time [3].

The use of SPCS is fundamentally changing the way disaster response and military conflicts are managed. The ability to transmit detailed information quickly and reliably to and from all parts of the globe helps streamline command and control, enabling faster deployment of highly mobile personnel capable of adapting quickly to changing conditions [1, 8]. The ability to integrate interactive data access with simultaneous video broadcasts opens new opportunities for information dissemination to roaming clients whose needs evolve with time.

The successful implementation of this system is equipment dependent. It requires the development of lightweight, man-portable ground station technologies.

1.2 Existing land-based direct satellite communication technology

All satellite communication systems are composed of a space segment and a ground segment. The Ground Station is responsible for transmitting, or uplinking, data to the satellite and receiving, or downloading, data from the satellite. Ground stations can also transmit data between themselves if they are within line-of-sight.

To fulfil this role ground stations are equipped with a user interface, a power system, a tracking system, a baseband processor, an up converter, an amplifier, and a parabolic dish antenna. Parabolic dish antennas are required for direct satellite communication as smaller, lighter antennas, such as dipoles and Yagi antennas do not generate the gain required for

direct satellite communication. The gain of the antenna is directly related to the aperture of the parabolic reflector.

Over time there has been a concerted research effort into miniaturizing the components of ground station terminals and reducing power consumption in order to increase portability [9]. Despite all these advances the portability of the system remains limited by the parabolic reflector. Reducing the size of the parabolic reflector in an attempt to increase the portability of the system, results in a reduction in the gain of the antenna and a reduction in performance. The challenge is to design a parabolic dish antenna which is lightweight and portable but which has the performance of a large reflector.

1.2.1 Portable rigid parabolic dish antennas

While fixed ground stations can handle large amounts of data which can then be relayed to individual users, mobile ground stations offer the ability to access the satellite network directly from multiple locations. Current mobile systems can be divided into two main categories: larger antennas that require a vehicle to transport them and smaller antennas that are intended for individual use but which are severely limited in performance due to their small size.

These two systems offer Communications-on-the-Halt (COTH) and Communications-on-the-Pause (COTP) [2, 10]. COTH is established where the user is stationed at a fixed location for a long period of time and can deploy a semi-permanent communications system. *Fig. 1* shows a typical military COTH ground station. COTP is deployed rapidly to establish connectivity and then rapidly dismantled in order for the user to continue on their way. *Fig. 2* shows a typical COTP ground station. The ability to implement COTP or COTH is equipment dependent, driving the development of lightweight, portable ground station technologies.

Communication kits have been developed that are typically housed in a weatherproof and ruggedized briefcase style carrier, and powered either by internal batteries or an external power source, these devices combine cryptography, and routing into a single human portable product [11]. With all the baseband equipment conveniently stored in a single suitcase, all that is needed is an antenna to connect to the appropriate network.

Fig. 1: Typical military Communications-on-the-Halt (COTH) ground station (image courtesy of US DoD)

Fig. 2: Typical military Communications-on-the-Pause (COTP) ground station (image courtesy of US DoD)

A parabolic dish antenna is the only antenna that produces the gain required for direct satellite communication. The gain of the antenna, and hence its performance, is directly related to the effective aperture of the reflector. As such the parabolic reflector is responsible for the greatest percentage of the size of the system and contributes significantly to its weight. If a parabolic dish reflector is to be used for portable satellite based personal communication the reflector and feed system will need to be replaced with a lightweight, stowable alternative without sacrificing performance. The provision of a small, lightweight, high gain antenna therefore presents the greatest design challenge and has the biggest impact on the portability of the unit.

1.2.2 Articulated parabolic dish antennas

To increase the portability of direct satellite communication systems without sacrificing performance a wide variety of deployable antennas have been developed, including mesh deployable, petal deployable and hybrid antennas [4, 5, 12]. A common feature of these antennas is that they can be stowed and then deployed when needed, thus reducing the size of the antenna during transit. As these systems are rigid they offer little if any reduction in weight.

The two most common deployable antennas are articulated mesh, or "umbrella" parabolic dish reflectors and petal deployable parabolic reflectors. Examples of these antennas are shown in *Fig. 3* and *Fig. 4*. Both forms of deployable antennas help to reduce the stowed volume of the parabolic dish antenna but neither solution offers a significant reduction in

weight. As weight also limits portability it is not sufficient to reduce the stowed volume alone, both factors must be reduced whilst maintaining performance.

Fig. 3: Typical articulated mesh, or umbrella, parabolic dish antenna (image courtesy of US DoD)

Fig. 4: Typical petal deployable parabolic dish antennas (image courtesy Thales and US of DoD)

The diameter of a parabolic dish antenna is the main factor that influences the gain of the antenna, hence the urge to increase the achievable size of portable systems, however the shape and surface accuracy must be maintained or the reflective characteristics of the antenna will be degraded to such a point as to render the antenna useless. When operating in the field equipment durability and reliability must also be demonstrated.

Articulated mesh, or umbrella, parabolic reflectors are mechanical systems whereby articulated ribs support a flexible mesh surface. The use of a mesh offers some weight reduction but the mechanical complexity of articulated system, combined with problems associated with shape accuracy, reduces their appeal. The shape accuracy of an articulated antenna is permanently limited by an effect known as pillowing [13]. Pillowing is caused by the localized stiffness of the ribs combined with the weight of the mesh. The pillowing effect means that the mesh surface will never achieve a true parabolic shape. The shape accuracy of an articulated antenna can be compromised even further if one of the ribs is bent or it fails to deploy as designed. The large number of joints in articulated antennas makes this type of design vulnerable to deployment defects. In remote or military scenarios this lack of resilience is unacceptable, especially when it is not possible to carry replacement reflectors.

Deployable petal antennas do not suffer from pillowing but their overall shape accuracy is dependent on the shape accuracy of the individual pieces being maintained and the accuracy of the assembly. In general this type of antenna is quite resilient but once one of the petals or any of the hinges is deformed the shape accuracy is permanently compromised.

When looking for ways to increase the size of a parabolic dish reflector whilst reducing stowed volume and weight inspiration can be drawn from the space environment where the limitations of launch vehicle size and lifting capacity have produced concepts for inflatable antennas. These inflatable antennas create the possibility of large diameter, high gain parabolic dish antennas for a fraction of the weight and volume, and hence cost, of their rigid counterparts. In the same way that inflatable space-based antennas overcome the limitations of launch, inflatable antennas could be used to overcome the limits on portability for land-based communication. To make this transition an inflatable antenna must be created that can match the performance of a rigid or articulated antenna under terrestrial conditions.

1.3 Existing Space-based Technology

Although there is fundamentally no difference between the antennas on satellites and those on the ground, the unique operating environments and the ability to establish the necessary infrastructure place limitations on both systems. The capacity of the launch vehicle places restrictions on the size, weight, and power of the satellite and subsequently each additional kilogram, cubic metre or Watt adds to the cost. This poses a complex problem as the performance of a parabolic reflector antenna is directly related to its size and power.

1.3.1 Rigid Space-based parabolic dish antennas

It has already been discussed that to maximize the gain of a parabolic dish antenna the aperture of the antenna should be maximized. As there is currently no capacity for orbital assembly the size of any space structure is either limited by the launch vehicle or it must be deployed post launch. Currently launch vehicles limit the diameter of rigid parabolic dish antennas to between 2 and 4 metres.

Deploying a structure post launch increases the achievable dimensions but it also introduces additional complexity to the system and increased risk. In the conservative context of space engineering and operation any risk must be justified by a significant improvement in performance [14]. The requirements for space systems are stringent; they must be capable of operating in extreme conditions whilst still maintaining the highest standards of reliability as they cannot be retrieved for maintenance or repair.

Maximizing the gain of an antenna is desirable to increase the capacity of the system but unless the shape and surface accuracy are maintained the performance will be degraded. The use of rigid parabolic dishes, whose behaviour in the space environment is understood, guarantees the required shape and surface accuracy will be maintained. The decision must then be made if a new technology offers a significant improvement in performance to justify the additional risk.

1.3.2 Articulated Space-based parabolic dish antennas

As in the terrestrial environment, deployable structures have been investigated to overcome the limitations of the launch vehicle [14]. In 1989 the Galileo probe was launched to study Jupiter's atmosphere, satellites and magnetosphere. Galileo used a deployable articulated antenna [15] as shown in *Fig. 5* to overcome the limitations of the launch vehicle and increase the size of the high gain antenna. The Galileo high gain antenna was a 4.8 metre diameter gold-plated metal mesh paraboloid stretched over 18 jointed ribs that were designed to unfold like an umbrella. When deployed the antenna would supply a bandwidth of 134,000 bits per second.

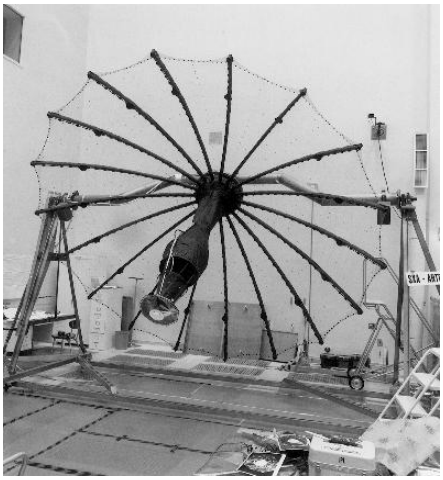

Fig. 5: Galileo High Gain Antenna (image courtesy of NASA)

Launching the antenna in a folded position served two purposes. The first and most important was that a larger diameter dish was possible and the second was that the antenna could be protected from thermal damage behind a sun shield until the craft was a safe distance from the sun [15]. *Fig. 6* shows the Galileo high gain antenna in the stowed position and *Fig. 7* shows the high gain antenna in the fully deployed position.

Fig. 6: Galileo High Gain Antenna in the stowed position (image courtesy of NASA)

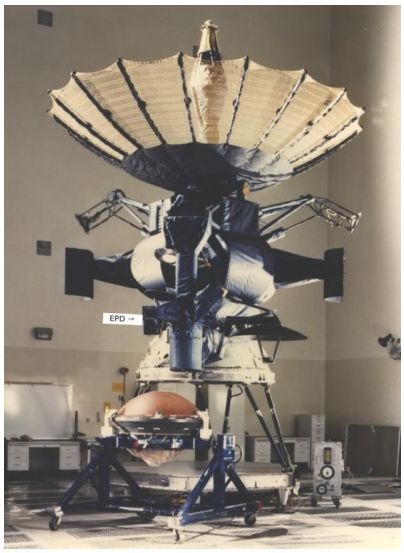

Fig. 7: Galileo High Gain Antenna in the fully deployed position (image courtesy of NASA)

In 1991 when engineers attempted to deploy the antenna they realized it was stuck. The problem was attributed to the sticking of a few antenna ribs due to friction between their standoff pins and their sockets [15]. The loss of the high gain antenna made the low gain antenna the prime source of communication and reduced the data rate to 160 bits per

second. This demonstrates the significant improvement in performance achievable with a larger diameter dish and the crippling impact of a failure to deploy as designed.

The operation of any mechanical system in the space environment has risks associated with it, the greater the number of joints and stages in the sequence, the higher the risk associated with it. Current concepts for mechanically deployable space structures tend to be complicated, requiring vast number of spring-loaded joints or motorized hinges, thereby increasing the possibility of a malfunction during deployment [16, 17]. Although these systems offer advantages in the achievable size of the structure they offer limited or no weigh saving and require additional power during deployment. The Galileo example also illustrated that should the deployment be off design the performance of the system is permanently diminished. The solution is not to abandon the concept of deployable structures but to look for reliable solutions that deliver maximum performance for minimum risk.

1.4 Inflatable Structures in the Space Environment

Until there is a viable facility to assemble structures in space, the size, weight and available power of space-based structures will be limited by the launch vehicle. There are many proposed space structure whose final dimensions are required to be much greater than that of the available launch vehicles, such as solar sails and shades, or whose performance would be improved by increased size such as antennas and remote sensing radar [6, 18].

The ability to deploy a structure after launch removes the limitations of the launch vehicle and increases the achievable size. Articulated structures have been used, however their mechanical complexity reduces their deployment reliability, and they offer little weight reduction [14]. Inflatable structures are an attractive option as they can achieve a weight saving of at least 50% and a reduction in stowed volume of up to 75% in addition to the significant increase in achievable size [6, 18].

1.4.1 Non-Precision Inflatable Structures in the Space Environment

The space environment presents many unique operating challenges including temperature extremes and solar radiation, but the absence of a gravitational field eliminates the need for high load bearing structures. The use of rigid truss structures in this environment concentrates the applied loads at the joints requiring them to be reinforced, which in turn increases the weight of the structure and the applied loads. The use of inflatable structures has a distinct advantage over rigid structures as the loads are evenly distributed over the entire surface. In inflatable structures the skin acts as a structural member eliminating the need for reinforced joints, and reducing the overall mass. As the skin is the main load bearing member, structural design, material selection and internal pressure are the key design factors.

The use of inflatable structures increases the achievable dimensions of the space structure whilst reducing the launch weight and their high packing efficiency reduces the stowed volume. Many applications already make use of the high packaging efficiency of inflatable structures and the strength and durability of thin films, such as solar sails, inflatable trusses and the impact attenuation system originally used for the Pathfinder mission and then again for the Mars Exploration Rover missions [19]. For example, the inflatable TransHab concept developed by NASA as a habitation module for the International Space Station (ISS) is designed to be launched inside the shuttle's cargo bay with a diameter of 4.3 metres, but once inflated is expanded to 8.2 metres, giving the crew of the ISS a 340 cubic metre facility [20].

All the examples provided benefit from the reduced weight, high packing efficiency and increased dimensions offered by inflatable structures but all are considered non-precision structures as they don't rely on shape accuracy to maintain performance.

1.4.2 Inflatable Antennas in the Space Environment

The designer of high gain antennas for space-based operations is limited by the capacity of the launch vehicle. As the gain of parabolic dish antennas is directly related to the aperture of the dish, maximum dish diameter and minimum weight are key drivers of the technology. The use of an articulated antenna increases the achievable aperture but the

weight saving is negligible and their mechanical complexity reduces their deployment reliability [15].

The use of inflatable structures increases the achievable dimensions of the space structure whilst reducing the launch weight and their high packing efficiency reduces the stowed volume. From *Fig. 8* and *Fig. 9* it can be seen that inflatable antennas perform better than either mesh deployable or precision deployable structures in the areas of weight and stowed volume. However, if inflatable structures are to be used for communications applications a number of additional structural and electromagnetic requirements must be met.

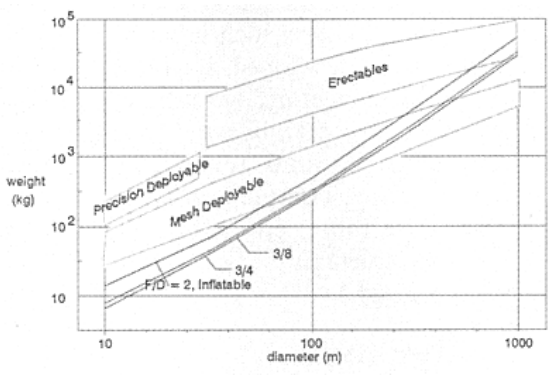

Fig. 8: Weight comparison of a range of deployable antennas (source JPL)

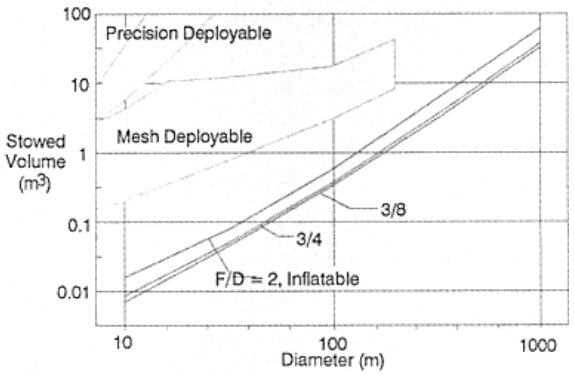

Fig. 9: Stowed volume comparison of a range of deployable antennas (source JPL)

Inflatable antennas are not a new concept in the space industry. The first successful space-based communications antenna was an inflatable structure. Echo 1A [6, 18], shown in *Fig. 10*, was launched in 1960. It was a 30.5 m diameter inflated sphere constructed from 0.0127 mm thick metalized polyester thin film. Echo designers utilised the fact that a uniform thickness spherical shell with uniform internal pressure behaves as a perfect membrane and resists its pressure load with a uniform membrane stress acting all over its surface. This allowed Echo designers to produce a structure that greatly exceeded the size of the launch vehicle whilst dramatically reducing the launch weight.

Fig. 10: Echo 1A (image courtesy of NASA)

Echo was a passive satellite which permitted signals to be “bounced” off its metalized surface and was successfully used to redirect transcontinental and intercontinental telephone, radio, and television signals. In addition to demonstrating the potential of satellite communications, Echo examined the dynamics of large inflatable structures in the space environment. Data was collected for the calculation of atmospheric density and solar pressure, indicating that Echo encountered significant orbital changes due to solar pressure, thereby highlighting an important consideration for future large inflatable structures. Instrumentation was also included to monitor the balloons skin temperature and internal pressure [6, 18].

The structure proved to be space worthy and surprisingly durable, laying the foundation for future inflatable space structures. Although NASA abandoned passive communications systems in favour of active satellites the success of Echo proved the validity of communications satellites and inflatable structures for use in space.

Despite the success of the Echo project it still fell into the category of a non-precision structure. The next major breakthrough in large inflatable antennas was the L’Garde Inflatable Antenna Experiment (IAE), shown in *Fig. 11*, launched in May 1996 as part of the NASA office of Space Access and Technology, In-Space Technology Experiments Program (IN-STEP) [21, 22, 7, 23, 24]. The objective of the experiment was to verify low cost and light weight precision structures by building a flight-quality reflector antenna, demonstrate deployment reliability in a realistic environment, and measure the reflector surface precision in a realistic gravity and thermal environment.

Fig. 11: L'Garde Inflatable Antenna Experiment (IAE) in orbit (image courtesy of L'Garde)

The IAE maintained the classical configuration of a conventional land-based antenna with a 14 metre diameter parabolic dish reflector and three struts supporting a feed system, or in this case photogrammetry equipment to measure the shape and surface accuracy of the reflector. The parabolic reflector was constructed from metalized thin film gores and a transparent canopy which formed an enclosure for inflation. The rim of the reflector assembly was supported by an inflatable torus which was then attached to the surface measurement system via three 28 metre long inflatable struts which rigidized after deployment. The total weight of IAE was 60 kg and the stowed antenna can be seen in Fig. *12*. So as not to compromise the Space Shuttle the mission utilized the recoverable Spartan spacecraft as the experiment carrier.

Fig. 12: L'Garde Inflatable Antenna Experiment (IAE) stowed ready for launch (image courtesy of L'Garde)

During the initial ejection and inflation of the structure it experienced unexpected dynamics. *Fig. 13* shows the deployment sequence of the IAE. The inflatable structure deployment did not proceed as predicted due to an unexpected amount of residual air in the stowed structure and a significant amount of strain energy release from the torus structure

[7]. This combination threatened to twist and tangle the structure which would be a catastrophic failure in the space environment.

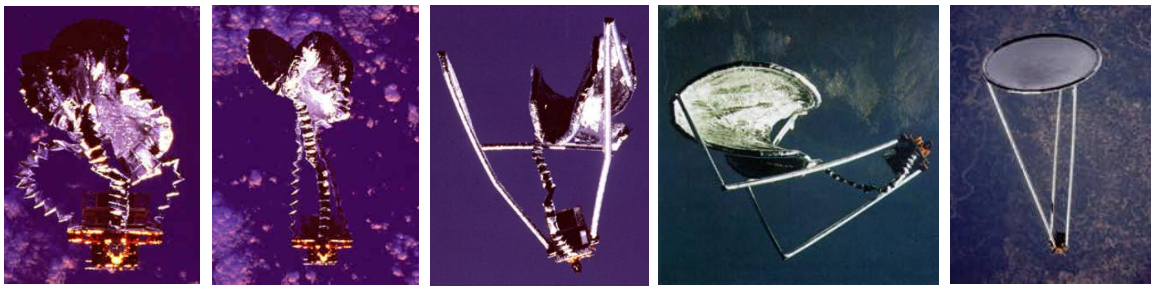

Fig. 13: Deployment of the L'Garde Inflatable Antenna Experiment (IAE) (images courtesy of L'Garde)

After reaching the desired orbit the antenna was jettisoned from the Spartan 207, and on the following day the Spartan 207 was successfully retrieved for return to Earth. For the mission to be considered successful it needed to demonstrate that the inflatable structure could achieve the required reflector shape and surface accuracy as well as maintain the dimensional relationship between the reflector and the feed. The IAE was measured to have a shape accuracy of within 2 mm RMS thus demonstrating that it was possible to manufacture a precision inflatable structure for space applications [7].

1.4.2.1 Current development of space-based inflatable antennas

NASA has continued to develop both non precision and precision inflatable technologies. Pappa et al [25] presented an overview of the technology development in progress at Goddard Space Flight Center, Langley Research Center, and Marshall Space Flight Center. JAXA, ESA and China also have programs to develop large deployable structures [26, 27, 28, 29, 30] although the majority of the work being conducted would be categorised as deployable or hybrid structures rather than inflatable.

Many of the problems associated with the development of large space-based antennas, whether they are inflatable or mechanically deployable, are the ability to test and evaluate the system and the ability to maintain the shape accuracy once deployed. The modelling and testing of large deployable structures is something that must be perfected if they are to become a mature technology. Ruggiero and Inman [31] presented a comprehensive overview of current modelling and testing techniques as well as some of the active control

mechanisms being introduced to maintain shape accuracy after deployment. Japan and China have made significant advances in the active control of mesh deployable and truss deployable antennas [26, 27, 31]. It is conceivable that some of these techniques could be adapted to the active control of inflatable structures.

1.4.3 Disadvantages of Using Inflatable Structures in the Space Environment

Despite the success of Echo and the Inflatable Antenna Experiment there are challenges associated with using inflatable structures in the space environment. These challenges fall into two main categories, the issues associated with the operating environment and the issues associated with deploying the structure.

In addition to the normal challenges such as temperature, atomic oxygen, radiation and micrometeorites, the large size of inflatable structures makes them more susceptible to solar winds. During its five year lifespan Echo encountered significant orbital changes due to solar pressure [6, 18]. Advances in material design are being used to address the structures resilience to the space environment but the dynamic response to solar pressure is more challenging as it is variable and unpredictable.

The deployment of the inflatable structure is an even greater challenge. The deployment and dynamic response of the Inflatable Antenna Experiment proved to be marginal. During the initial ejection and inflation of the structure it experienced unexpected dynamics. *Fig. 13* shows the deployment sequence of the IAE. If the antenna had twisted and tangled it would have been a catastrophic failure.

Following the IAE a great deal of attention was devoted to understanding and controlling the dynamic response of large inflatable structures, in particular during deployment [33, 34]. Another active area of research was in rigidization techniques for inflatable structures [35, 36]. By rigidizing an inflatable structure after deployment it behaves like a rigid structure and the dynamic response in better understood. Conversely, the advantage of high natural damping is lost. Recent development has concentrated on the modelling of the structural dynamics to better understand and predict the behaviour of inflatable structures.

Many of the problems faced in the space environment are of no concern in the terrestrial environment but the advantages of increased size, reduced weight and reduced stowed volume are common. It is proposed that in addition to pursuing the development of inflatable antennas in the space environment they can be developed for the terrestrial environment to address the issue of portability for direct satellite communication.

1.5 Comparison of Space-based Parabolic Antenna Structures

There are many other parabolic antenna designs that have been used in the space environment and many more are being developed. The main categories have been explored; rigid, mechanical deployable and inflatable, but there are many variations and combinations of these.

Each approach has both its advantages and disadvantages, and the ultimate selection is made taking all the mission requirement into consideration. The characteristics of the most common parabolic dish antenna structures are summarised in *Table 1*.

Type of Antenna	Achievable Diameter	Shape Accuracy	Stowed Volume	Weight	Mechanical Complexity	Risk	Durability	Maturity of Technology	Cost
Rigid	Limited by launch vehicle	Excellent	High	High	Very Low	Very Low	High	Mature	Low
Petal Deployable	Medium	Good	Medium	High	Medium	Medium	High	Mature	Medium
Mesh Deployable	Large	Good	Medium	Medium	High	Medium/ High	Medium	Mature	High
Cable Truss	Large	Good	Medium	Medium	High	High	Medium	Immature	Medium/ High
Hybrid	Very Large	Good	Low	Low	Medium	Medium/ High	Medium	Immature	Medium
Inflatable	Extremely Large	Good	Very Low	Very Low	Low	Medium/ High	Medium/ Low	Immature	Medium/ Low

Table 1: Comparison of space-based parabolic antenna structures [4-7, 14-18, 21-36]

1.6 Inflatable Antennas in the Terrestrial Environment

After reviewing the types of parabolic dish antennas used in the space environment it is proposed that in the same way that inflatable antennas have been used to overcome the limitations of the launch vehicle, inflatable antennas could be used in the terrestrial environment to overcome limitations on the portability and performance of personal satellite-based communication systems. The ability to stow the antenna when it is not needed, carry it without the need for a vehicle and deploy it when required, creates the possibility of personal direct satellite access for mobile military applications, emergency response teams and remote media broadcasting.

To develop an inflatable antenna that can be used in a terrestrial environment, it must be demonstrated that a precision inflatable structure can be developed from a material with the necessary electromagnetic characteristics that can achieve the required shape and surface accuracy and maintain the dimensional relationship between the antenna elements whilst under the influence of environmental conditions.

The design presented in this thesis uses similar thin film materials and construction techniques as those used for the space-based inflatable antenna. Unlike the IAE the inflatable antenna presented in this thesis can support its own weight and maintain its dimensional stability under terrestrial conditions without being rigidized. This allows the inflated structure to maintain all the positive qualities of a pressure vessel like distributing the applied loads through the skin and excellent vibration damping as well as maintaining the ability to be deflated and stowed for reuse. The use of a single enclosure for inflation also allows the antenna to be inflated without risk of tangling.

The inflatable antenna concept, including gossamer feed horn, presented in this thesis was first published in February 2003 along with preliminary results for the gossamer feed horn fed by a microstrip patch. Since that date an alternative design for a terrestrial inflatable antenna has been commercialised by GATR Technologies. The GATR design, shown in *Fig. 14*, was first published in May 2003 and again in July 2005 by Phase IV Systems and SRS Technologies in Huntsville, Alabama [37, 38] and GATR Technologies was incorporated in 2004 to commercialise the antenna.

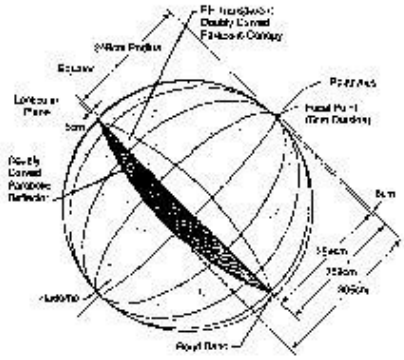

Fig. 14: GATR Technologies inflatable antenna (images courtesy of GATR)

The GATR Technologies antenna uses an inflatable sphere to support a rigid feed horn and inflatable lenticular. It is currently the lightest antenna of its size on the market and has the smallest stowed volume. However, the use of a rigid feed assembly makes it heavier and larger than the inflatable antenna presented in this thesis. The positioning of the rigid feed assembly at the focal point of the dish creates aperture blockage and acts to unbalance the antenna on its curved base.

In the following chapters the concept for an inflatable parabolic dish antenna and feed horn constructed entirely from thin film materials will be presented. It will be shown that using a combination of structural design and material selection an inflatable antenna can be constructed that matches the performance of an identical rigid antenna under terrestrial conditions. It will also be shown that using a microstrip patch to feed the gossamer horn further reduces the weight and stowed volume of the antenna and reduces the cost of manufacturing the antenna, producing a low cost solution to human portable direct satellite communication.

2 Design

For mobile direct satellite communication to be a reality, an antenna with an aperture large enough to generate the gain necessary for voice, data and video transmission, whist small enough and light enough to be human portable, is needed. It has been demonstrated that using inflatable structures in the space environment can reduce launch weight and volume whilst increasing the achievable size [18]. It has been further demonstrated that in the space environment an inflatable structure can maintain the shape accuracy and dimensional stability required to operate as an antenna [7].

An inflatable antenna is a precision structure, which means the performance of the antenna is directly related to the dimensional stability of the structure. This includes both the shape accuracy of the individual components and the dimensional relationship between the antenna elements. It is proposed that it is possible to manufacture an inflatable structure that performs reliably as an antenna under terrestrial conditions.

The following chapter explores how this can be achieved using a combination of structural design, material selection and internal pressure.

2.1 Material

The inflatable antenna concept presented makes use of a design technique known as a monocoque design. This is a design technique commonly used in aircraft fuselages and submarines where a combination of the design and the internal pressure enable the skin to carry bending and compression loads beyond the ability of the material alone. The skin acts as a structural member eliminating the need for reinforced joints, and reducing the overall mass. As the skin is the main load bearing member, structural design, material selection and internal pressure are the key design factors.

The use of the skin as the main load bearer in monocoque structures makes the material selection critical. As well as carrying the applied loads, the skin in an inflatable structure has additional requirements. For the structure to be stowed and then inflated the material must be foldable and have low gas permeation to sustain the inflation. The material when

stowed must not become permanently deformed and to maintain inflation it must be durable, and tear and puncture resistant. The materials that best fulfil these requirements are polymer thin films, including polyesters, ploymides and polyamides. These thin films are often referred to as membrane or gossamer materials as they have a small thickness, which allow them to be folded for storage, but are incapable of carrying compressive or bending loads.

If the gossamer material is to be used to construct a non-precision structure, high packing efficiency and durability are the key factors for material selection. If the final product is to be a precision structure the dimensional stability of the material becomes critical and if the structure is intended for a communications application the electromagnetic properties of the material must also be considered. The electromagnetic properties required for the material to be used to construct an antenna are explored in *section 2.4.1*.

Thin films are available commercially in thicknesses from 12 um to 350 um and their properties can be manipulated with a variety of additives, treatments and coatings. In a commercial context the material would be designed to provide the required properties. For the purpose of demonstrating the concept a prototype was constructed using polyester thin films donated by VISIPAK. The structural and electromagnetic testing of the materials is outlined in *section 3.3* and the results are presented in *section 4.2*.

2.2 Pressure vessels

The internal pressure gives the structure its desired shape and stability and introduces membrane stresses which enable the skin to carry bending and compression loads beyond the ability of the material alone. The most efficient pressure vessel to contain uniform pressure is a uniform thickness spherical shell. Such a vessel behaves as a perfect membrane and resists its pressure load with a uniform membrane stress acting all over its surface.

Pressure vessels are not limited to spherical shells; other curved structures such as cylinders, paraboloids and cones can be used. For curved panels under combined compression and internal pressure, the following interaction equation applies

$$R_C{}^2 - R_P = 1.0 \qquad \textit{Eq. 1}$$

Where

$$R_C = \frac{f_C}{F_{C_{CR}}} \qquad \textit{Eq. 2}$$

$f_C =$ applied compression stress

$F_{C_{CR}} =$ critical buckling stress for curved panel under compression stress only

$$R_P = \frac{q}{p_{CRIT}} \qquad \textit{Eq. 3}$$

$q =$ applied internal pressure

$p_{CRIT} =$ external inward pressure that would buckle a cylinder of which the curve panel is a part.

Shear buckling stress of curved panels under internal pressure:

$$R_S{}^2 - R_P = 1 \qquad \textit{Eq. 4}$$

Where

$$R_S = \frac{f_S}{F_{S_{CR}}} \qquad \textit{Eq. 5}$$

$f_S =$ applied shear stress

$F_{S_{CR}} =$ critical buckling stress for curved panel under shear stress only

It can be seen that the introduction of membrane stresses in the skin due to pressurisation, increases the buckling stress level for panels under compression and shear and thus the loads the overall structure can carry.

A parabolic dish reflector was chosen because it offers the high gain necessary for direct satellite communication and the curvature of the dish can be generated by forming an enclosed environment between the reflector and the canopy which can then be pressurized. *Fig. 15* shows the inflatable antenna design under consideration.

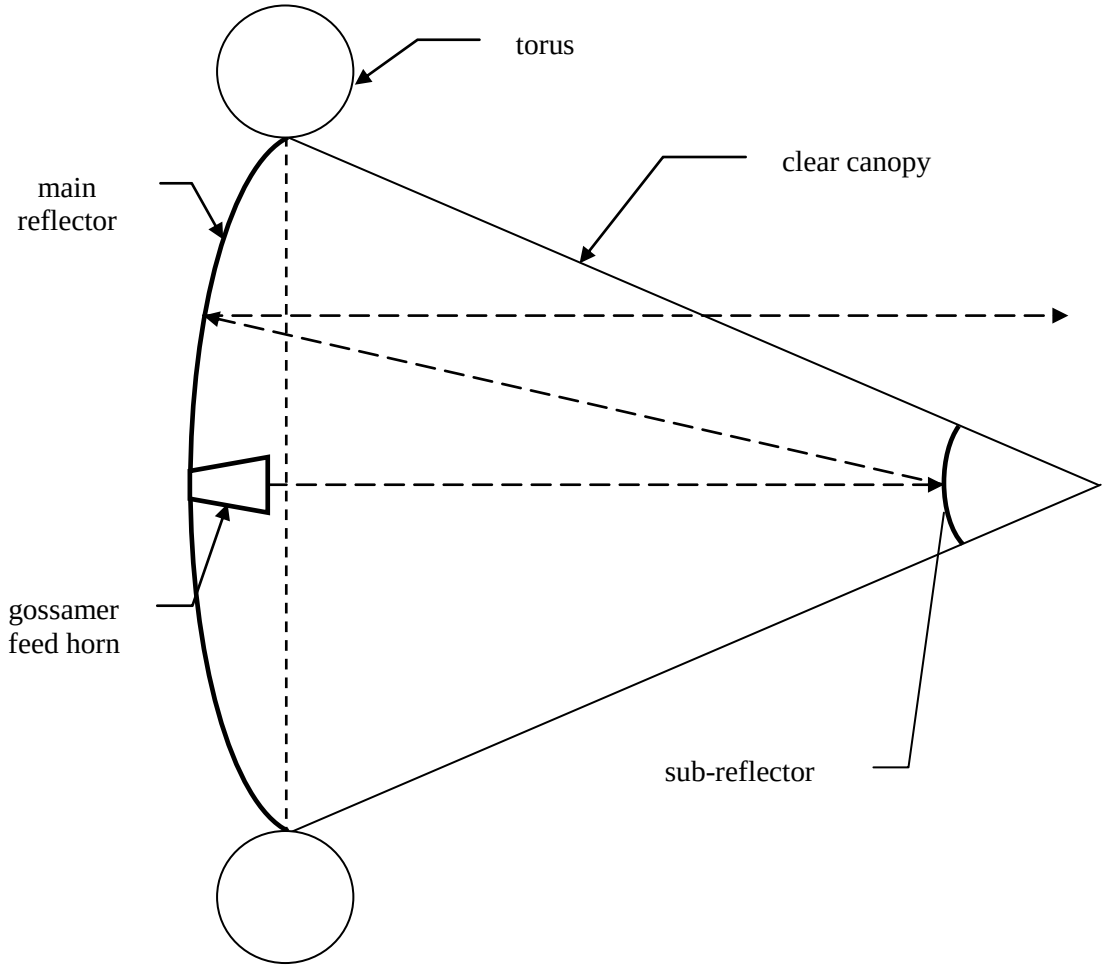

Fig. 15: Layout of inflatable antenna

Both the parabolic reflector and the conical canopy are surfaces of revolution. The reflector surface is a parabola of revolution, or paraboloid and the canopy is a cone.

2.2.1 Parabolic reflector

A paraboloid is best approximated as an ellipsoid of revolution. In this case half of the ellipsoid is used, as shown in *Fig. 16.*

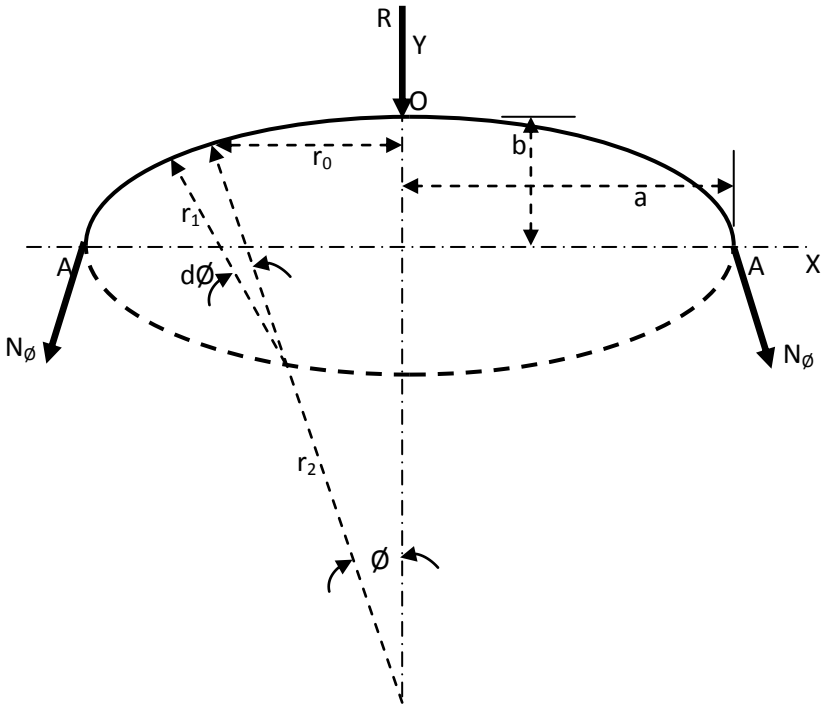

Fig. 16: Membrane forces in parabolic reflector

The principal radii of curvature in the case of an ellipse with semi axes a and b are given by the formulas

$$r_1 = \frac{a^2 b^2}{(a^2 \sin\varphi^2 + b^2 \cos\varphi^2)^{\frac{3}{2}}} \qquad \textit{Eq. 6}$$

$$r_2 = \frac{a^2}{(a^2 \sin\varphi^2 + b^2 \cos\varphi^2)^{\frac{1}{2}}} \qquad \textit{Eq. 7}$$

If the resultant of the total load on the shell is denoted by R, the equation of equilibrium is given by

$$2\pi r_0 N_\varphi \ \sin\varphi + R = 0 \qquad \textit{Eq. 8}$$

Once N_φ is known N_θ can be calculated from

$$\frac{N_\varphi}{r_1} + \frac{N_\theta}{r_2} = -Z \qquad \textit{Eq. 9}$$

Where N_φ and N_θ are the membrane forces per unit length in the two meridian planes.

If q is the internal pressure, then for a parallel circle of radius r_0, giving $R = -\pi q r_0^2$ and

$$N_\varphi = \frac{q r_0}{2\sin\varphi} = \frac{q r_2}{2} \qquad \textit{Eq. 10}$$

$$N_\theta = r_2 p - \frac{r_2}{r_1} N_\varphi = q\left(r_2 - \frac{{r_2}^2}{2r_1}\right) \qquad \textit{Eq. 11}$$

At the top of the shell, point O,

$$r_1 = r_2 = \frac{a^2}{b} \qquad \textit{Eq. 12}$$

Giving

$$N_\varphi = N_\theta = \frac{q a^2}{2b} \qquad \textit{Eq. 13}$$

At the equator AA,

$$r_1 = \frac{b^2}{a} \qquad \text{and} \qquad r_2 = a$$

Giving

$$N_\varphi = \frac{qa}{2} \qquad \textit{Eq. 14}$$

and

$$N_\theta = qa\left(1 - \frac{a^2}{2b^2}\right) \qquad \textit{Eq. 15}$$

In the case of a sphere where a = b it can be seen that

$$N_\varphi = N_\theta = \frac{qa}{2} \qquad \textit{Eq. 16}$$

Confirming that in a spherical shell membrane forces are equal in all directions.

2.2.2 Conical canopy

The membrane forces in the conical canopy will be considered next. *Fig. 17* shows the conical canopy and the membrane stress distribution due to internal pressure.

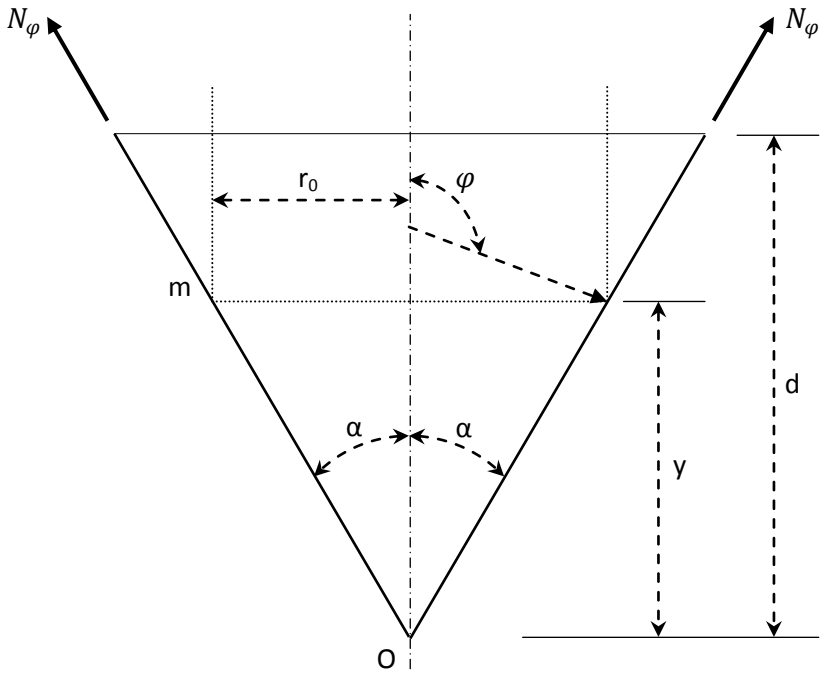

Fig. 17: Membrane stress distribution in conical canopy

In the case of the conical canopy membrane stresses are produced by a force applied at the top of the cone. If a force P is applied in the direction of the axis of the cone, the stress distribution is symmetrical, and

$$N_{\varphi} = -\frac{P}{2\pi r_0 \cos\alpha} \qquad \textit{Eq. 17}$$

Substituting *Eq. 17* into *Eq. 9* gives

$$N_{\theta} = 0$$

If lateral forces are symmetrically distributed over the conical surface due to internal pressure, the membrane stresses can be calculated by using *Eq. 8* and *Eq. 9*. Since the curvature of the meridian in the case of a cone is zero, $r_1=\infty$; we can write these equations in the following form:

$$N_{\varphi} = -\frac{R}{2\pi r_0 \sin\varphi} \qquad \textit{Eq. 18}$$

$$N_{\theta} = -Zr_2 = -\frac{Zr_0}{\sin\varphi} \qquad \textit{Eq. 19}$$

Each of the resultant forces N_{φ} and N_{θ} can be calculated independently provided the load distribution is known.

The membrane stresses in the skin provide the structural rigidity needed to maintain the position of the sub-reflector. It can be seen from the previous analysis that when an external load is applied to the canopy, due to environmental conditions like wind, the load will be transferred through the skin to the torus.

A conical canopy was chosen as opposed to a parabolic canopy for additional rigidity. The formation of a cone from a gossamer material applies a pre-stress in the skin which allows the cone to maintain its shape under the influence of gravity even without internal pressure. This pre-stress provides additional stability which allows the canopy to maintain

the dimensional relationship between the antenna elements and makes the antenna performance less dependent on the internal pressure.

2.2.3 Torus

If the junction between the parabolic reflector and the conical canopy was unrestrained the internal pressure and membrane stresses will act to balance the stress in the skin and ripples will form around the edge of the reflector, reducing the shape accuracy of the reflector, and degrading the antenna performance. To counteract this force an inflatable torus is used to maintain the diameter of the dish. *Fig. 18* shows the torus and the membrane stress distribution.

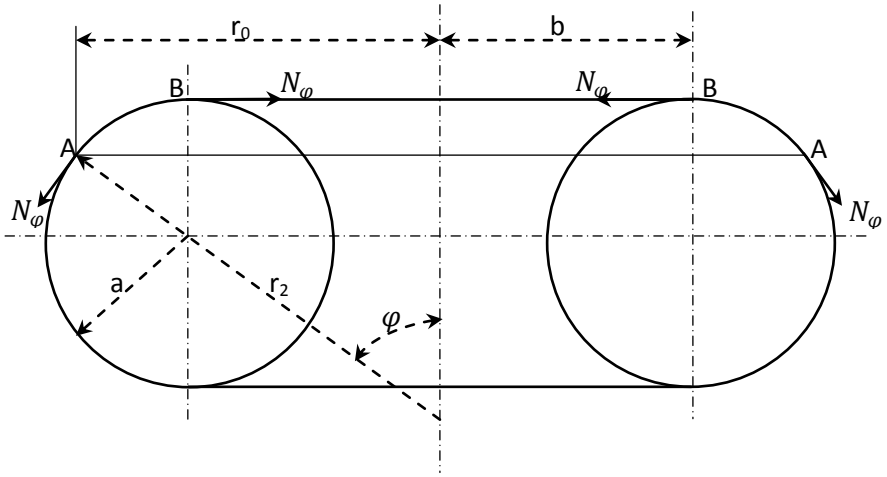

Fig. 18: Membrane stress distribution in torus

If a torus is obtained by rotation of a circle of radius a about a vertical axis the forces N_φ are obtained by considering the equilibrium of the ring-shaped portion of the shell AB. Since the forces N_φ along the parallel circle BB are horizontal, we need consider only the forces N_φ along the circle AA and the external forces acting on the ring when discussing equilibrium in the vertical direction. Assuming the shell is under uniform internal pressure p, we obtain the equation of equilibrium.

$$2\pi r_0 N_\varphi \sin\varphi = \pi q({r_0}^2 - b^2) \qquad \textit{Eq. 20}$$

From which

$$N_{\varphi} = \frac{q({r_0}^2 - b^2)}{2r_0 \sin\varphi} = \frac{qa(r_0 - b)}{2r_0} \qquad \textit{Eq. 21}$$

Substituting this expression in *Eq. 9* we find

$$N_{\theta} = \frac{qr_2(r_0 - b)}{2r_0} = \frac{qa}{2} \qquad \textit{Eq. 22}$$

Which is logical since the torus is circular.

2.3 Internal pressure

If the walls of a vessel are relatively thin and have no abrupt changes in thickness, slope or curvature and if the loading is uniformly distributed or smoothly varying, the stresses σ_1 and σ_2 are practically uniform throughout the thickness of the wall and are the only important ones present. The radial stress σ_3 and such bending stresses as occur are negligibly small.

Despite the fact that the antenna design proposed uses a cone for the canopy, the vessel will be approximated as a sphere to calculate an initial pressure. For a spherical pressure vessel the internal pressure can be calculated using

$$\sigma_1 = \sigma_2 = \frac{qr}{2t} \qquad \textit{Eq. 23}$$

Where

q = uniform internal pressure
r = radius of the sphere
t = thickness of the sphere

The operating pressure is the pressure required to remove the wrinkles from the material after being stowed. *Freeland et al.* [21] showed that for a metalized PET thin film an internal pressure of 6.89 MPa was required to remove the wrinkles after deployment.

Referring to *section 4.2.1* the thickness of the metalized thin film was measured as 50 μm and the thickness of the clear thin film was measured as 25 μm. To be conservative the greater of the two will be used. Substituting into *Eq. 23* gives

$$6.89\times10^{6}=\frac{q\times0.25}{2\times50\times10^{-6}}$$

$$q=2.75kPa$$

It can be seen that only a very low internal pressure is needed to remove the wrinkles from the skin. Starting at this minimum, the pressure can then be optimized to provide the best shape accuracy. The internal pressure generates membrane stresses that add to the stability of the structure but over inflation can cause the structure to pillow. Pillowing is caused by the localized stiffening created by the seams combining with the flexibility of the membrane material and the internal pressure to degrade the shape accuracy.

The maximum operating pressure is limited by the strength of the material. The material will fail when the material's tensile strength is exceeded but the maximum operating pressure is determined by the yield strength of the material. When the yield strength is exceeded the inflatable structure will no longer be able to maintain its dimensional stability and the performance will be degraded. Of the two materials used to construct the inflatable antenna the yield strength of the metalized PET thin film was measured to have a lower yield strength than the clear PET thin film. Substituting the yield strength and thickness stated in *section 4.2.1* into *Eq.23,* and assuming the seams have the same strength as the material, the maximum operating pressure is given by

$$31.25\times10^{6}=\frac{q\times0.25}{2\times50\times10^{-6}}$$

$$q=12.5kPa$$

To increase the maximum operating pressure of the antenna a material with a higher yield strength should be chosen.

The combination of the pressurized elements detailed above, produces a structure that can withstand the external forces of gravity and other environmental conditions. In addition, the high natural damping characteristics of inflatable structures act to stabilize any transient loading such as wind gusting. It must then be shown that the structure provides the dimensional stability to perform reliably as an antenna.

2.4 Rigidizing inflatable structures

During the initial investigations into inflatable structures in the space environment emphasis was placed on rigidizing the structure after deployment to increase their durability [35, 36]. Rigidizing the structure after deployment is necessary for structures that are not capable of maintaining their structural integrity or dimensional stability but there are some major disadvantages associated with rigidizing inflatable structures.

The ability of an inflatable structure to distribute the applied loads through the skin reduces the overall weight of the structure and increases its vibration damping. The extreme flexibility of the skin, combined with internal pressure, produces only local deformation when an external point load is applied rather than exciting any of the global modes [39]. If the structure is rigidized it loses these characteristic and behaves like a rigid structure, concentrating loads at the joints rather than distributing the load over the skin. Maintaining vibrational damping in a terrestrial environment is important as it helps to minimize the impact of varying wind conditions.

The inflatable antenna design presented can maintain its structural integrity without relying on rigidization. Not rigidizing makes the antenna re-usable and eliminates the risk of rigidizing the structure in a deformed state; it also eliminates the weight and added complexity of an additional system.

2.5 Antenna configuration

The antenna design presented is a dual reflector antenna, so it consists of a feed system, a primary reflector and secondary reflector which must maintain their dimensional relationship relative to one another to maintain communication. The most common dual

reflector antennas are Cassegrain and Gregorian antennas. The Cassegrain antenna consists of a primary concave reflector and a secondary convex reflector. In a Gregorian antenna both the primary reflector and the secondary reflector are convex. The inflatable antenna concept presented can be used to generate either a Cassegrain or a Gregorian antenna of varying dimensions. It can also be used to generate offset Cassegrain or Gregorian antennas. For the purpose of discussion a Cassegrain antenna will be considered.

A dual reflector configuration was chosen to reduce the loading on the canopy and improve the balance of the structure. However, dual reflector antennas have a range of other features that make them appealing. They have increased focal length, all the transmitting and receiving equipment can be housed in the same unit as the positioning and tracking equipment behind the main reflector, and the antenna noise is reduced because the feed is facing the cool sky.

In a prime focus antenna the feed assembly is placed at the focal point of the reflector. Positioning the feed assembly at this point places a lot of weight at the end of a long moment arm which places strain on the support structure and in turn the reflector, causing distortions. To maintain shape accuracy the antenna structure must be reinforced which then adds weight and reduces portability. In the case of rigid antennas the feed is supported by either a single strut in an attempt to reduce aperture blockage and weight, or three struts to distribute the load evenly through the reflector. In an inflatable antenna the support structure is a thin film canopy. The clear canopy eliminates any aperture blockage caused by struts but is incapable of supporting the weight of a rigid feed horn.

Using a dual reflector configuration significantly reduces the loading on the canopy by placing the feed assembly at the centre of the primary reflector and all transmitting and receiving equipment behind the primary reflector. As a result, the only non thin film component the inflatable structure must support is the metallic sub-reflector. The surface and shape accuracy required of the hyperbolic sub-reflector and its small size means that machining it from a lightweight Aluminium alloy is the preferred solution.

Placing all the electronics behind the primary reflector also minimizes the transmission loss which occurs if the feed is placed at the focal point. The elimination of transmission lines from the feed assembly at the focal point to the processing equipment behind the

reflector also eliminates scattering of the signal and the possibility of the cables puncturing the inflatable antenna due to either friction or heat concentration.

The greatest advantage of using the clear thin film canopy to support the sub-reflector is that it eliminates any aperture blockage and scattering of the signal due to support struts. The aperture blockage caused by the sub-reflector is also significantly less than the blockage caused by a feed assembly.

The antenna design presented is manufactured entirely from polyester thin film with the exception of the sub-reflector and the microstrip patch used to feed the horn. The use of a microstrip patch to feed the horn reduces the weight and stowed volume of the antenna further and enhances the balance of the structure. The use of this feed system also reduces the manufacturing cost of the system. A single patch antenna could not produce the gain required for direct satellite communication and even using a patch array the aperture of the antenna would need to be significantly increased. The placement of a rigid flat patch array on the surface of a gossamer reflector would also distort the dish and reduce the effective area.

Using a microstrip patch to feed a gossamer conical horn increases the gain of the feed and produces a narrow beamwidth whilst minimizing the weight and size of the feed assembly.

The antenna under consideration is intended to operate under terrestrial conditions. It will therefore be necessary for the antenna to operate under the influence of gravity and atmospheric pressure. In addition to these basic parameters the antenna must operate under a range of temperature extremes, wind conditions, rain, and snow and be durable enough to operate reliably in both military and disaster response situations.

Rigid antenna dishes suffer distortions due to gravity, wind and particles such as snow and rain settling in the dish. To maintain the required shape a rigid dish is supported by a rigid structure to prevent distortion. An inflatable antenna constructed from thin film is so light that the internal pressure is sufficient to counteract the impact of gravity. The cone provides an aerodynamic profile which minimizes the wind loading on the entire structure and transfers the load through the skin to the torus. The clear canopy also acts as a radome which prevents the dish acting like a sail and stops any particles settling in the dish.

2.5.1 Skin depth

To maintain antenna performance the inflatable structure must maintain the shape accuracy of the individual components and the relationship between the components whilst under the influence of the operating environment. Any components which will act as a canopy must be radio frequency (RF) transparent at the operating frequency and any components acting as a reflector must be metalized such that the signal is reflected without loss. The thickness of the metal coating can be calculated using the principle of skin effect [40] which varies depending on the wavelength of the signal to be reflected and the conductivity of the material used for the coating. The thickness of the metalized layer can be calculated using

$$\delta = \sqrt{\frac{2}{\varpi\mu\sigma}} \qquad \textit{Eq. 24}$$

$\omega = 2\pi F$ giving

$$\delta = \frac{1}{\sqrt{\pi F\mu\sigma}} \qquad \textit{Eq. 25}$$

Where

δ = skin depth

F = frequency (Hz)

$\mu = 4\pi\times10^{-7}$ (H/m)

σ = conductivity (mhos/m)

$= 3.55\times10^{7}$ mhos/m for Aluminium sheet

At the chosen operating frequency of 12.5 GHz

$$\delta = 7.55\times10^{-5}\ \text{m}$$

$$= 0.76\ \mu\text{m}$$

2.5.2 Basic antenna parameters

The characteristics of pressurized monocoque structures that will give the inflatable antenna dimensional stability have been explored and the electromagnetic properties of the thin films required to construct the antenna have been examined. This approach is not limited to any particular size or design but for the purposes of testing the hypothesis a design must be specified.

The inflatable antenna concept presented is a dual reflector antenna but before this configuration can be tested it is important to understand the behaviour of each of the components. As such the testing will be conducted in the following stages.

1. Microstrip patch
2. Gossamer conical feed horn for prime focus antenna fed by microstrip patch
3. Inflatable prime focus antenna supported by rigid mount fed by gossamer horn
4. Inflatable prime focus antenna supported by inflatable torus fed by gossamer horn
5. Gossamer conical feed horn for Cassegrain antenna fed by microstrip patch
6. Inflatable Cassegrain antenna supported by rigid mount fed by gossamer horn
7. Inflatable Cassegrain antenna supported by inflatable torus fed by gossamer horn

The following section presents the design of the various components used to test the hypothesis that an inflatable antenna can be manufactured that matches the performance of an identical rigid antenna under terrestrial conditions. Each component will be manufactured as a rigid structure and an inflatable structure. The performance of the rigid structure and the inflatable structure will then be compared.

The behaviour of parabolic reflector antennas can be explained using the principles of physical optics. These principles can be applied as microwaves fall in the region between radio waves and visible light. The surface of the dish reflector is defined by rotating a parabola about its axis. This ensures that a signal originating at the focal point is reflected by the dish as plane waves and conversely any incoming signal collected by the dish is reflected to the focal point. This reciprocity means parabolic dish antennas can be used equally for receiving and transmitting signals.

When fed efficiently from the focal point paraboloidal reflectors produce a high gain pencil beam with low side lobes and good cross polarization characteristics. This type of antenna is widely used for low noise applications and is considered a good compromise between performance and cost. The frequency of operation, bandwidth, beamwidth, gain and cross polarization level are among the main design parameters and directly influence the performance of the antenna. Using these parameters, the performance of the inflatable antenna will be compared to that of an identical rigid antenna.

A paraboloidal reflector antenna operates efficiently, provided that it has an aperture exceeding 10 wavelengths, a surface roughness less than 1/8 wavelength and the profile of the antenna is maintained. The wavelength is related to the frequency of the signal and the velocity of propagation by

$$\lambda_m = \frac{v_{m/s}}{F_{Hz}} \qquad \textit{Eq. 26}$$

Since radio waves propagate at the speed of light 300,000,000 m/s, the expression for wavelength can be written as

$$\lambda_m = \frac{300}{F_{MHz}}$$

As the antenna is intended for direct satellite communications it must operate in the Ku band (12 – 18GHz). A frequency of 12.5GHz has been chosen for demonstration purposes but the inflatable antenna concept can be applied to other frequencies.

At 12.5GHz the wavelength is

$$\lambda = \frac{0.3}{12.5}$$

$$= 0.024 \text{ m}$$

Thus the antenna must be at least 0.24 m in diameter and the surface roughness must be less than 3 mm.

The gain of a parabolic antenna is a function of several factors, dish diameter, feed illumination and surface accuracy. The dish diameter should be large compared with its depth. For a standard dish

$$0.5 < \frac{f}{D} < 1.0$$

For demonstration purposes an average value of $\frac{f}{D} = 0.75$ and a diameter of 0.5 m was chosen giving a focal length of 0.375 m.

Each of these factors can be varied to optimize the design for specific applications but as this antenna is for proof of concept only, little attention has been paid to refining the design.

2.5.3 Conical feed horn for prime focus antenna

Now that the size and shape of the reflector have been determined a feed horn can be designed to maximize the feed illumination. Feed illumination refers to how evenly the feed element radiates to the reflector surface.

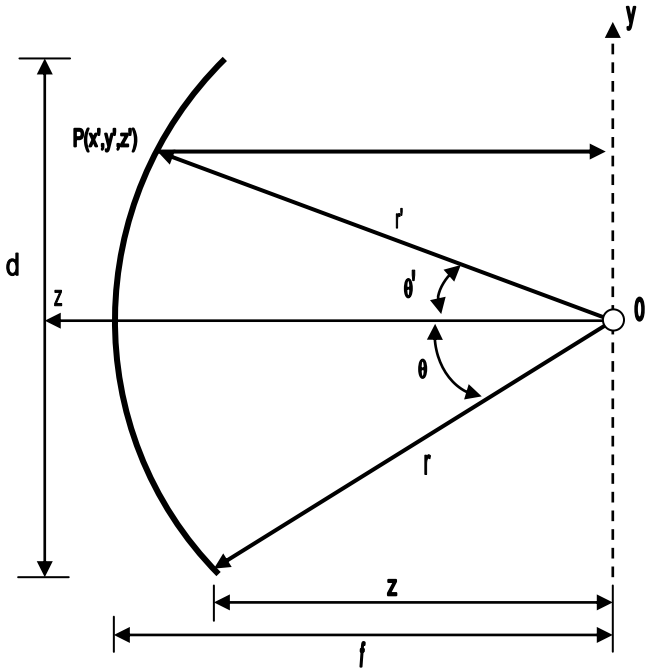

Fig. 19: Layout of prime focus parabolic dish antenna

$$\theta_o = \tan^{-1}\left|\frac{\frac{1}{2}\left(\frac{f}{d}\right)}{\left(\frac{f}{d}\right)^2 - \frac{1}{16}}\right| \qquad \textit{Eq. 27}$$

$$= \tan^{-1}\left|\frac{0.5 \times 0.75}{0.75^2 - 0.0625}\right|$$

$$= 36.8°$$

$2\theta_0$ is referred to as the included angle and is used to calculate the optimum feed required to fully illuminate the main reflector.

$$2\theta_0 = 73.6°$$

From basic geometry

$$z_o = f - \frac{d^2}{16f} \qquad \textit{Eq. 28}$$

$$= 0.375 - \frac{0.5^2}{16 \times 0.375}$$

$$= 0.333\text{m}$$

and

$$r^2 = z^2 + \left(\frac{d}{2}\right)^2 \qquad \textit{Eq. 29}$$

$$r^2 = 0.333^2 + 0.25^2$$

$$r = 0.416m$$

The next step is to consider the directivity and aperture efficiency of the main reflector and how they are impacted on by the primary feed. To simplify the analysis it is assumed that the feed pattern is circularly symmetric.

The antenna directivity in the forward direction is given by

$$D_0 = \left(\frac{\pi d}{\lambda}\right)^2 \left\{ \cot^2\left(\frac{\theta_0}{2}\right) \left| \int_0^{\theta_0} \sqrt{G_f(\theta')} \tan\left(\frac{\theta'}{2}\right) d\theta' \right|^2 \right\} \qquad \textit{Eq. 30}$$

The factor $\left(\frac{\pi d}{\lambda}\right)^2$ is the directivity of a uniformly illuminated constant phase aperture. Therefore the ideal directivity would be 4283.68.

This can be represented in decibels as

$$\begin{aligned} \text{D(dB)} &= 10 \log \text{D} \\ &= 36.3 \text{ dB} \end{aligned}$$

The remaining part of the equation defines the aperture efficiency, therefore

$$\varepsilon_{ap} = \cot^2\left(\frac{\theta_o}{2}\right) \left| \int_0^{\theta_o} \sqrt{G_f(\theta')} \tan\left(\frac{\theta'}{2}\right) d\theta' \right|^2 \qquad \textit{Eq. 31}$$

From *Eq. 31* it can be seen that efficiency is a function of the subtended angle θ_o and the feed pattern $G_f(\theta)$ of the reflector.

To illustrate the variation of the aperture efficiency as a function of the feed pattern and the angular extent of the reflector, the following feed patterns can be used

$$\begin{aligned} G_f(\theta') &= \{G_0^{(n)} \cos^n(\theta') && 0 \le \theta' \le \pi/2 \\ G_f(\theta') &= \{0 && \pi/2 \le \theta' \le \pi \end{aligned}$$

Where $G_0^{(n)}$ is a constant for a given value of n. The intensity in the back region $(\pi/2 < \theta' \le \pi)$ was assumed to be zero in order to avoid interference between the direct radiation from the feed and scattered radiation from the reflector.

The constant $G_0^{(n)}$ can then be determined from

$$\oiint_S G_f(\theta')d\Omega = \oiint_S G_f(\theta')\sin\theta' d\theta' d\phi' = 4\pi \qquad \textit{Eq. 32}$$

Which becomes

$$G_0^{(n)} \int_0^{\pi/2} \cos^n\theta' \sin\theta' d\theta' = 2 \Rightarrow G_0^{(n)} = 2(n+1) \qquad \textit{Eq. 33}$$

For even values of n=2 through n=8

$$\varepsilon_{ap}(n=2) = 24\left\{\sin^2\left(\frac{\theta_0}{2}\right) + \ln\left[\cos\left(\frac{\theta_0}{2}\right)\right]\right\}^2 \cot^2\left(\frac{\theta_0}{2}\right)$$

$$\varepsilon_{ap}(n=4) = 40\left\{\sin^4\left(\frac{\theta_0}{2}\right) + \ln\left[\cos\left(\frac{\theta_0}{2}\right)\right]\right\}^2 \cot^2\left(\frac{\theta_0}{2}\right)$$

$$\varepsilon_{ap}(n=6) = 14\left\{2\ln\left[\cos\left(\frac{\theta_0}{2}\right)\right] + \frac{[1-\cos(\theta_0)]^3}{3} + \frac{1}{2}\sin^2(\theta_0)\right\}^2 \cot^2\left(\frac{\theta_0}{2}\right)$$

$$\varepsilon_{ap}(n=8) = 18\left\{\frac{1-\cos^4(\theta_0)}{4} - 2\ln\left[\cos\left(\frac{\theta_0}{2}\right)\right] + \frac{[1-\cos(\theta_0)]^3}{3} - \frac{1}{2}\sin^2(\theta_0)\right\}^2 \cot^2\left(\frac{\theta_0}{2}\right)$$

Fig. 20 shows the variations of *Eq. 33* as a function of the angular aperture of the reflector θ_0 or the f/d ratio. From this figure the value of n that gives the highest aperture efficiency can be determined.

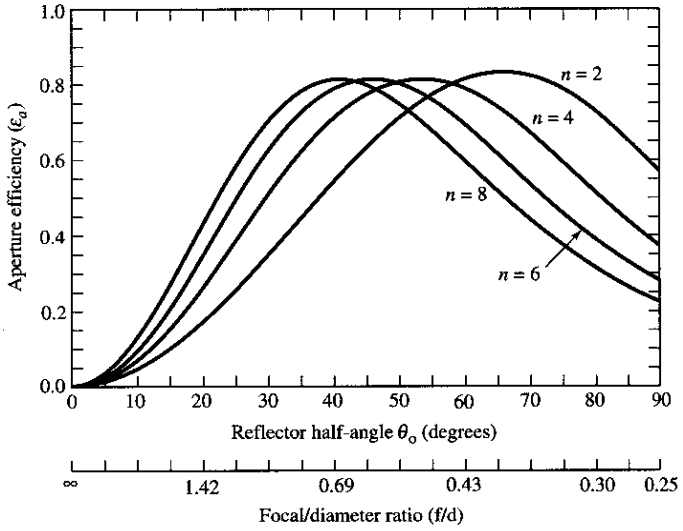

Fig. 20: Aperture efficiency as a function of reflector half-angle [source: Constantine A. Balanis, Antenna Theory: Analysis and Design (2nd Ed.), John Wiley & Sons, 1997]

The aperture efficiency is a product of:

- spillover efficiency ε_s - the fraction of the total power that is radiated by the feed, intercepted, and collimated by the reflecting surface
- taper efficiency ε_t - the uniformity of the amplitude distribution of the feed pattern over the surface of the reflector
- polarization efficiency ε_x - the phase uniformity of the field over the aperture plane
- blockage efficiency ε_b – the fraction of the total power blocked by a physical obstruction such as the feed assembly or struts
- random error efficiency ε_r – the accuracy of the reflector surface

This gives

$$\varepsilon_{ap} = \varepsilon_s\, \varepsilon_t\, \varepsilon_p\, \varepsilon_x\, \varepsilon_b\, \varepsilon_r$$

Thus for a reflector half angle of 36.8° the highest aperture efficiency, ε_{ap} is achieved for n=8. ε_{ap}= 0.8 or 80%

Using n=8

$$\varepsilon_{ap}(n=8) = 18\left\{\frac{1-\cos^4(\theta_0)}{4} - 2\ln\left[\cos\left(\frac{\theta_0}{2}\right)\right] + \frac{[1-\cos(\theta_0)]^3}{3} - \frac{1}{2}\sin^2(\theta_0)\right\}^2 \cot^2\left(\frac{\theta_0}{2}\right)$$

ε_{ap} = 18{0.147+0.105-0.003-0.179}^{2}9.037

= 0.8 or 80%

Which agrees with the result taken from the graph in *Fig. 20.*

Referring back to *Eq. 30*, if the factor $\left(\frac{\pi d}{\lambda}\right)^2$ is the directivity of a uniformly illuminated constant phase aperture and the remaining part of the equation defines the aperture efficiency

$$D_0 = D\varepsilon_{ap}$$

D_0 = 4283.68 x 0.8

= 3426.9

= 35.35 dB

Taper and spillover efficiencies are obtained from the graph in *Fig. 21*.

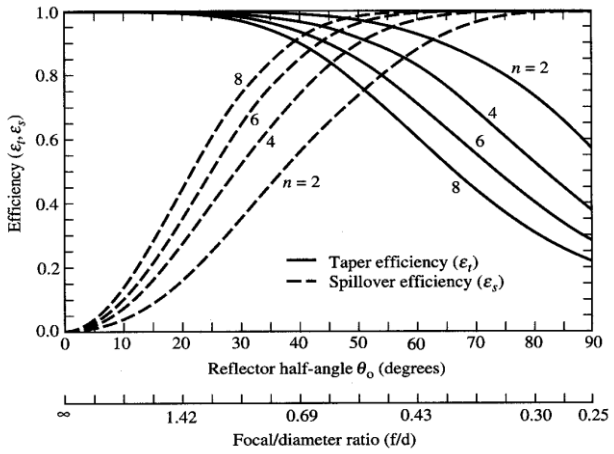

Fig. 21: Taper and spillover efficiency as a function of reflector half-angle [source: Constantine A. Balanis, Antenna Theory: Analysis and Design (2nd Ed.), John Wiley & Sons, 1997]

From *Fig. 21*, it can be seen that for a reflector half angle of 36.8° the best compromise for taper and spillover efficiency is obtained from n=8. This supports the result for aperture efficiency. From *Fig. 21* taper efficiency ε_t= 0.93 and spillover efficiency ε_s= 0.86

Taper and spillover efficiency dominate the aperture efficiency. The values taken from *Fig. 21* support the value taken from *Fig. 20.* Thus aperture efficiency ε_{ap}= 0.8 and n=8 will be used to determine the relative field strength.

From *Fig. 22* it can be seen that for n=8 the relative field strength is 10.2 dB.

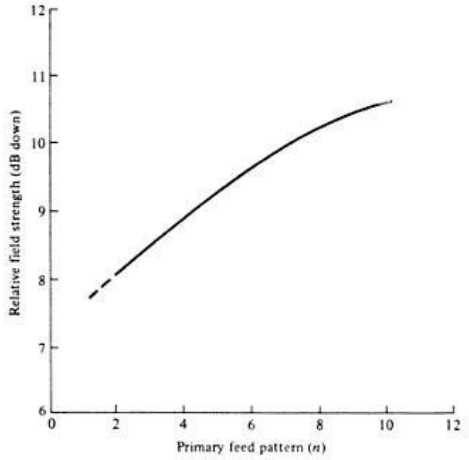

Fig. 22: Relative field strength of feed pattern along reflector edge bounds as a function of primary feed pattern number [source: S. Silver (ed.), Microwave Antenna Theory and Design, MIT Radiation Lab. Series Vol. 12, McGraw-Hill, New York, 1949]

If the feed pattern of the reflector is given by

$$G_f(\theta') = \{G_0^{(n)} \cos^n(\theta') \qquad 0 \le \theta' \le \pi/2$$
$$G_f(\theta') = \{0 \qquad \pi/2 \le \theta' \le \pi$$

Where

$$G_0^{(n)} \int_0^{\pi/2} \cos^n \theta' \sin\theta' d\theta' = 2 \Rightarrow G_0^{(n)} = 2(n+1)$$

for n=8 $\quad G_o^{(8)} = 18$

thus $G_f(\theta) = 18 \cos^8(36.8)$

$= 3.04$

In decibels

$$G_f(\theta) = 10 \log 3.04$$
$$= 4.82\text{dB}$$

This gives the gain of the feed at the edge of the reflector. To calculate the gain of the feed we need

$$G_f(\theta) \text{ at } \theta = 0$$

Thus

$$G_f = 18$$

In decibels

$$G_f = 10 \log 18$$
$$= 12.55 \text{ dB}$$

The feed directivity in the forward direction is given by

$$D_c(dB) = 10\log_{10}\left[\varepsilon_{ap}\frac{4\pi}{\lambda^2}(\pi a^2)\right] \qquad \textit{Eq. 34}$$
$$= 10\log_{10}\left(\frac{C}{\lambda}\right)^2 - L(s)$$

Where

C = circumference of the feed horn (m)
s = quadratic phase factor

The first term in *Eq. 34* represents the directivity of a uniform circular aperture and the second term is a correction figure to account for the loss in directivity due to the aperture efficiency. This loss figure is calculated in decibels by using

$$L(s) \approx \left(0.8 - 1.71s + 26.25s^2 - 17.79s^3\right) \qquad \textit{Eq. 35}$$

H-plane and E-plane universal patterns for a conical horn are used to select a value for s. From *Fig. 23* and *Fig. 24* it can be seen that as s increases the beamwidth gets broader and the asymmetry between E-plane and H-plane increases. A broader beamwidth leads to a loss in gain and reduced aperture efficiency. From *Fig. 23* and *Fig. 24* it can be seen that s<0.2 produces a reasonable pattern, whilst larger values of s give significantly distorted patterns.

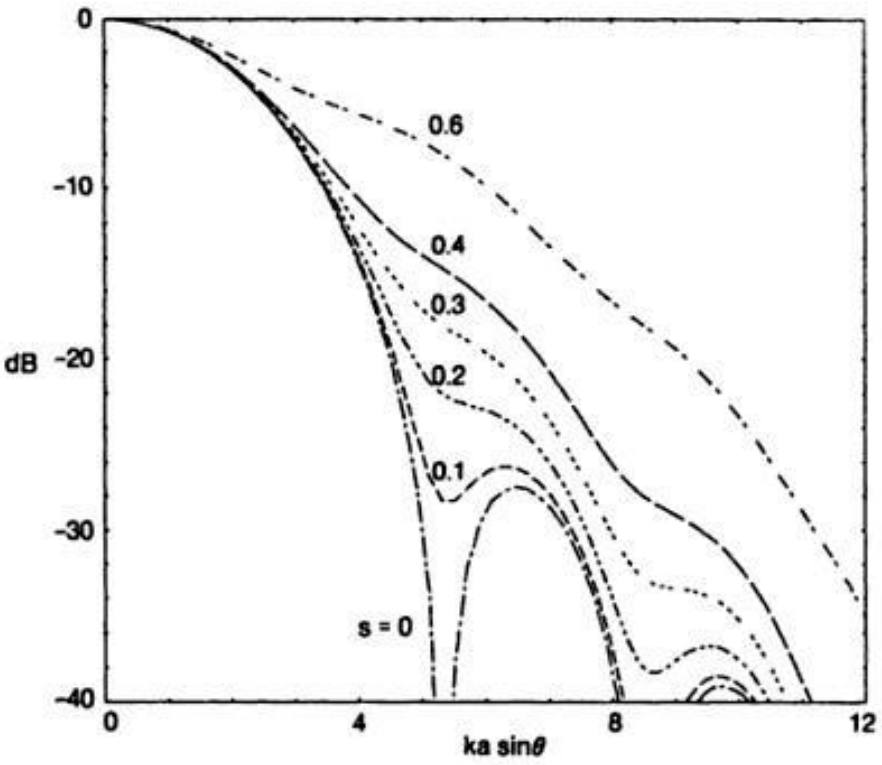

Fig. 23: H-plane universal pattern for a conical horn [source: A. D. Olver, P. J. B. Clarricoats, A. A. Kishk and L. Shafai, Microwave Horns and Feeds, IEE Electromagnetic Wave Series 39, IEEE Press 1994]

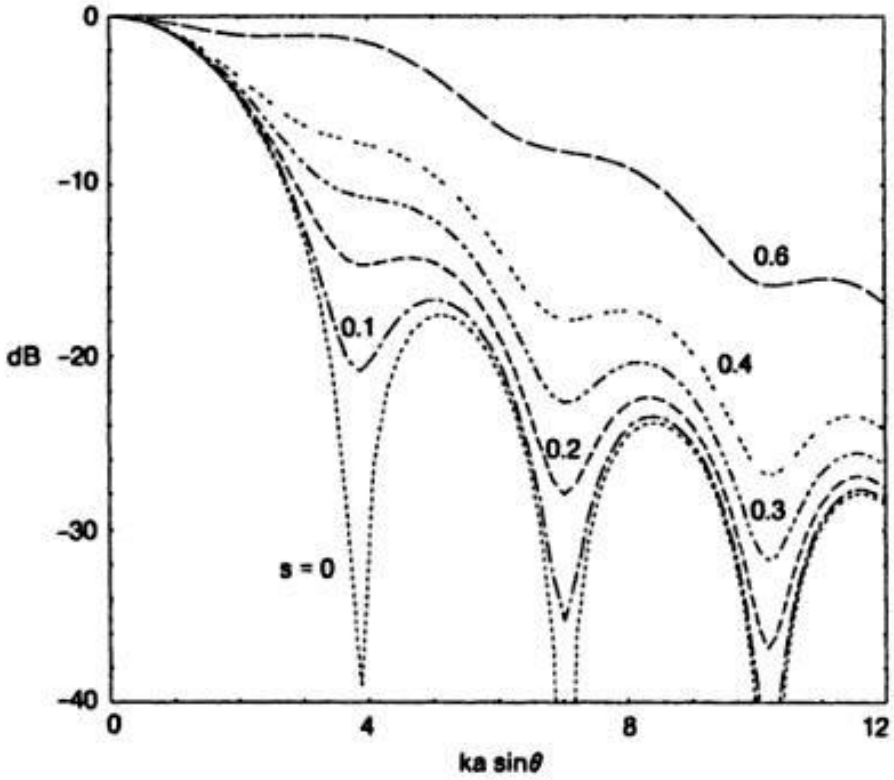

Fig. 24: E-plane universal pattern for a conical horn [source: A. D. Olver, P. J. B. Clarricoats, A. A. Kishk and L. Shafai, Microwave Horns and Feeds, IEE Electromagnetic Wave Series 39, IEEE Press 1994]

Substituting s = 0.1 into *Eq. 10*

$$L(s) = \left(0.8 - 1.71s + 26.25s^2 - 17.79s^3\right)$$

$$\mathrm{L}(0.1) = 0.87\mathrm{dB}$$

From *Eq. 34*

$$\text{Peak gain} = 10\log_{10}\left(\frac{C}{\lambda}\right)^2 - L(s)$$

$$12.55 = 10\log_{10}\left(\frac{C}{0.024}\right)^2 - 0.87$$

Giving a horn circumference, C = 0.1125 m, and a horn radius, R = 0.0179 m

The quadratic phase factor is given by

$$s = \frac{R^2}{2l\lambda} \qquad \textit{Eq. 36}$$

$$0.1 = \frac{(0.0179)^2}{2 \times l \times 0.024}$$

l = 0.0668 m

from geometry θ = 15.5°

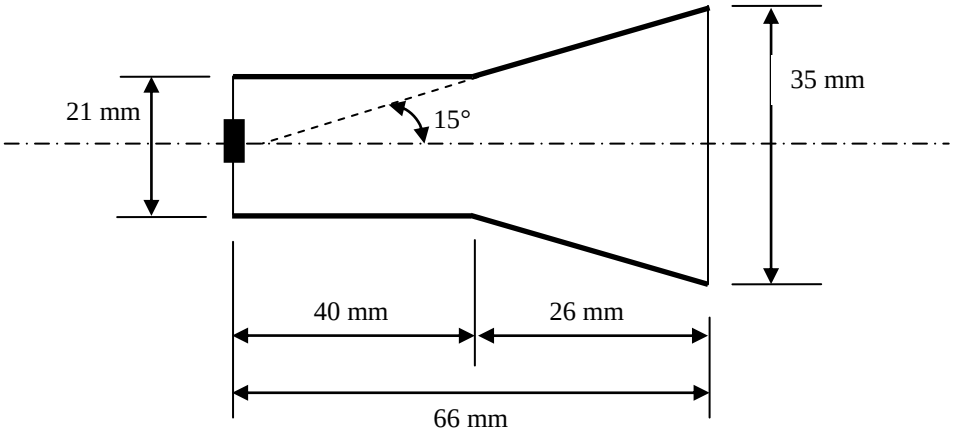

Fig. 25: Layout of conical horn

2.5.3.1 Phase Centre

The phase centre of a feed is the local centre of the spherical wavefront of the radiated field from the feed and is located along the axis of the horn. It is important to position the feed horn such that the focus of the reflector coincides with the phase centre.

There is no single phase centre for a horn: each plane of radiation has its own phase centre. It is therefore necessary to calculate an average value for the phase centre using formulae based on the predicted phase pattern for the horn. For a conical horn the universal phase centre curves shown in *Fig. 26* have been plotted in terms of the relative position of the phase centre as a function of the total length of the horn.

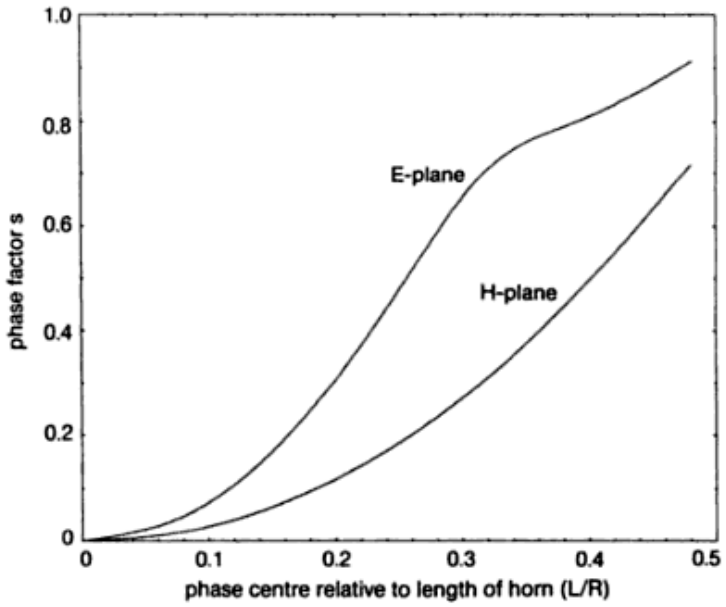

Fig. 26: Universal phase-centre curves for conical horns [source: A. D. Olver, P. J. B. Clarricoats, A. A. Kishk and L. Shafai, Microwave Horns and Feeds, IEE Electromagnetic Wave Series 39, IEEE Press 1994]

From *Fig. 23* and *Fig. 24* it was established that s = 0.1. Referring to *Fig. 26,* when s=0.1, L/R = 0.12 in the E-plane and L/R = 0.19 in the H-plane. Given the radius of the horn R = 0.0179m, in the E-plane the phase centre is positioned 2.15mm from the aperture and in the H-plane the phase centre is located 3.40mm from the aperture. Taking the average places the phase centre at 2.77mm from the aperture. This difference means that there is no single position for a conical horn to be positioned when used as a feed for a reflector. This feed misalignment causes a phase variation over the reflector aperture which results in a symmetrical increase in side lobes and filling of the antenna pattern nulls.

2.5.4 Prime focus antenna

The primary reflector is defined by a parabola rotated about its axis or paraboloid.

$$y^2 = ux \qquad \textit{Eq. 37}$$

From geometry we know that when y = 0.25, x = 0.042. This gives a value of u = 1.5. Therefore the reflective dish is defined by

$$y^2 = 1.5x$$

The inflatable antenna must then be constructed such that the parabolic reflector achieves the above geometry and the phase centre of the feed horn is positioned at the focal point of the reflector. *Fig. 27* shows the layout of the inflatable antenna used to achieve this.

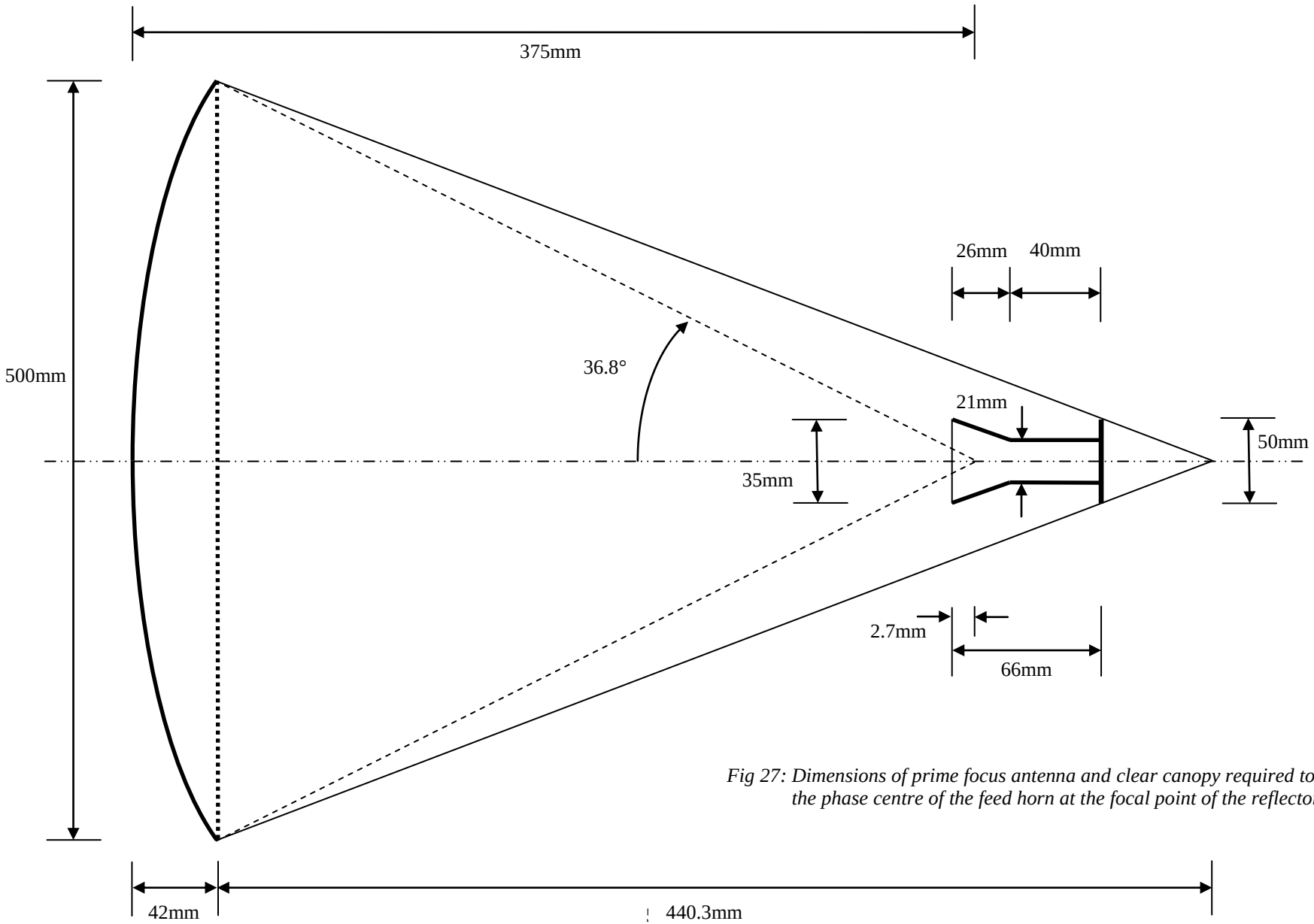

Fig 27: Dimensions of prime focus antenna and clear canopy required to position the phase centre of the feed horn at the focal point of the reflector

2.6 Cassegrain antenna and horn

To maintain consistency in testing the same primary reflector design that was used for the prime focus antenna will be used for the Cassegrain antenna. Ideally the diameter of the sub-reflector will be 10% of the diameter of main reflector to minimize aperture blockage. However, with the parameters specified, the flare angle of the horn would need to be so large that it would cause more aperture blockage than the sub-reflector.

The software package PCAAD was used to find a compromise between the size of the sub-reflector and the flare angle of the feed horn needed to efficiently illuminate the sub-reflector. *Fig. 28* shows the layout of the Cassegrain antenna and *Fig. 29* shows the dimensions of the conical horn feed horn for the antenna. This design will result in a poor antenna but the purpose of the investigation is to demonstrate the ability to manufacture an inflatable antenna that matches the performance of a rigid antenna not to evaluate the quality of the design.

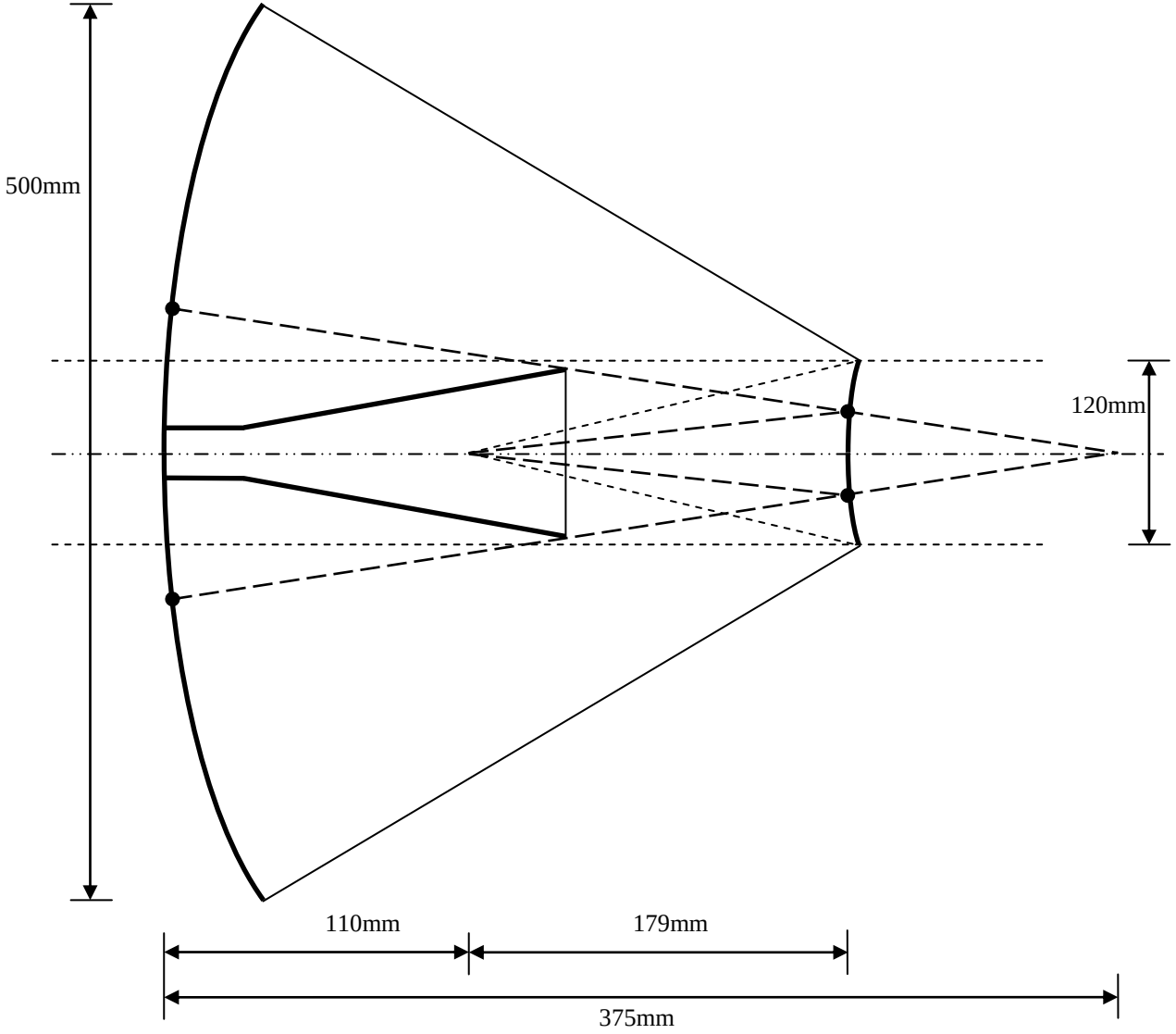

Fig 28: Layout of Cassegrain antenna

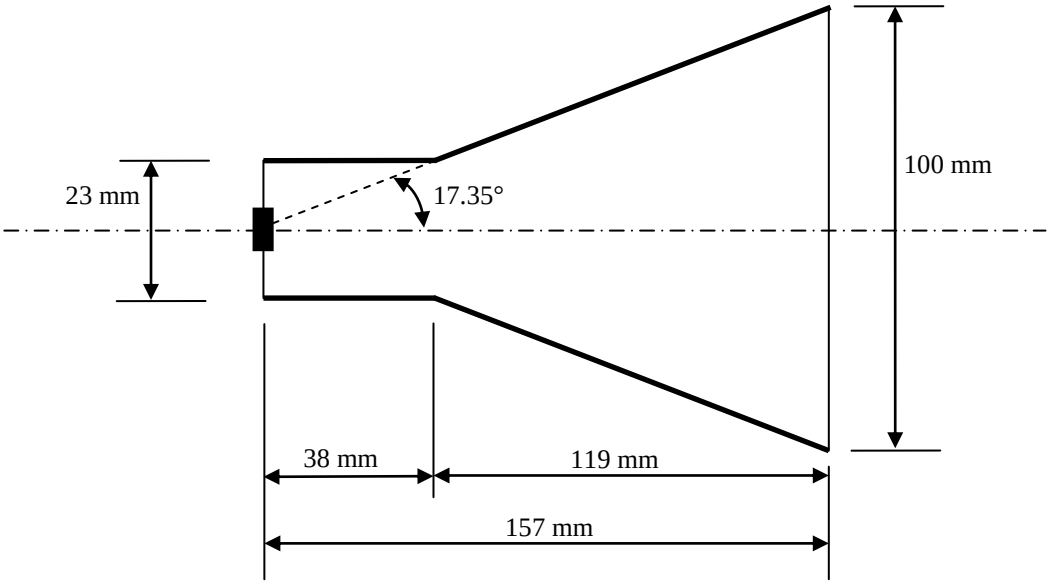

Fig. 29: Cassegrain antenna horn design

The above designs will be manufactured as both rigid and inflatable structures and their performance compared. The diameters of the circular waveguides in the two horns are 21mm and 23mm, respectively. For the dominant mode TE11 excitation, this diameter is large and can generate other higher order modes. If these higher order modes are excited this should be observed equally in the rigid and gossamer horns. Future work would include the design of a more efficient antenna. This thesis explores the ability to effectively replicate a rigid parabolic dish antenna and conical feed horn as a gossamer structure. Any reduction in efficiency due to a loss in shape and surface accuracy or dimensional stability will result in a decrease in gain, an increase in beamwidth, an increase in side lobe level, an increase in the number of side lobes and an increase in cross polar levels. These parameters will be used to measure of the stability of the inflatable antenna.

From the above calculations it can be seen that increasing the effective area of antenna has the greatest impact on its gain. *Table 2* presents a comparison of the theoretical gain for various apertures assuming the operating frequency and f/d are kept constant. From this comparison it can be seen why emphasis is placed on maximizing the diameter of the dish and why an inflatable antenna that can be stowed for transportation, and then inflated to a size greater than any existing portable antenna, is of interest.

F	12.5GHz	12.5GHz	12.5GHz
f/d	0.75	0.75	0.75
d	0.5m	1.0m	5.0m
f	0.375m	0.75m	3.75m
λ	0.024m	0.024m	0.024m
θ	36.8°	36.8°	36.8°
z_0	0.333m	0.667m	3.333m
r	0.416m	0.833m	4.16m
D (ideal)	36.3dB	42.34dB	56.32dB
ε_{ap}	0.8	0.8	0.8
G	35.35dB	41.37dB	55.34dB

Table 2: Comparison of antenna gain for various apertures

2.7 Microstrip patch

To further reduce the weight and stowed volume of the feed assembly and reduce the loading on the inflatable antenna it was decided to investigate using a microstrip patch to feed the gossamer feed horn. Replacing the waveguide with a microstrip patch reduces the weight and stowed volume of the feed assembly and significantly reduces the manufacturing cost of the antenna. This combination not only increases the portability of the system, it also makes it possible to carry multiple antennas. The ability to carry multiple antennas can be used to either provide redundancy at a single frequency or to carry antennas that operate at multiple frequencies.

The design of the microstrip patch is beyond the scope of this investigation. The microstrip patch requirements were given to Dr Kamran Ghorbani at RMIT University who designed a variety of patch antennas which were then manufactured by RMIT technician, Mr. David Welch.

The impedance characteristics and the radiation patterns of each patch were measured and the results compared. The patch with a resonant frequency closest to the design frequency

of 12.5 GHz and which demonstrated the lowest cross polar radiation was selected. The patch selected to feed the gossamer horn was a proximity patch with the dimensions shown in *Fig. 30*.

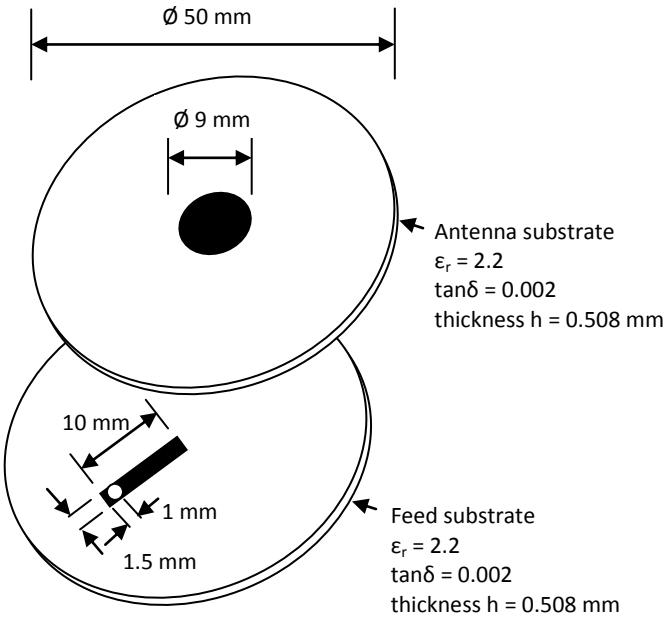

Fig. 30: Dimensions of microstrip patch

The proposed inflatable concept is not limited to the design presented; it can be applied to a variety of antenna designs, sizes and operating frequencies. The design presented is intended to demonstrate the concept, it is not necessarily the most efficient design, but an example to facilitate the direct comparison between the performance of an inflatable and rigid antenna. The testing procedure is presented in *section 3* and the results are presented in *section 4*.

3 Fabrication Methodology and Measurement Set-Up

3.1 Antenna design to be tested

This chapter presents the methodology used to construct and test the inflatable antenna presented in *section 2*. The antenna design presented will be manufactured and tested to demonstrate that it is possible to construct an inflatable antenna that provides the shape accuracy and dimensional stability required for portable direct satellite communication under terrestrial conditions. To validate this, the performance of an inflatable antenna will be compared to the performance of an identical rigid antenna under terrestrial conditions.

The inflatable antenna concept presented is a dual reflector antenna but before this configuration can be tested it is important to understand the behaviour of each of the components. As such the testing will be conducted in the following stages.

1. Microstrip patch
2. Gossamer conical feed horn for prime focus antenna fed by microstrip patch
3. Inflatable prime focus antenna supported by rigid mount fed by gossamer horn
4. Inflatable prime focus antenna supported by inflatable torus fed by gossamer horn
5. Gossamer conical feed horn for Cassegrain antenna fed by microstrip patch
6. Inflatable Cassegrain antenna supported by rigid mount fed by gossamer horn
7. Inflatable Cassegrain antenna supported by inflatable torus fed by gossamer horn

Basic antenna design principles were used to design the antenna and feed assembly. Complete calculations are included in *section 2.4* and the main parameters are listed below.

Operating frequency 12.5GHz

$$\lambda = 0.024m.$$

$$\frac{f}{d} = 0.75$$

$$d = 0.5m$$

$$f = 0.375m$$

The surface of the reflector dish is defined by rotating a parabola about its axis. The dish is defined by

$$y^2 = 1.5x$$

For complete calculations refer to *section 2.4.2*. *Fig. 19* showing the prime focus antenna dimensions is reproduced below.

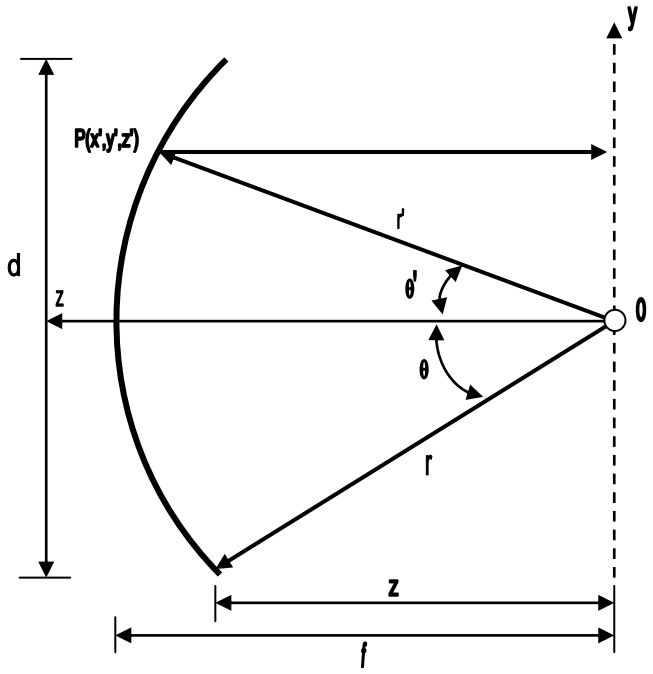

Fig. 19: Primary focus antenna design (reproduced from section 2.4.2)

A feed horn was designed to feed this antenna in a prime focus configuration. For complete calculations refer to *section 2.4.3*. *Fig. 25* showing the dimensions of the conical feed horn used to feed the prime focus antenna is reproduced below.

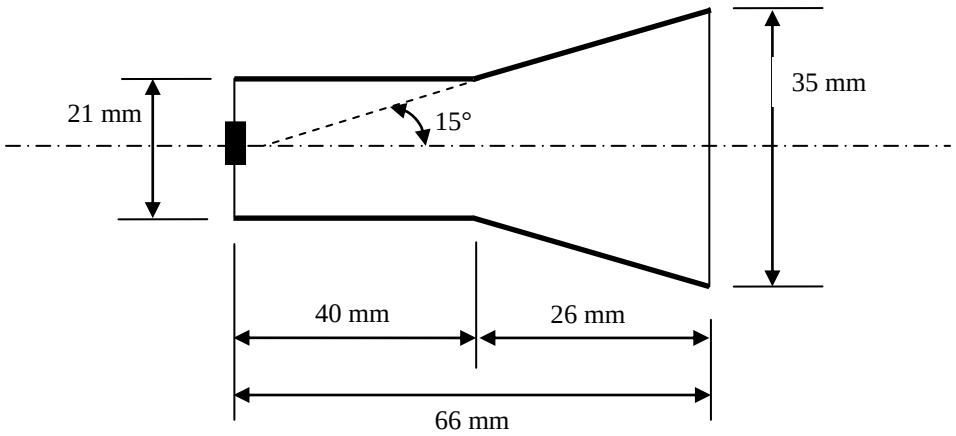

Fig. 25: Prime focus antenna horn design (reproduced from section 2.4.3)

A feed horn was designed to feed the Cassegrain antenna. For complete calculations refer to *section 2.4.5*. *Fig. 29* showing the dimensions of the conical feed horn used to feed the Cassegrain antenna is reproduced below.

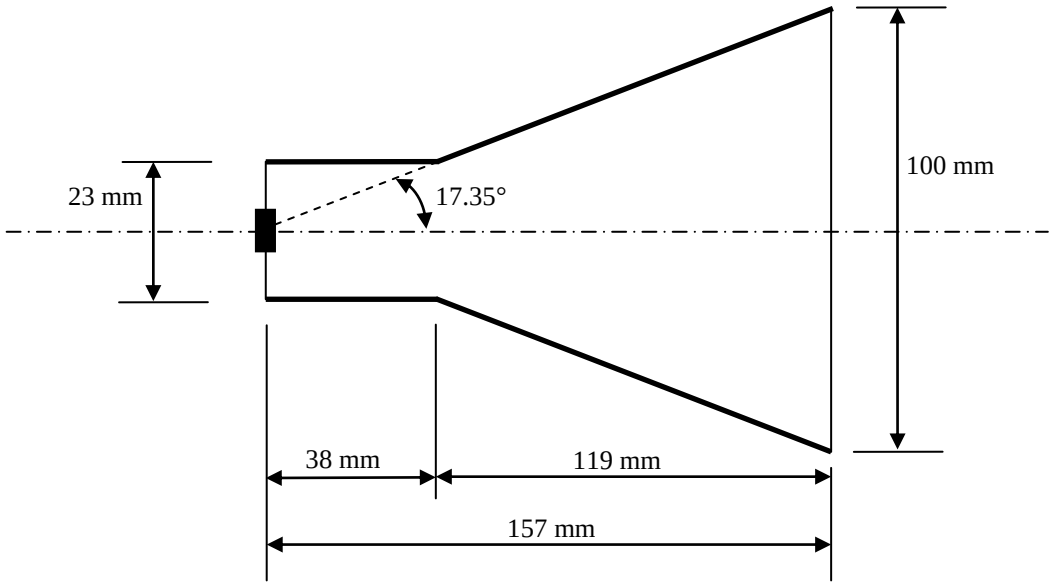

Fig. 29: Cassegrain antenna horn design (reproduced from section 2.4.5)

3.2 Simulation

The patch and horns were modelled using CST Microwave Studio. The author would like to thank Dr Christophe Granet of CSIRO's Electromagnetics and Antennas Group for generating the models and results. The simulation results are presented in *section 4.1* and an analysis is presented in *section 5.1*.

The patch was simulated and an impedance plot generated to confirm that it should resonate at the desired frequency. The prime focus antenna feed horn was then simulated. To compare the effects of feeding the horn with a patch instead of a standard waveguide input, the horn was simulated with both a standard TE11 circular-waveguide feed and the microstrip patch. Impedance and radiation plots were generated.

The analysis was repeated for the Cassegrain antenna feed horn. The horn was simulated with both a standard TE11 circular-waveguide feed and the microstrip patch. Impedance and radiation plots were generated.

To evaluate the performance of the inflatable horn and the inflatable antenna the impedance and radiation characteristics will be compared to those of identical rigid structures. It is known that pillowing, and aperture blockage adversely affects the performance of a reflector antenna. To facilitate the interpretation of the measured results I generated a series of simulations using the antenna simulation software, GRASP, progressing from a perfect paraboloid, to one with ribs but no pillowing, and then to one with ribs and pillowing. I generated a similar series of simulations using GRASP progressing from no struts supporting the feed horn, to a single strut supporting the feed horn, and then three struts supporting the feed horn. These results are presented in *section 4.1.6.*

3.3 Material testing

3.3.1 Structural properties

The clear thin film and the metalized thin film used to construct the gossamer feed horn and the inflatable antenna was donated by VISIPAK. The material specifications for the two thin films were not available but it is known that both thin films were polyesters. It is known that the clear thin film has a layer of Linear Low Density Polyethylene (LLDPE) on one side of the polyester core and it is known that the second film was metalized with Aluminium by vapour deposition and then sandwiched between two layers of LLDPE.

Thin films are available commercially in thicknesses from 12 um to 350 um and their properties can be manipulated with a variety of additives, treatments and coatings. The most common polyester thin film is Polyethylene Terephthalate (PET). PET is produced by DuPont Teijin Films under a variety of trade names including Mylar [41].

The material properties of the two thin films that would be used to construct the inflatable antenna and feed horn were measured and compared to the properties stated for the most common Mylar thin film, Type A 48-1400 Gauge as specified by DuPont [41]. The materials were weighed and the thickness of the two materials was measured using a micrometer with a tolerance of ±0.1 μm. A series of five tensile tests were conducted on

each material and the average taken. These tests measured the yield strength of the material, the tensile strength and the elongation at break. For results refer to *section 4.2.1*.

3.3.2 Electromagnetic properties

The electromagnetic properties of the clear thin film and the metalized thin film were tested using a Vector Network Analyser and the arrangement shown in *Fig. 30*. Any material used for a canopy must transmit a signal without loss at the operating frequency whilst a material used as a reflective surface must reflect a signal without loss at the operating frequency. A signal was generated in Port 1 and received in Port 2. The material under test was sandwiched between two waveguides connected to the respective ports with coaxial cable. The intended operating frequency of the inflatable antenna is 12.5 GHz so measurements were made at frequencies between 12 GHz and 13 GHz at increments of 0.5 GHz. For results refer to *section 4.2.2*.

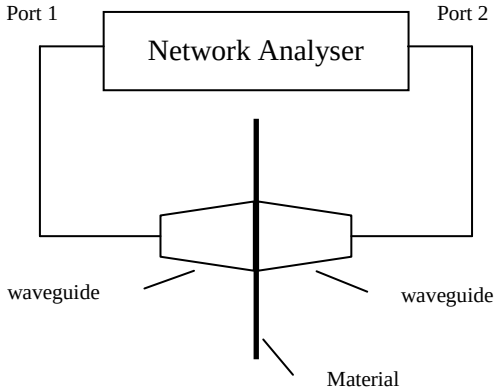

Fig. 31: Testing electromagnetic properties using network analyser

3.4 Microstrip patch

To further reduce the weight and stowed volume of the feed assembly and reduce the loading on the inflatable antenna it was decided to investigate using a microstrip patch to feed the gossamer feed horn. The use of a microstrip patch also significantly reduces the manufacturing cost of the antenna.

The design of the microstrip patch is beyond the scope of this investigation. The microstrip patch requirements were given to Dr Kamran Ghorbani at RMIT University who designed

a variety of patch antennas which were then manufactured by RMIT technician, Mr. David Welch.

I then tested the impedance characteristics of each patch using a Network Analyser and measured the radiation characteristics of each patch in the anechoic chamber at RMIT. The RMIT anechoic chamber is XX m long, XX m wide and XX m high, allowing far field measurements to be recorded. The test antenna was mounted on a turntable such that the phase centre of the antenna was positioned at the centre of the turnstile. The height of the test antenna and the source were aligned as shown in *Fig. 32.* During the testing procedure the turnstile was rotated at a constant velocity and measurements were recorded at 1° intervals using a network analyser. Co-polar and cross polar measurements were taken by rotating the source antenna and repeating the procedure. This method and procedure were repeated to test the horn and the parabolic reflector.

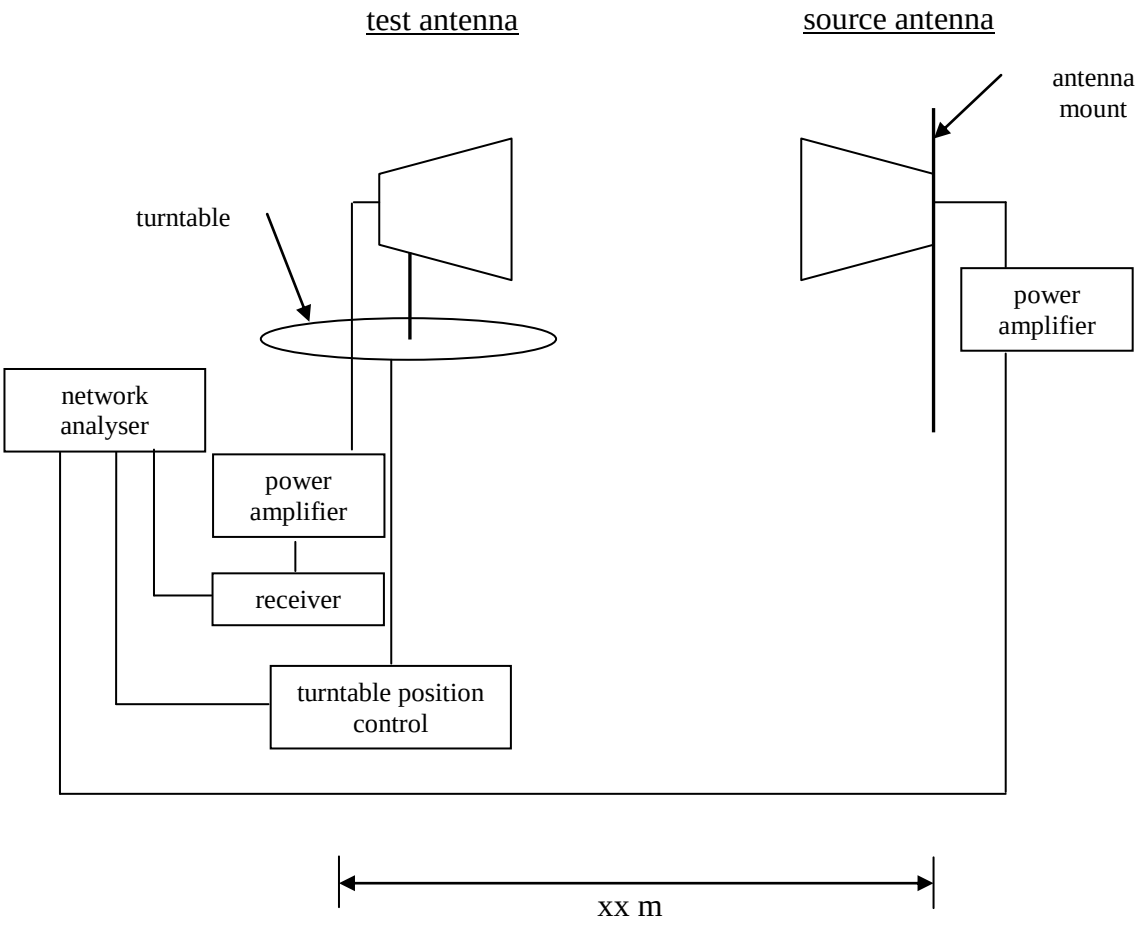

Fig. 32: Schematic of test setup in anechoic chamber

The patch with a resonant frequency closest to the design frequency of 12.5 GHz and which demonstrated the lowest cross polar radiation was then selected. The patch selected was a proximity fed patch. The dimensions of the patch are presented in *section 2.4.6* and reproduced below in *Fig. 32*. The patch is shown in *Fig. 33*.

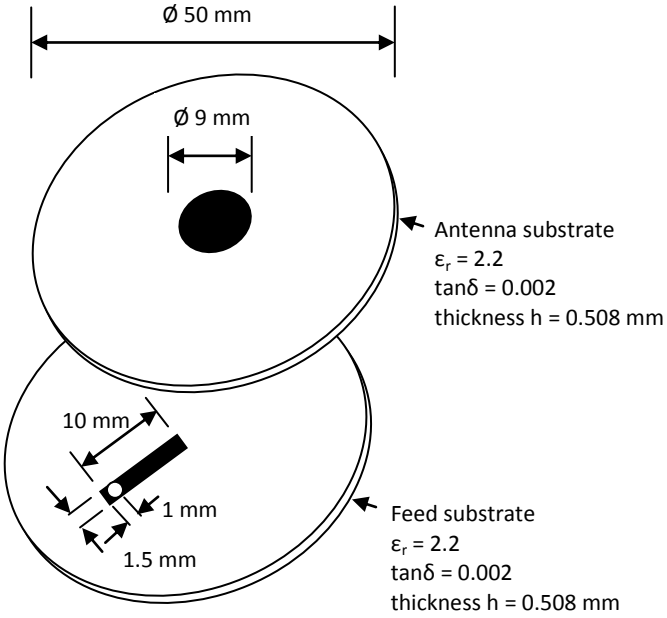

Fig. 30: Dimensions of microstrip patch (reproduced from section 2.4.6)

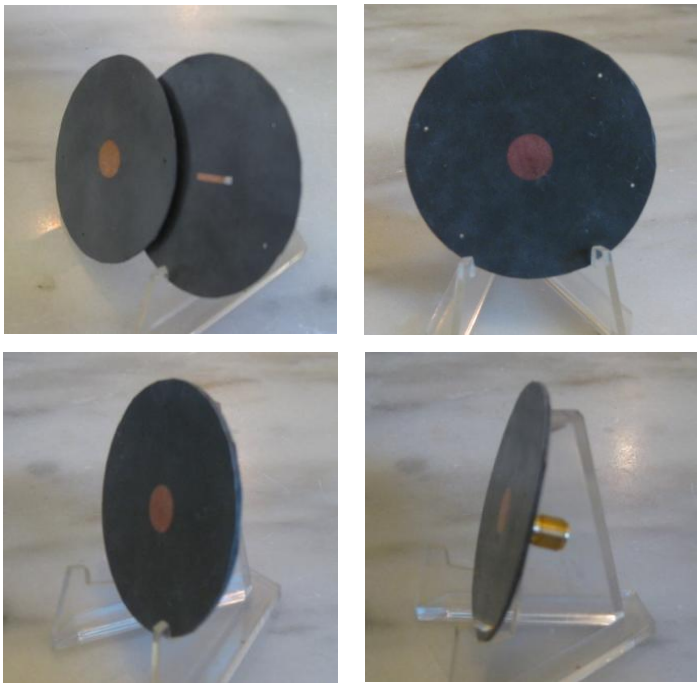

Fig. 33: Microstrip patch

3.5 Feed horn

After demonstrating that the thin film selected has the structural and electromagnetic qualities needed to construct an antenna, it must then be demonstrated that an antenna can be manufactured from this material such that it matches the performance of a rigid antenna.

A rigid horn was machined from Aluminium as per the design. I would like to acknowledge RMIT technician, Mr. David Welch, for the manufacture of the Aluminium feed horn. The Aluminium feed horn is shown in *Fig. 34*.

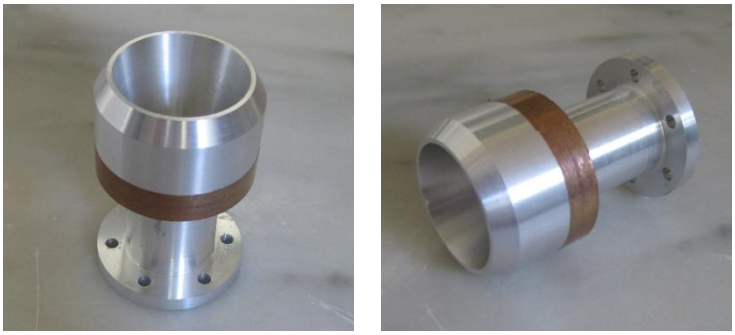

Fig. 34: Aluminium feed horn

As the antenna is being constructed from a flat, dimensionally stable gossamer material, the shape is established using pattern making techniques and seaming the panels together to form an enclosed structure which can then be inflated. For components such as the feed horn and the canopy, which are constructed from tubular or conical sections having curvature in one direction, a flat pattern can be easily produced using basic geometry. Despite the simplicity of the geometry care must be given to the accuracy of the seam allowance calculation and the cutting precision.

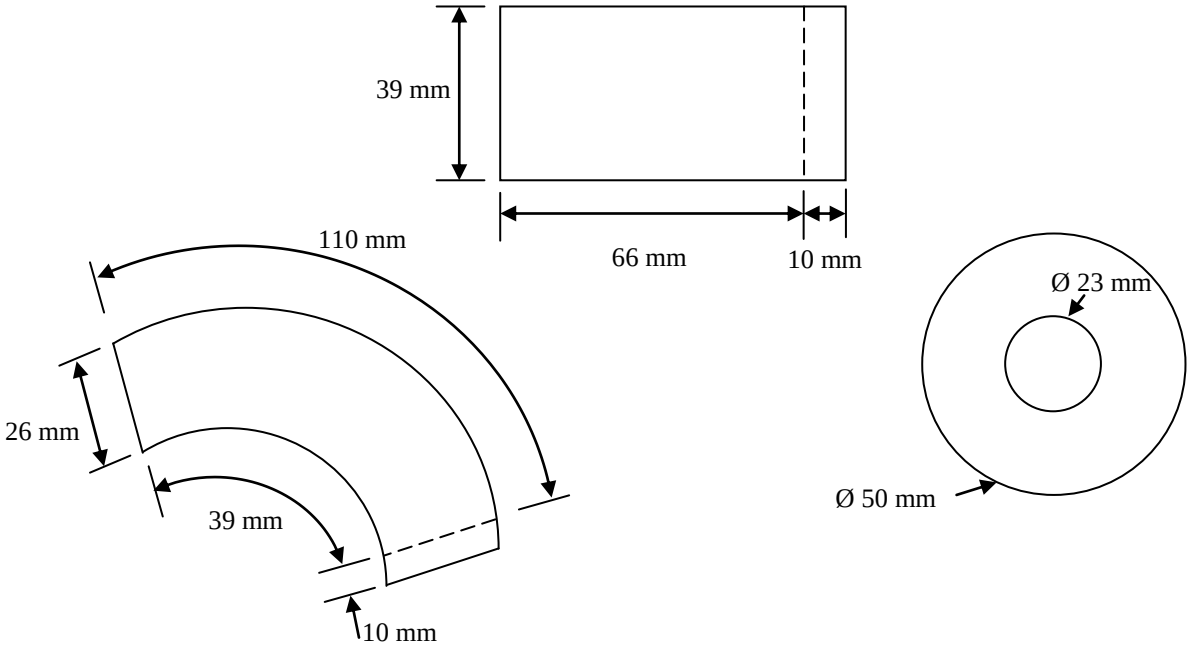

Fig. 35: Patterns for prime focus antenna feed horn components

Fig. 36: Cutting pattern pieces for prime focus antenna feed horn components

Once a pattern has been produced for each of the components the pieces can be connected and the components assembled. The flexible nature of the material can impede the accurate assembly of the shaped components. It was found that using a plug assisted in the assembly of the components. *Fig. 36* shows how the use of a plug can aid the accurate assembly of the individual components.

Fig. 37: Assembly of individual horn components with the assistance of shaped plugs

To reduce the stiffness of the seams and minimize surface irregularity a highly adhesive transfer tape was used to seal the seams. Transfer tape is a pressure sensitive tape pre-applied to a special release liner. As the tape is applied to the first surface the release liner is removed ready for the second surface to be connected and pressure applied. As it has no backing it is highly flexible and can bond gossamer materials without causing localized stiffening. Transfer tapes are available with a variety of adhesive properties including high tack, high temperature resistance, exceptional moisture or solvent resistance and adhesion to low surface energy plastic. *Fig. 38* shows the specialist applicator used to apply the transfer tape.

Fig. 38: Transfer tape applicator

Tape is strongest in plane or shear mode and weakest in tensile mode. *Fig. 39* shows the technique used to seal the individual components of the feed horn. It can be seen that each of the components are connected using lap joints and so all seams are loaded in shear.

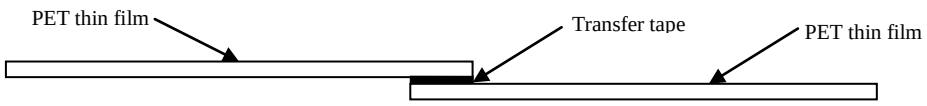

Fig. 39: Lap joint used to assemble feed horn components

Fig. 40: Individual components of feed horn

Once the individual components have been assembled they need to be connected to form the feed horn. Because of the angle of the joints it was impractical to tape the joints. A variation on heat welding was used to connect the components.

Heat welding uses a combination of temperature and pressure to, melt two thermoplastic layers, force them to combine, and then allow the combined layer to harden to an extremely strong bond. Heat welding can be used to produce bonded joints with mechanical properties that approach those of the base material. The PET thin film has a layer of Linear Low Density Polyester (LLDPE), which melts at approximately 80°C, allowing it to be heat welded.

A hot glue gun was used to heat weld the horn components together. The glue is raised to a temperature which partially melts the LLDPE layer and combines with it to form a robust bond. This technique produces a bond which is adequate for testing the prototype horn.

Fig. 41: Hot glue gun used to assemble feed horn pieces

Fig. 42 shows the fully assembled gossamer horn and the Aluminium horn.

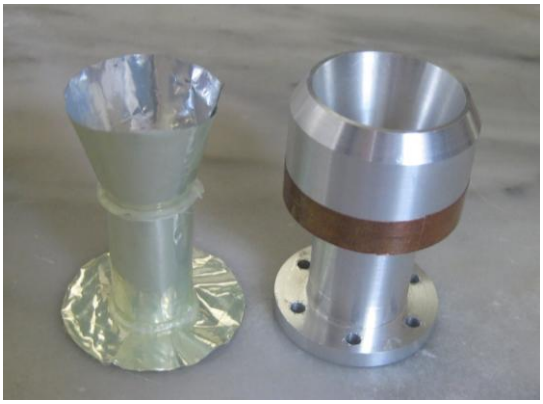

Fig. 42: Assembled gossamer horn with Aluminium horn

Once the horn has been assembled the microstrip patch is attached with transfer tape. Care must be taken that the resonating patch is located in the centre of the horn and that the seal is complete. Any gaps between the microstrip patch and the horn will result in interference. The microstrip patch is attached to the Aluminium horn using the same method. *Fig. 43* shows the gossamer horn with the microstrip patch and *Fig. 44* shows the Aluminium horn with the microstrip patch. Before testing both horns were weighed.

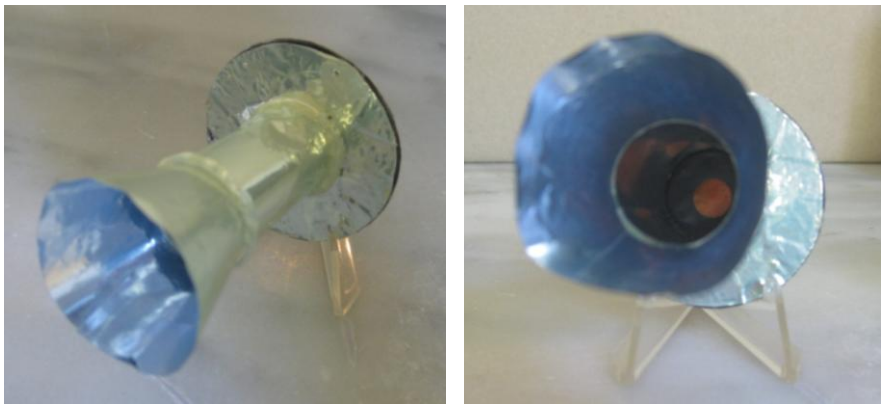

Fig. 43: Gossamer horn with microstrip patch

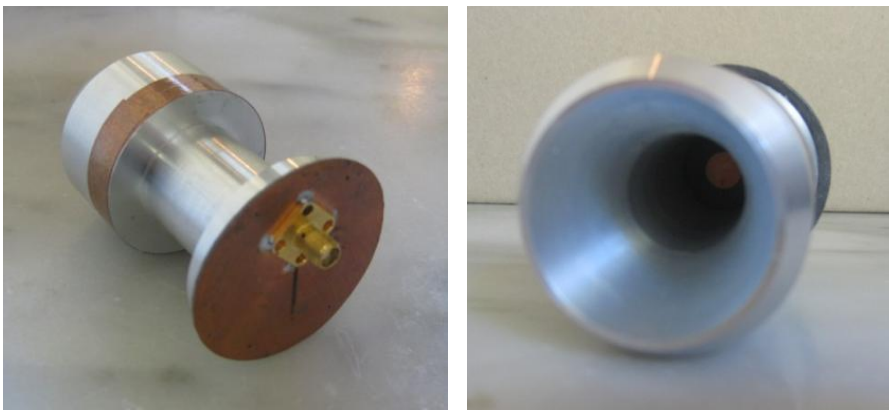

Fig. 44: Aluminium horn with microstrip patch

The impedance characteristics of the Aluminium horn were tested and compared to the simulated results to measure how well the system is matched and verify that a microstrip patch can be used to feed a conical horn. The impedance characteristics of the gossamer horn were then measured and compared to those of the Aluminium horn. The impedance characteristics of the gossamer horn were also tested after the horn had been crushed and then returned to its original shape, to simulate a horn that had been stowed and then deployed.

Once it was confirmed that a microstrip patch can be used to feed a conical horn without affecting the impedance characteristics the radiation patterns of the horns were measured and compared.

The rigid Aluminium horn and the gossamer horn fed by the same microstrip patch were tested in the anechoic chamber at RMIT at 12.576 GHz and the results normalized with respect to a standard gain horn. The tests were conducted in an anechoic chamber as detailed in s*ection 3.4* and shown in *Fig. 32* to eliminate the impact of wind. The antenna system is ultimately required to operate reliably under all environmental conditions; however before the impact of environmental conditions such as wind and rain can be considered the impact of the material and the structural design must be fully understood.

The radiation patterns for both horns were measured in the E-plane, H-plane, 45-plane, E-cross pole, H-cross pole and 45-cross pole.

3.6 Parabolic reflector

After demonstrating that the gossamer conical feed horn fed by a microstrip patch matched the performance of the Aluminium horn of the same design it was possible to progress to the testing of a parabolic reflector. As the characteristics of the gossamer horn were now defined it will be used as the feed for the parabolic reflector.

The shape of the parabolic reflector is generated by forming an enclosed environment between the reflector and a canopy and then pressurising it.

The use of a pressurised structure distributes the load through the skin. Unless the structure is constrained the natural tendency is for the structure to deform until the stress is evenly distributed. The parabolic reflector and clear canopy are connected at a sharp angle. Unless this connection is supported the internal pressure will act to round out this connection and creases will form. An exaggerated simulation of what would happen to the antenna if the internal pressure was increased and there was no rim support is shown in *Fig. 45*. This simulation does not show the creases around the rim because the material in the simulation has elasticity and so will stretch rather than crease. In the final antenna the connection between the reflector and the canopy, which is also the circumference of the reflector, will be supported by an inflatable torus. To eliminate the torus as a variable and investigate the performance of the parabolic reflector the circumference was supported by a rigid frame.

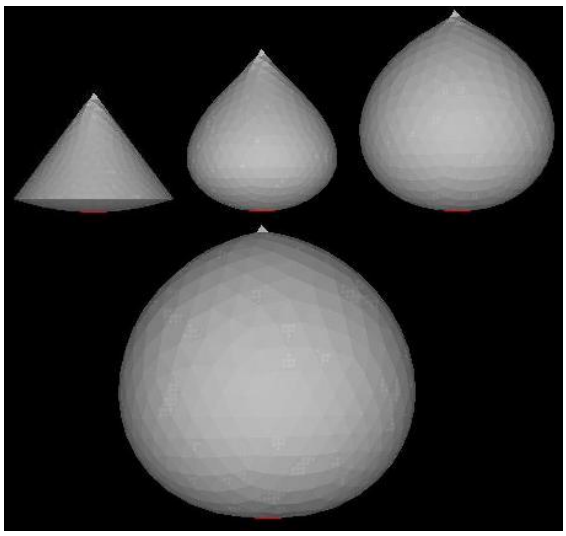

Fig. 45: Simulation of increasing antenna pressure without rim support

A cone was selected as the shape for the canopy because of its dimensional stability and the way this shape transfers the load in the skin to the rim support. Forming a cone from thin film pre-stresses the skin and gives the final structure good dimensional stability. As the conical canopy has curvature in only one dimension it was assumed that it performed in the same way as the conical horn. The increase in scale does introduce some pillowing and limited modelling was performed to understand how much allowance needs to be made for the movement in the feed or sub-reflector due to this pillowing. It was shown that a conical canopy at low pressure with a good rim support experienced minimal pillowing. It was decided not to make allowances for any pillowing in the canopy in the initial testing. However, it is recommended that this be reviewed in any further testing.

To test if it is possible to construct a parabolic reflector from thin film the radiation characteristics of the gossamer reflector were measured and compared to the radiation characteristics of a rigid parabolic reflector of the same design to facilitate the assessment of the shape accuracy.

Basic antenna design principles were applied then replicated using thin film materials in such a way that the integrity of the design is maintained. The surface of the reflector dish is defined by rotating a parabola about its axis. The dish is defined by

$$y^2 = 1.5x$$

A plug was machined to aid in the construction of the thin film reflector. The plug was also used to manufacture a rigid parabolic dish from composite materials. A woven pre-preg was laid over the reflector plug and cured in an autoclave. This was done with the assistance of RMIT technician Terry Rosewarne. The reflector plug and the composite dish are shown in *Fig. 46*. The composite dish was then coated with Aluminium foil to make it RF reflective.

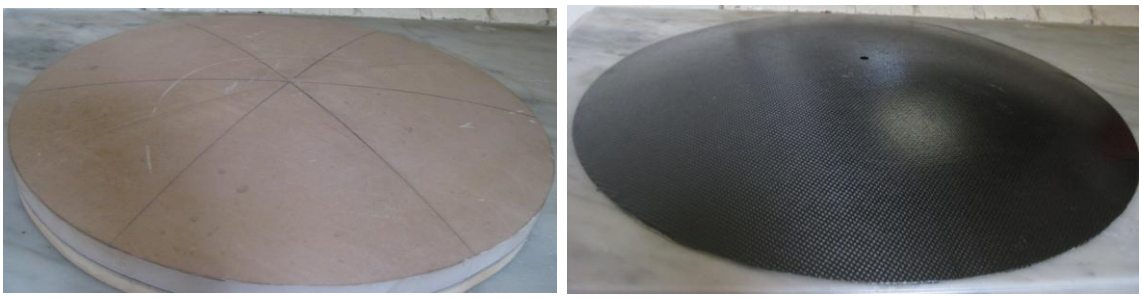

Fig. 46: Reflector plug and rigid composite reflector dish manufactured using reflector plug

The radiation characteristics of the rigid reflector fed by the gossamer horn were tested in the anechoic chamber. An adjustable platform was used to support the dish and the horn. *Fig. 47* shows the platform with the rigid dish and gossamer horn in the anechoic chamber. The platform facilitated the adjustment of the horn height and distance from the dish. The radiation patterns were measured in the E-plane, H-plane, 45-plane, E-cross pole, H-cross pole and 45-cross pole.

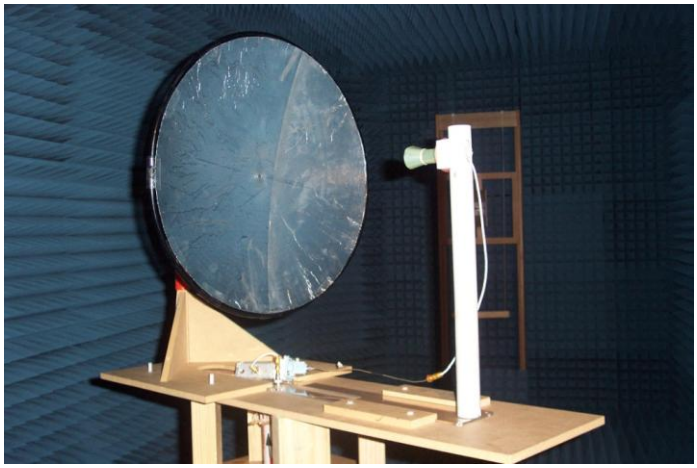

Fig. 47: Rigid reflector dish fed by gossamer horn in anechoic chamber

To construct the gossamer parabolic reflector, a surface with curvature in two directions must be constructed from a flat, dimensionally stable material. This was achieved using a gored construction.

A Computer Aided Design (CAD) program was used to generate a three dimensional model of the antenna. This program was then used to generate a flat pattern of the reflector. To produce the desired curvature a minimum number of gores are required. The more gores that are used the more curvature that can be imparted; on the other hand the seams create both surface and shape inaccuracies that reduce the performance. It was found that six gores was the best compromise between shape and surface accuracy. A seam allowance was added around the circumference of the reflector to allow the reflector to be attached to a rigid frame for testing. *Fig. 48* shows one of six identical gores used to construct the reflector.

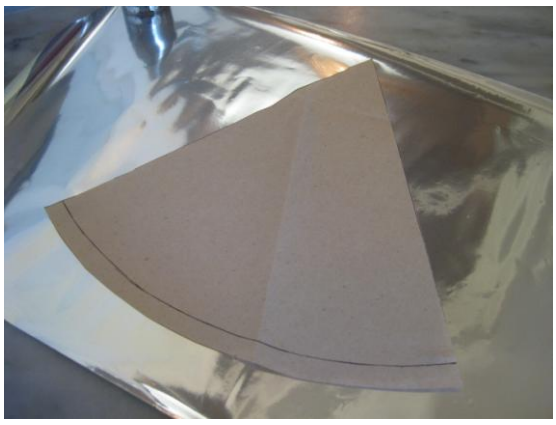

Fig. 48: Pattern for one of six identical gores used to construct the gossamer reflector dish

Six identical gores were cut from Aluminized thin film taking care to maintain cutting precision. To provide the maximum flexibility the gores were assembled using transfer tape. Tape is strongest in plane or shear mode and weakest in tensile mode. *Fig. 49* shows the technique used for taping the gores together to form the parabolic reflector. It can be seen that each of the panels are connected using lap joints and so all of these seams are loaded in shear.

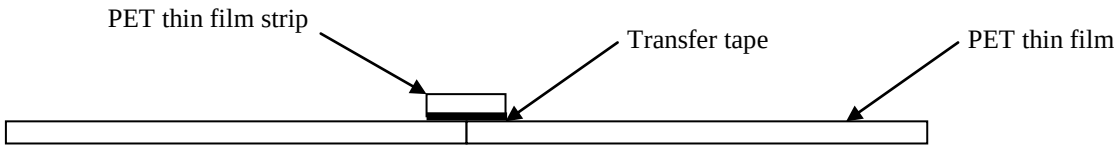

Fig. 49: Lap joint used to assemble gores in parabolic dish reflector

As with the gossamer horn a plug was used to assist in the assembly of the gossamer reflector. The plug was marked to indicate the desired position of the gores. The plug helped to align the gores and apply the tape to curved seams. *Fig. 50* shows how the use of a plug can aid the accurate assembly of the individual components.

Fig. 50: Assembly of gossamer reflector

The internal pressure of the inflatable antenna acts on the parabolic reflector to form the curved surface. To generate this internal pressure an enclosed environment is formed between the parabolic reflector and the clear canopy. In the case of the prime focus antenna the canopy will support the feed horn and in the Cassegrain design the canopy will support the sub-reflector. *Fig. 27* showing the dimensions of the conical canopy used to position the phase centre of the feed horn at the focal point of the reflector has been reproduced from *section 2.4.4*. *Fig. 51* shows the flat pattern for the canopy. A seam allowance is added to form the cone and to attach the cone to the reflector. The position of the patch is marked on the cone to facilitate the alignment of the horn.

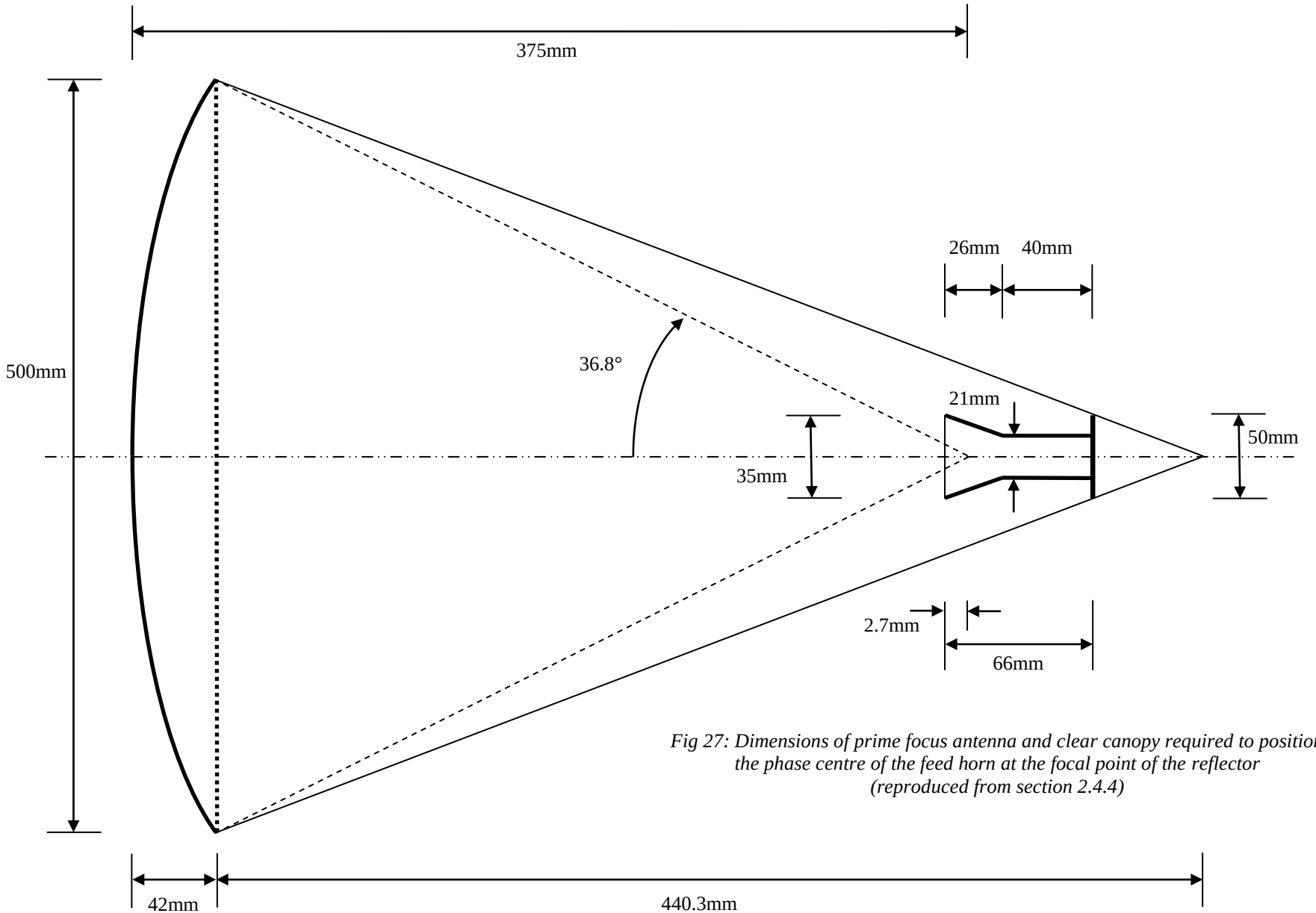

Fig 27: Dimensions of prime focus antenna and clear canopy required to position the phase centre of the feed horn at the focal point of the reflector (reproduced from section 2.4.4)

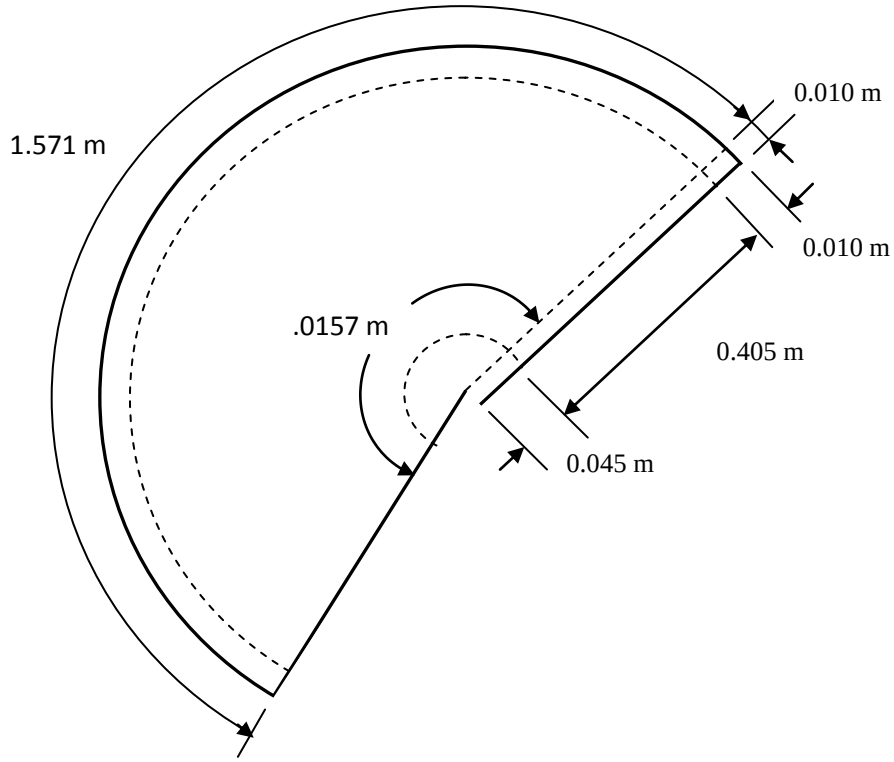

Fig. 51: Clear canopy pattern

The clear canopy is cut from clear thin film and assembled using transfer tape. *Fig. 52* shows the flat pattern of the cone and the clear polyester thin film.

Fig. 52: Conical canopy pattern and clear polyester thin film

To help position the feed horn accurately the cone was marked with the correct position and a connector was added to the feed horn. *Fig. 53* shows the conical feed horn with the adapter and the feed horn installed in the apex of the clear canopy.

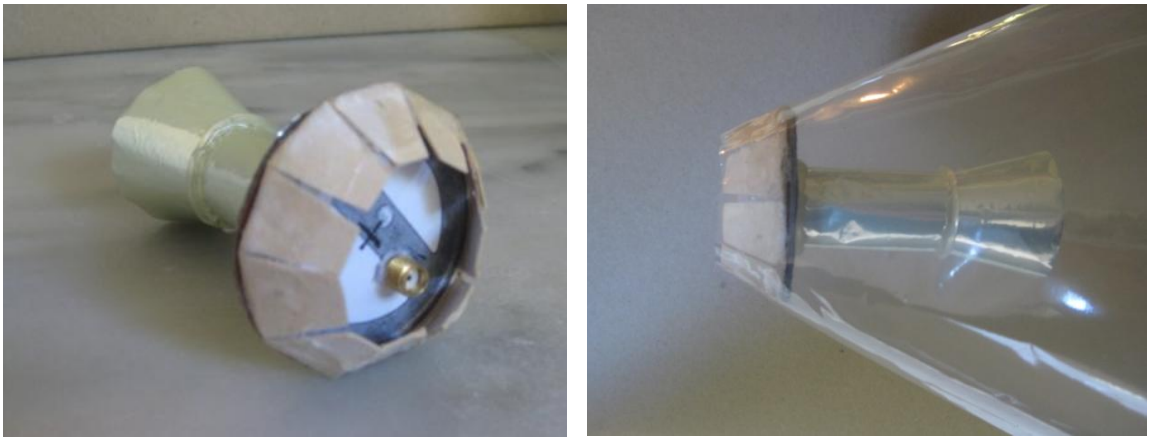

Fig. 53: Conical feed horn and adapter. Conical feed horn installed in the apex of the clear canopy

When a thin film vessel is pressurized the skin deforms until it reaches a state of equilibrium. The antenna was inflated using a compressor connected to a small valve at the edge of the dish. The pressure was controlled using a regulator. The antenna required a large volume of air but operates at just above atmospheric pressure. A pressure regulator and cutoff switch was used to achieve the desired pressure but once inflated the antenna could maintain its shape.

The parabolic reflector and clear canopy are connected at a sharp angle. Unless this connection is supported the internal pressure will act to round out this connection and creases will form. In the final antenna the connection between the reflector and the canopy, which is also the circumference of the reflector, will be supported by an inflatable torus. To eliminate the torus as a variable and isolate the parabolic reflector the circumference was supported by a rigid frame. The prime focus antenna mounted on the rigid frame can be seen in *Fig. 54*. *Fig. 54* also shows a template of the desired reflector shape being held next to the inflated antenna. As any contact would cause the reflector to conform to the shape of the template care was taken not to make contact with the reflector.

Fig. 54: Inflatable antenna with gossamer horn mounted on rigid frame

The radiation characteristics of the prime focus inflatable antenna fed by the gossamer horn were tested in the anechoic chamber as detailed in s*ection 3.4* and shown in *Fig. 32*. The antenna was supported by a rigid frame and rotated about the axis of the dish. *Fig. 55* shows the inflatable antenna in the anechoic chamber. The radiation patterns were measured in the E-plane, H-plane, 45-plane, E-cross pole, H-cross pole and 45-cross pole.

Fig. 55: Inflatable antenna with gossamer horn mounted on rigid frame in anechoic chamber

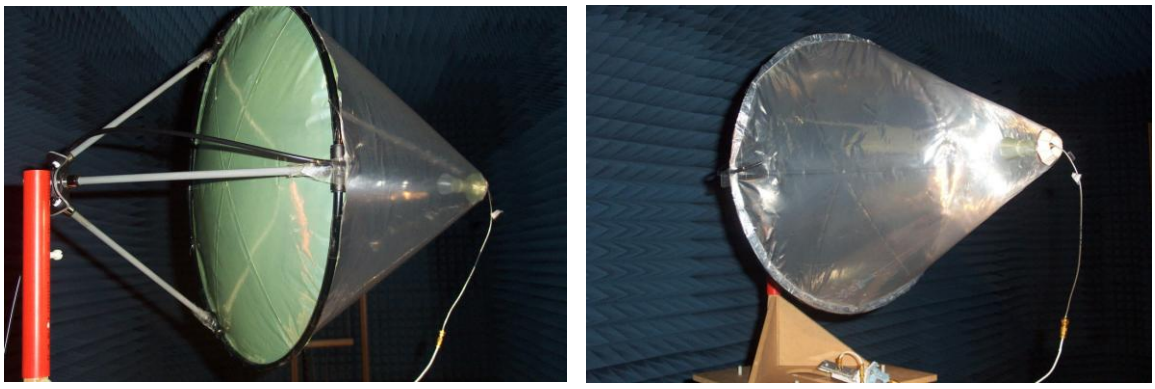

Fig. 56: Inflatable antenna with gossamer horn mounted on rigid frame in anechoic chamber

The reflectors were both tested at 12.5GHz using an inflatable feed horn at the focal point. The test was conducted in an anechoic chamber to eliminate the impact of wind. It will be necessary for the final antenna system to operate reliably under all environmental conditions however this test is concerned with the ability to manufacture the reflector dish.

The rationale for this investigation is to increase the portability of direct satellite communication systems. As such, the weight and stowed volume of the system are pivotal. The weight of the inflatable antenna and gossamer horn were measured and compared to the weight of the rigid antenna and gossamer horn. Both antennas were weighed without the support structure. The results are presented in *section 4.4*.

The gossamer antenna and feed horn were folded and stowed and the volume calculated. *Fig. 57* shows the stowed antenna.

Fig. 57: Inflatable antenna with gossamer horn stowed for travel

The results from this analysis are presented in *section 4* and an analysis of the results is presented in *section 5*.

4 Results

All the simulated and measured results collected during this investigation are presented in this section. The methods and procedures used to collect the data presented in this section have been defined in *section 3*. An evaluation of the results is presented in *section 5*.

4.1 Simulation

The following simulations were generated:

- microstrip patch
- prime focus antenna conical feed horn with patch feed and waveguide feed
- prime focus antenna fed by feed horn with patch feed and feed horn with waveguide feed
- Cassegrain antenna conical feed horn with patch feed and waveguide feed
- Cassegrain antenna fed by feed horn with patch feed and feed horn with waveguide feed

4.1.1 Microstrip patch

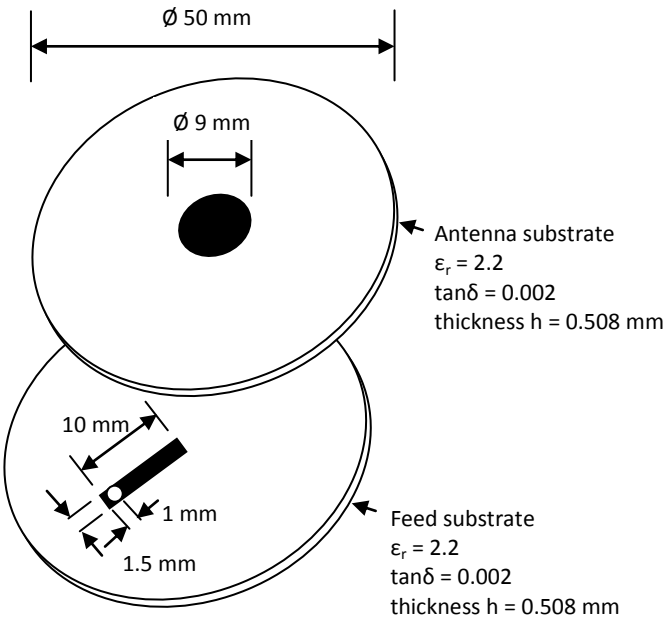

Fig. 31: Dimensions of microstrip patch (reproduced from section 2.4.6)

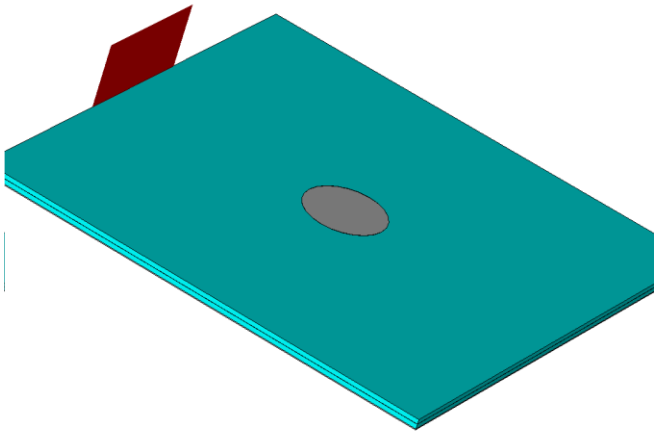

Fig. 58: Simulated microstrip patch

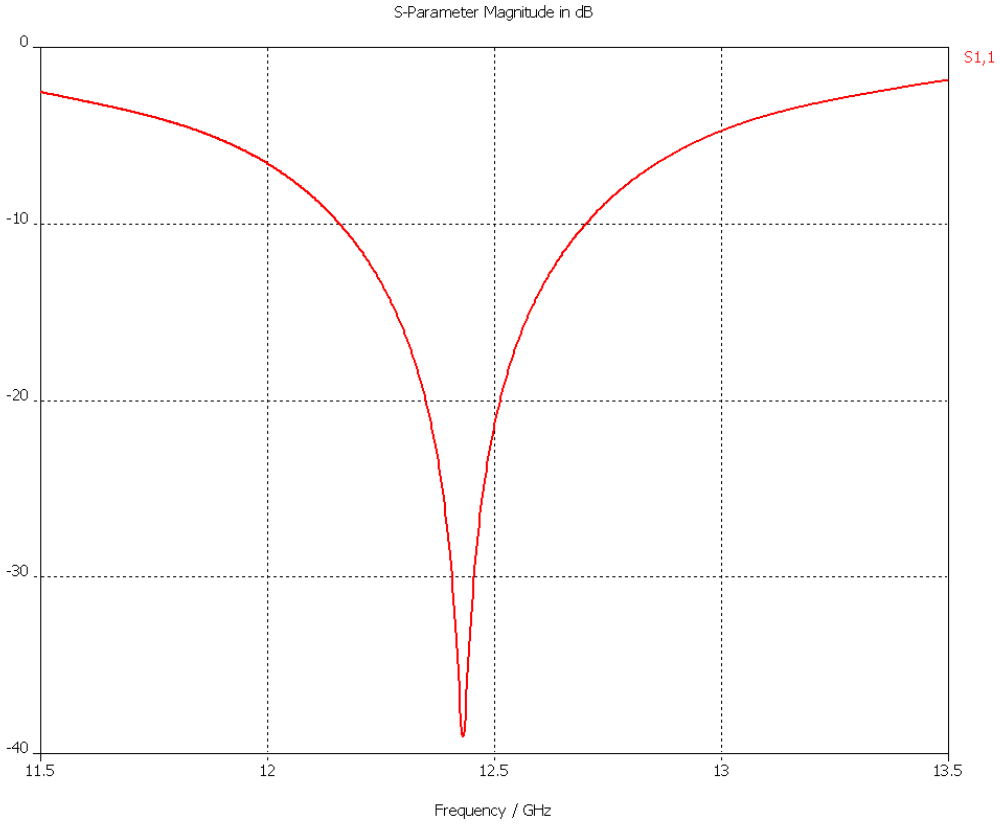

Fig. 59: Simulated S11 (Return Loss) of the patch

4.1.2 Conical horn fed by microstrip patch for prime focus antenna

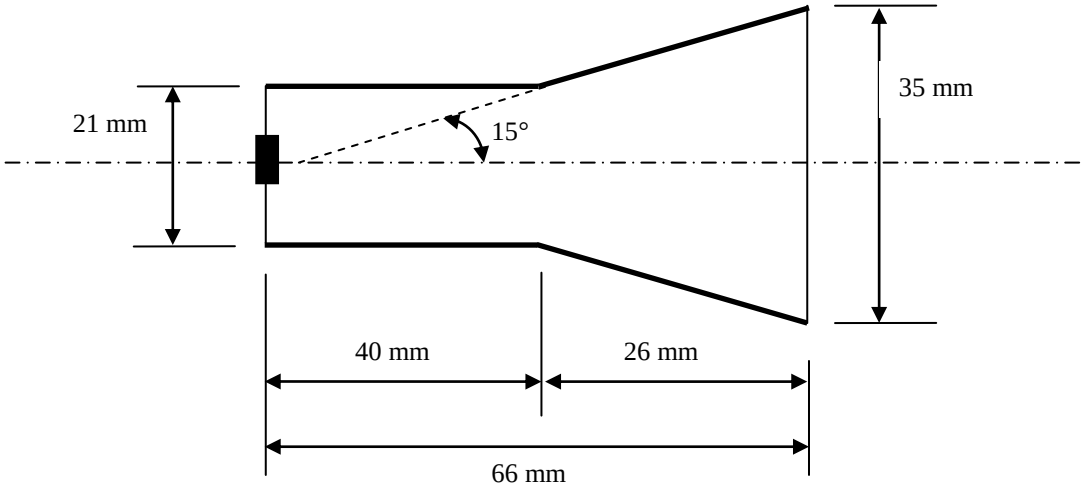

Fig. 25: Layout of conical horn (reproduced from section 2.4.3)

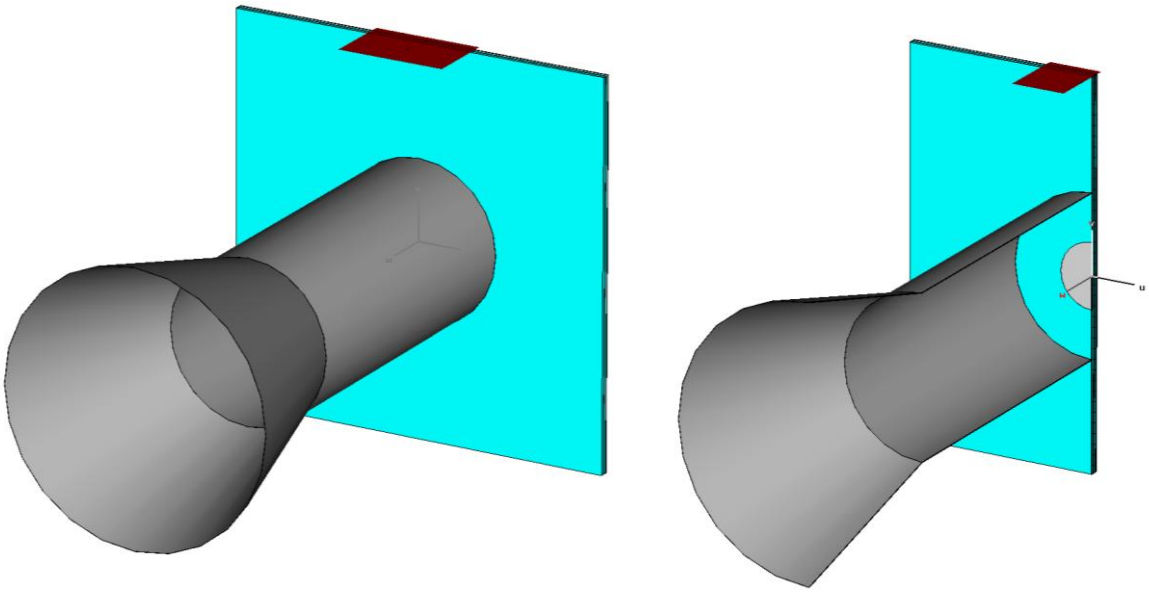

Fig. 60: Simulated horn for prime focus antenna fed by microstrip patch

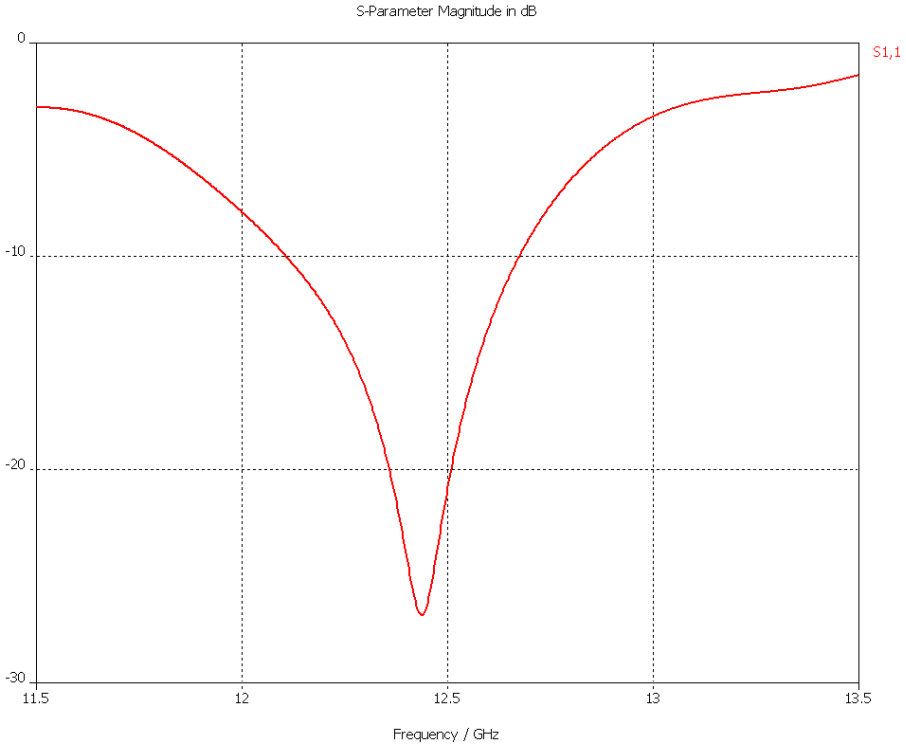

Fig. 61: Simulated S11 (Return Loss) of the conical horn fed by microstrip patch

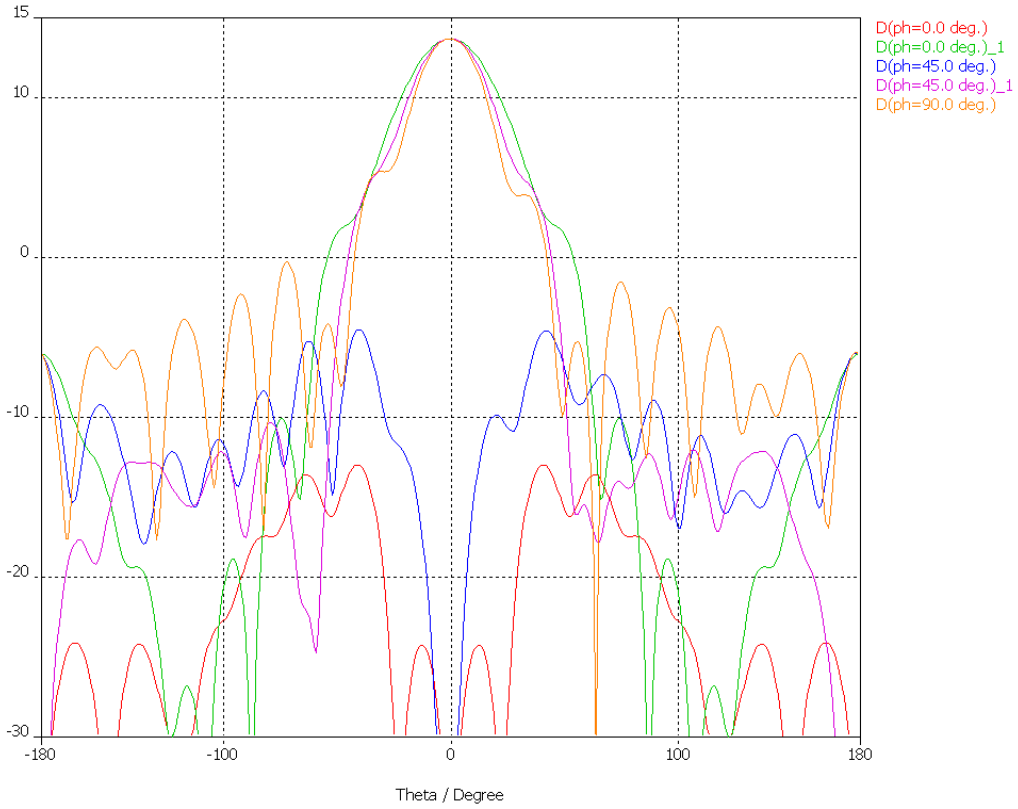

Fig. 62: Simulated co and cross polar radiation patterns of a conical horn fed by microstrip patch at 12.50 GHz. (Peak=13.72 dBi)

To compare the effects of feeding the horn with a patch instead of a standard waveguide input, the horn was simulated fed by a standard TE11 circular-waveguide mode (best theoretical feeding mechanism).

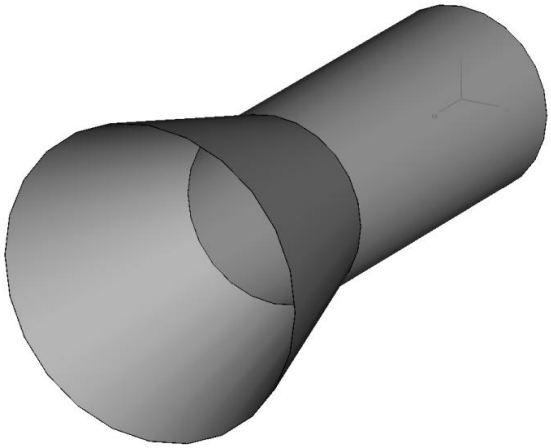

Fig. 63: Simulated horn fed by TE11 circular-waveguide mode

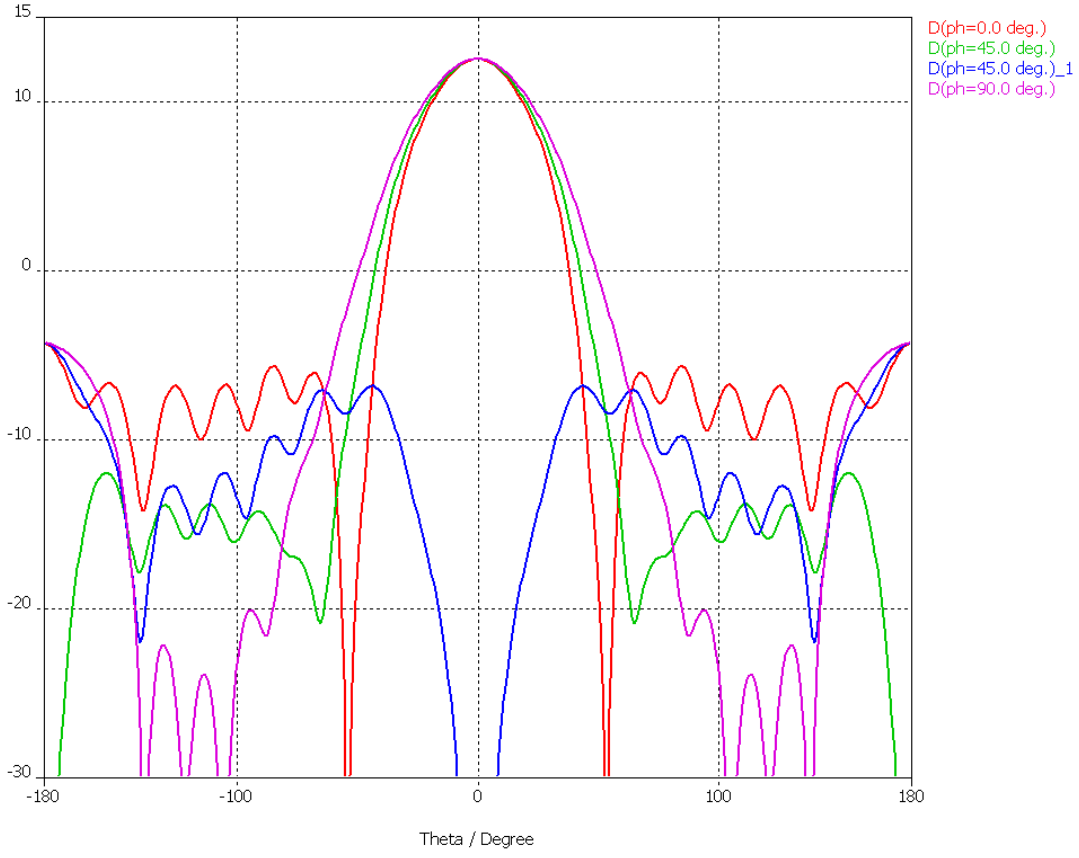

Fig. 64: Simulated co and cross polar radiation patterns of a conical horn fed by a TE11 circular waveguide mode at 12.5 GHz (Peak=12.58 dBi)

4.1.3 Conical feed horn fed by microstrip patch for Cassegrain antenna

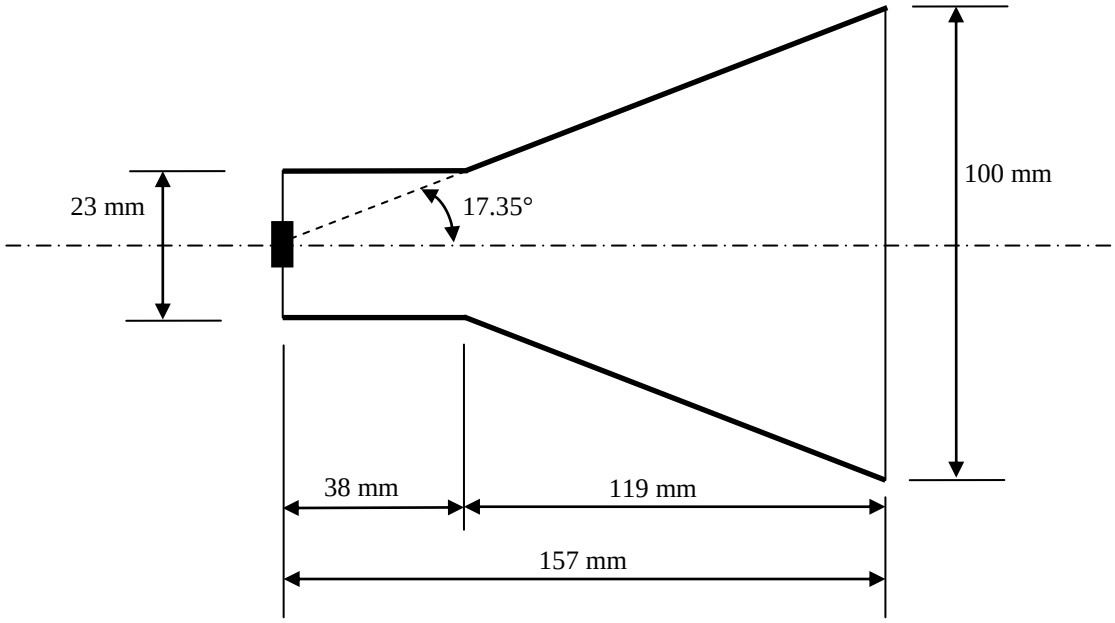

Fig. 29: Cassegrain antenna horn design (reproduced from section 2.4.5)

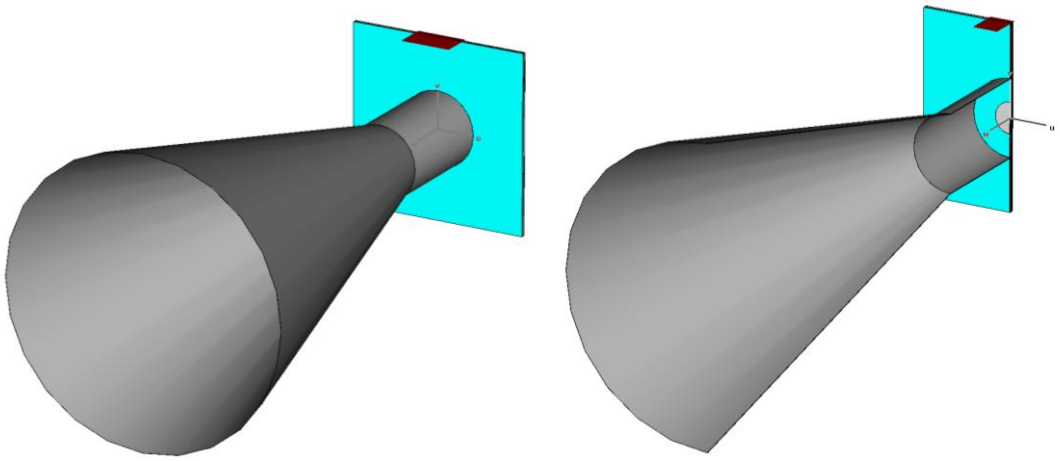

Fig. 65: Simulated horn for Cassegrain antenna fed by microstrip patch

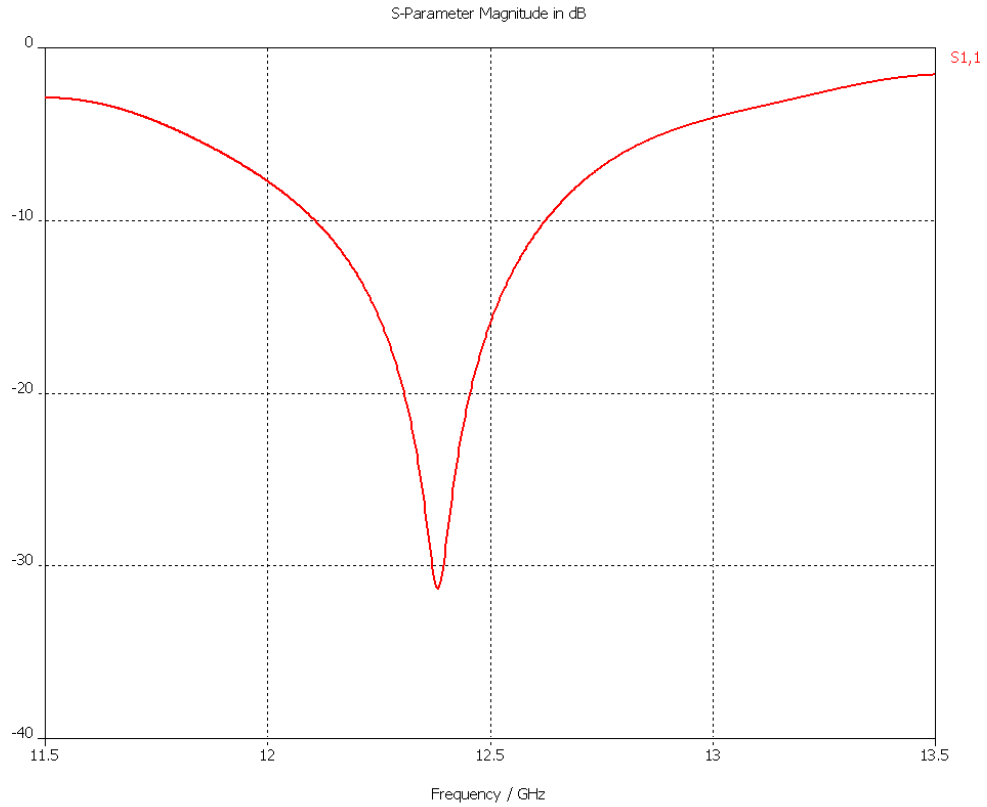

Fig. 66: Simulated S11 (Return Loss) of the conical horn for Cassegrain antenna fed by microstrip patch

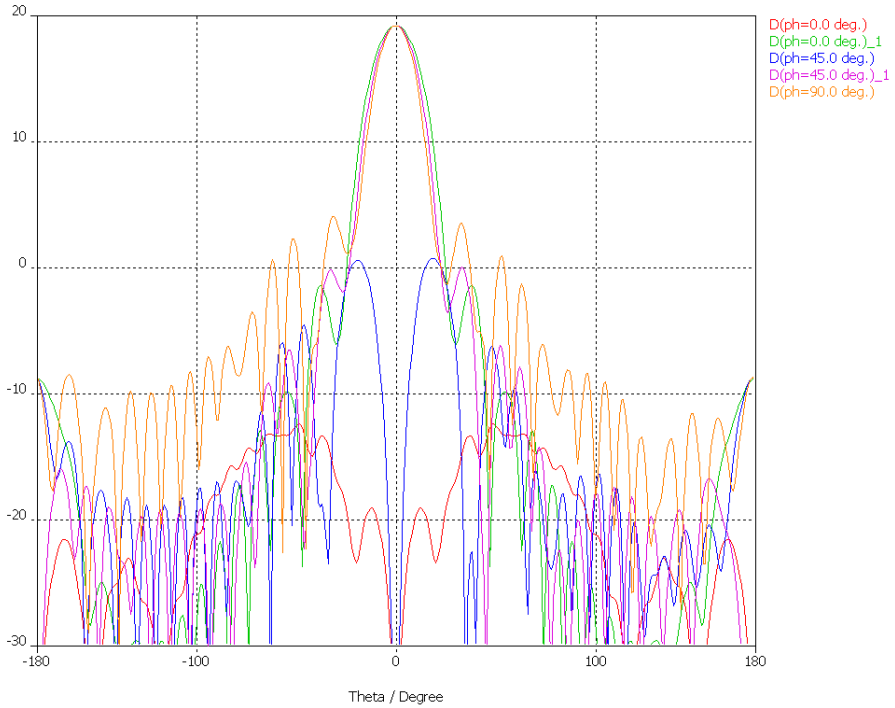

Fig. 67: Simulated radiation pattern of conical horn for Cassegrain antenna fed by microstrip patch at 12.50 GHz. (Peak=19.26 dBi)

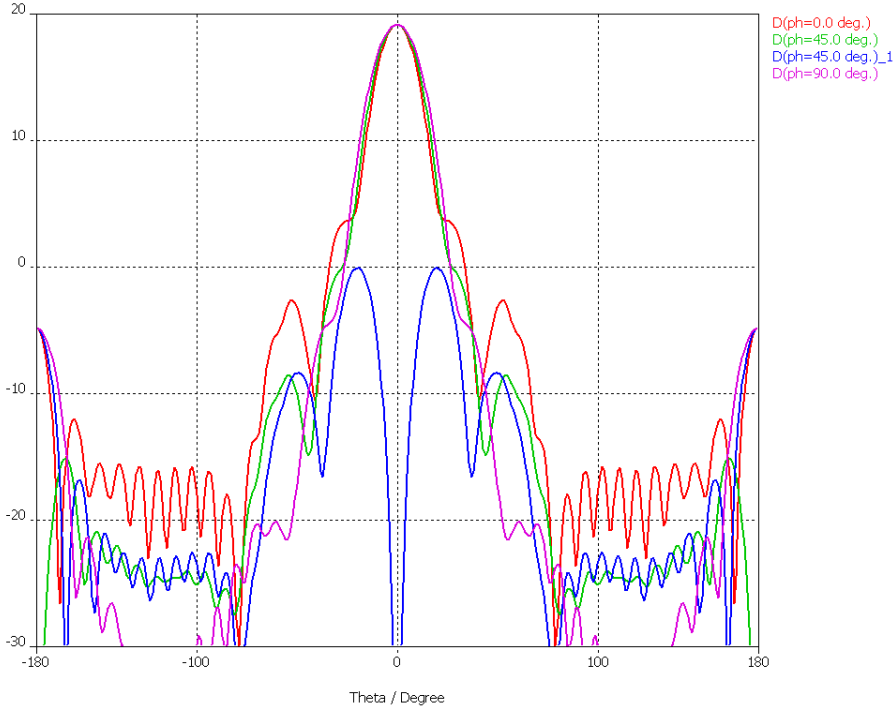

Fig. 68: Simulated radiation pattern of conical horn for Cassegrain antenna fed by a TE11 circular waveguide mode at 12.5 GHz (Peak=19.2 dBi)

4.1.4 Impact of support struts, ribs and pillowing on antenna performance

The impact of struts, ribs and pillowing was simulated using the TICRA GRASP simulation software. These simulations were generated by the author to aid the evaluation of the inflatable antennas performance. The following simulations were generated:

- single parabolic reflector fed by point source
- single parabolic reflector fed by point source supported by single 0.005m diameter strut
- single parabolic reflector fed by point source supported by three 0.005m diameter struts
- single parabolic reflector fed by point source
- single parabolic reflector fed by conical feed horn
- single parabolic reflector fed by point source, 8 ribs, no pillowing
- single parabolic reflector fed by conical feed horn, 8 ribs, no pillowing
- single parabolic reflector fed by point source, 8 ribs with pillowing
- single parabolic reflector fed by conical feed horn, 8 ribs with pillowing
- single parabolic reflector fed by point source, 12 ribs, no pillowing
- single parabolic reflector fed by conical feed horn, 12 ribs, no pillowing
- single parabolic reflector fed by point source, 12 ribs with pillowing
- single parabolic reflector fed by conical feed horn, 12 ribs with pillowing
- single parabolic reflector fed by point source, 16 ribs, no pillowing
- single parabolic reflector fed by conical feed horn, 16 ribs, no pillowing
- single parabolic reflector fed by point source, 16 ribs with pillowing
- single parabolic reflector fed by conical feed horn, 16 ribs with pillowing

All simulations were conducted keeping the following parameters constant:

Frequency: 12.5GHz
Wavelength: 0.024m
Main reflector diameter: 0.5m
Main reflector focal length: 0.375m
Distance between main reflector axis and parabola axis: 0

Point source

Taper angle: 36.869898 (ideal – automatically generated)

Taper: -12 (ideal – automatically generated)

Conical feed horn

Aperture radius: 0.0175015m

Flare length: 0.067184m

Phase displacement: 0

Modes: type TE11, amplitude 1, phase 0, rotation 0

4.1.4.1 Rigid parabolic reflector fed by point source

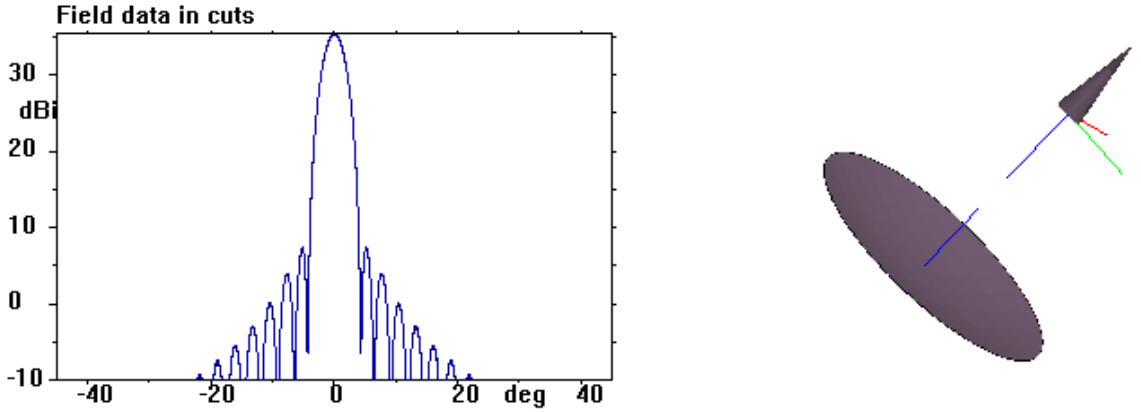

Fig. 69: Simulated radiation pattern of single rigid parabolic reflector fed by point source (Black: E-field / Blue: H-field / No cross polar)

4.1.4.2 Impact of single strut on the radiation patterns

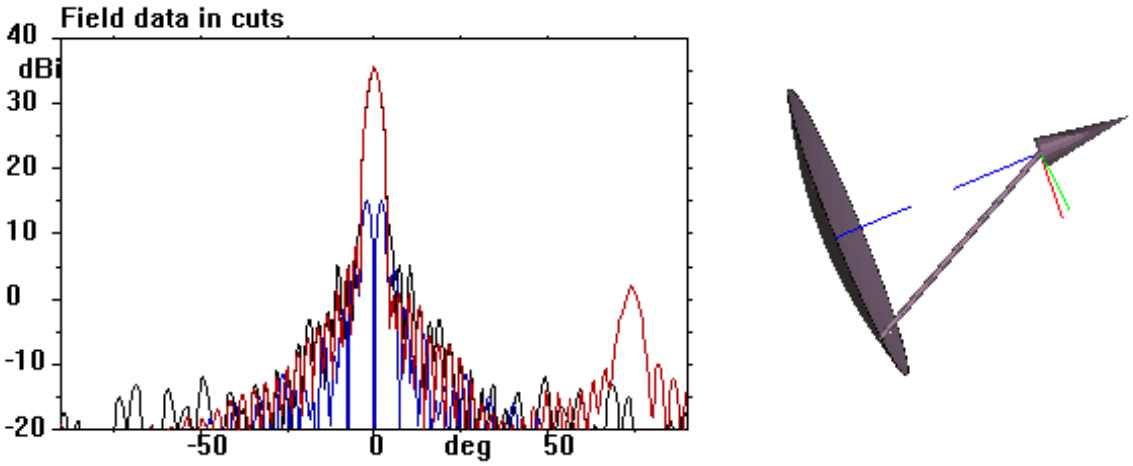

Fig. 70: Simulated radiation pattern of single rigid parabolic reflector fed by point source supported by single 0.005m diameter strut (Black: E-field / Red: H-field / Blue: cross polar (E) / No cross polar (H))

The final radiation plot above is a combination of the following two effects:

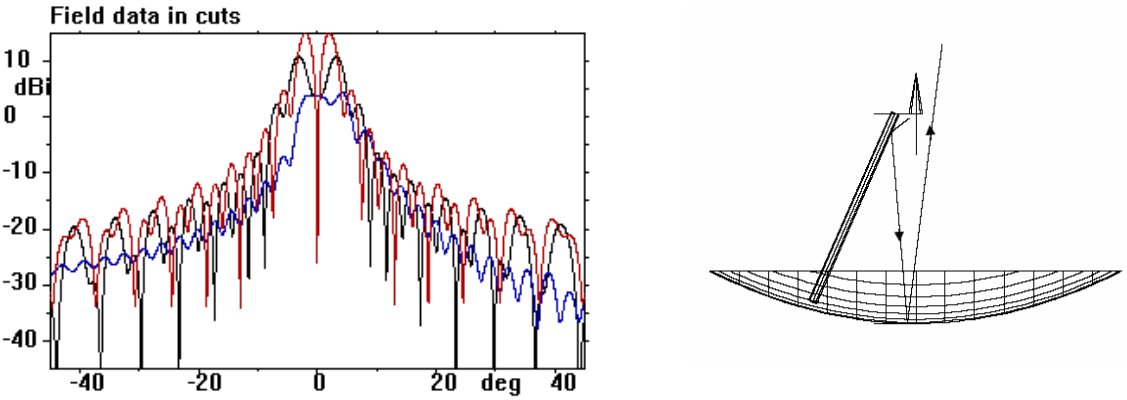

Black: E-field / Blue: H-field / Red: cross polar (E) / No cross polar H

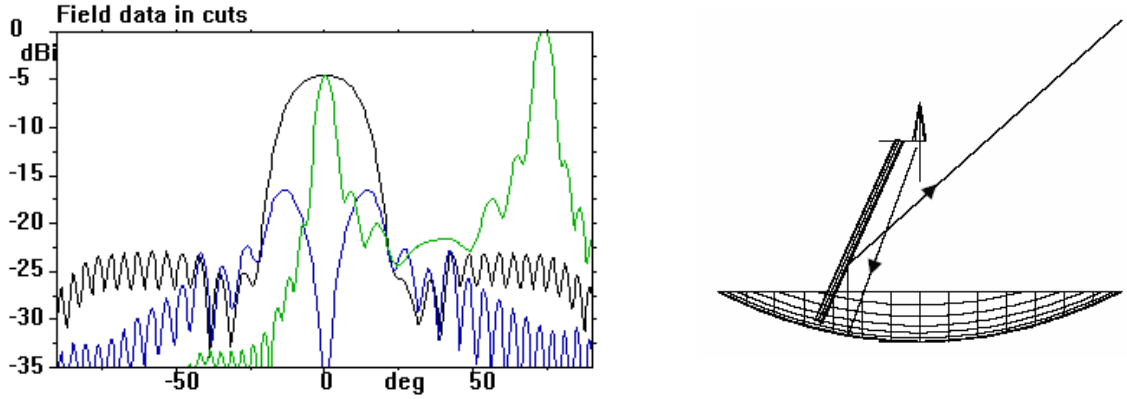

Black: E-field / Green: H-field / Blue: cross polar (E) / No cross polar H

4.1.4.3 Impact of three struts on the radiation patterns

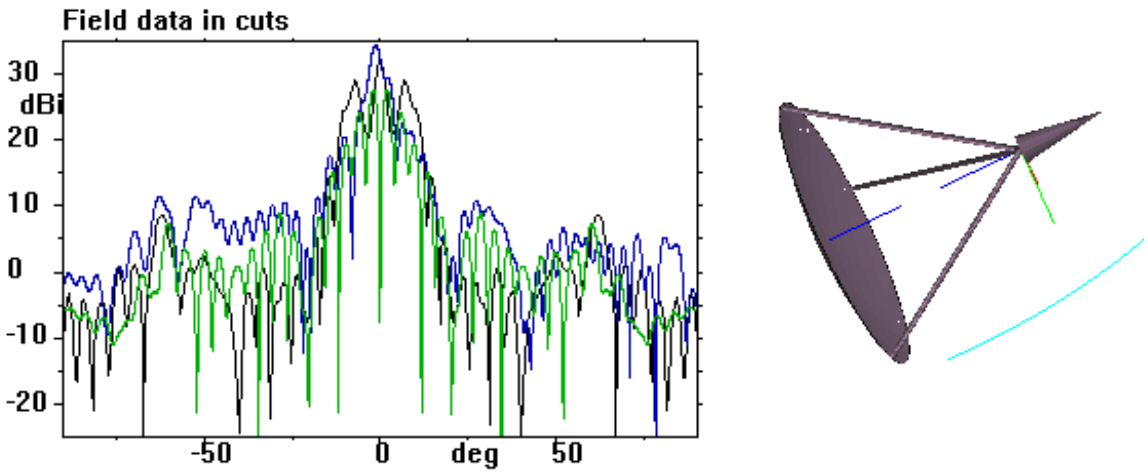

Fig. 71: Simulated radiation pattern of single rigid parabolic reflector fed by point source supported by three 0.005m diameter strut (Black: E-field / Blue: H-field / Green: cross polar (E) / No cross polar (H))

Final radiation plot is a combination of the following two effects:

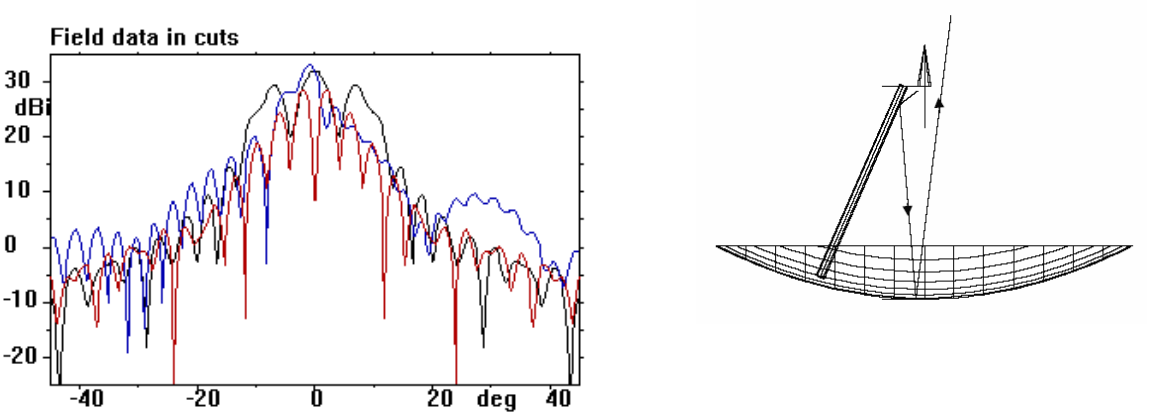

Black: E-field / Blue: H-field / Red: cross polar (E) / No cross polar (H)

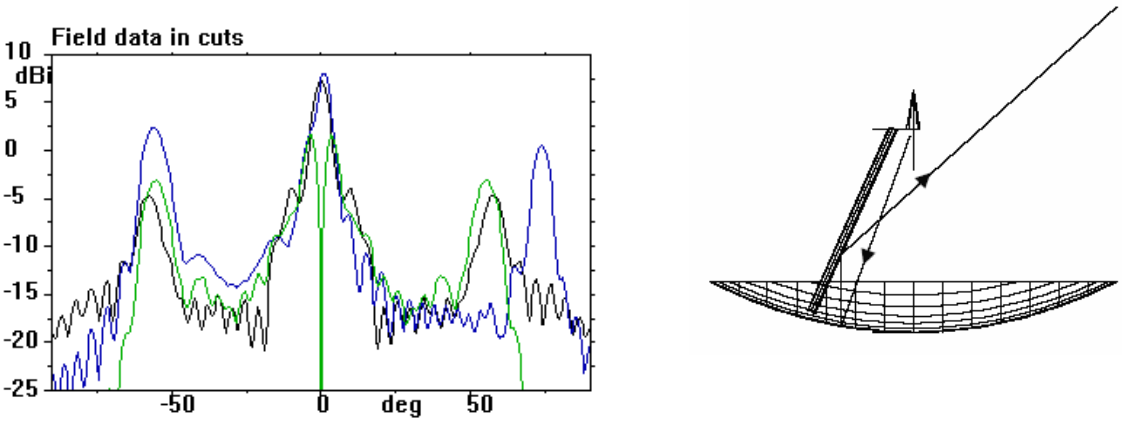

Black: E-field / Blue: H-field / Green: cross polar (E) / No cross polar (H)

4.1.4.4 Comparison of point source and horn feed

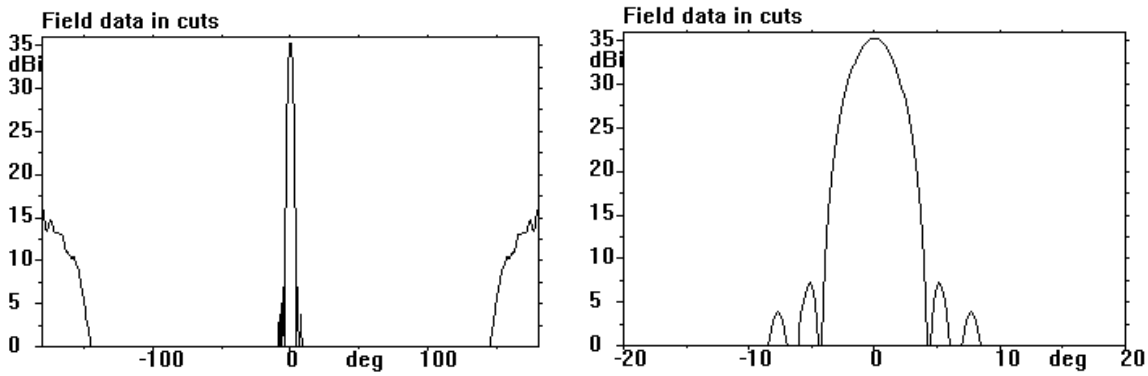

Fig. 72: Simulated radiation pattern of single parabolic reflector fed by point source, with no ribs and no pillowing (E-field)

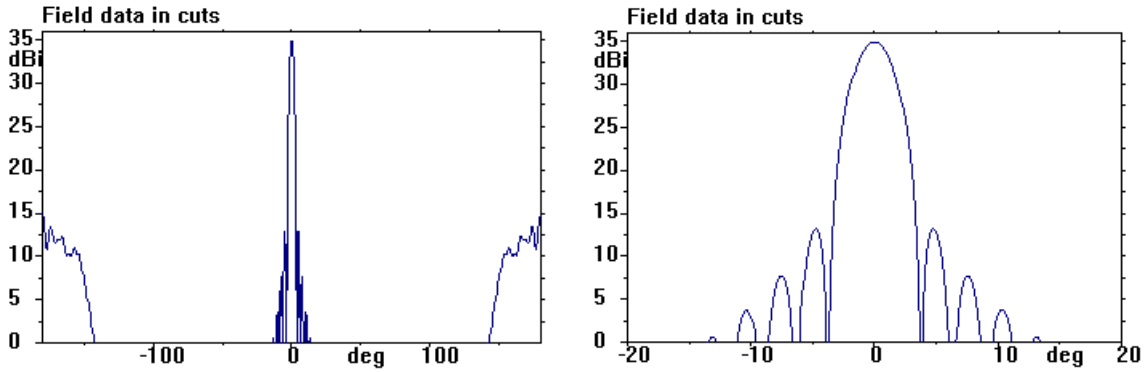

Fig. 73: Simulated radiation pattern of single parabolic reflector fed by conical horn, with no ribs and no pillowing (E-field)

4.1.4.5 Impact of pillowing in an antenna with 8 ribs

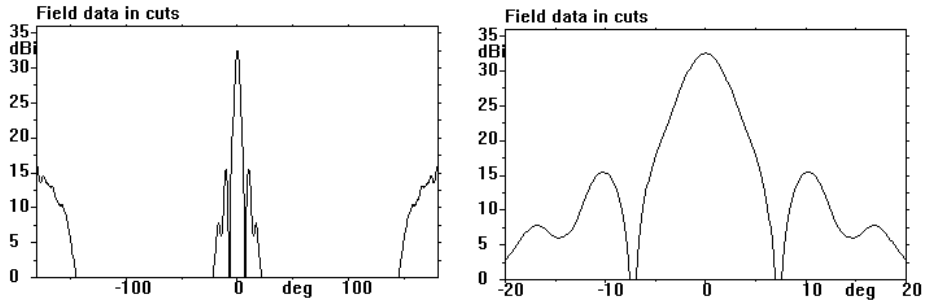

Fig. 74: Simulated radiation pattern of single parabolic reflector fed by point source, with 8 ribs and no pillowing (E-field)

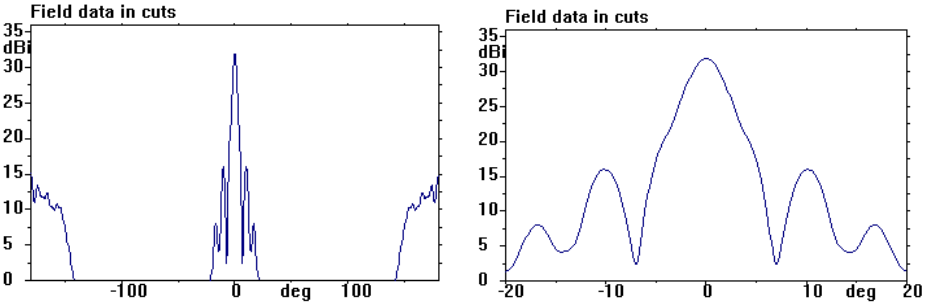

Fig. 75: Simulated radiation pattern of single parabolic reflector fed by conical horn, with 8 ribs and no pillowing (E-field)

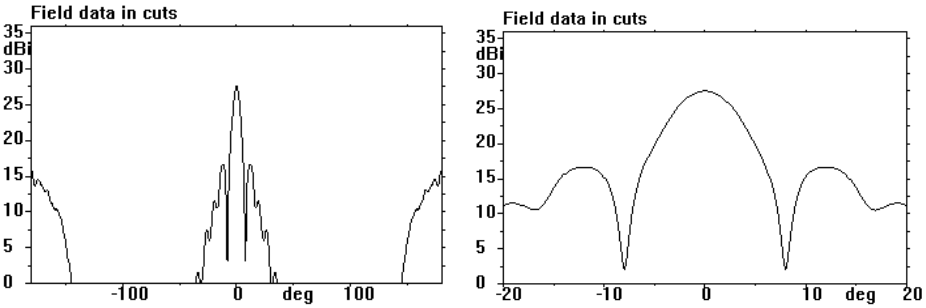

Fig. 76: Simulated radiation pattern of single parabolic reflector fed by point source, with 8 ribs and pillowing (E-field)

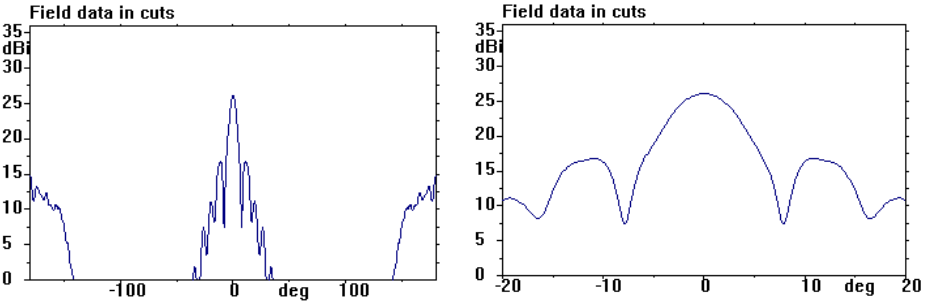

Fig. 77: Simulated radiation pattern of single parabolic reflector fed by conical horn, with 8 ribs and pillowing (E-field)

4.1.4.6 Impact of pillowing in an antenna with 12 ribs

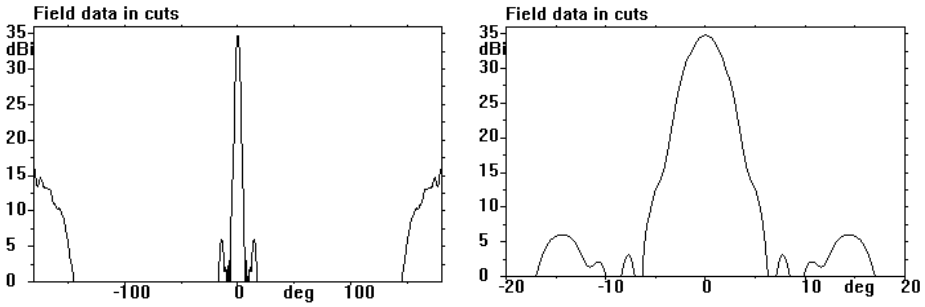

Fig. 78: Simulated radiation pattern of single parabolic reflector fed by point source, with 12 ribs and no pillowing (E-field)

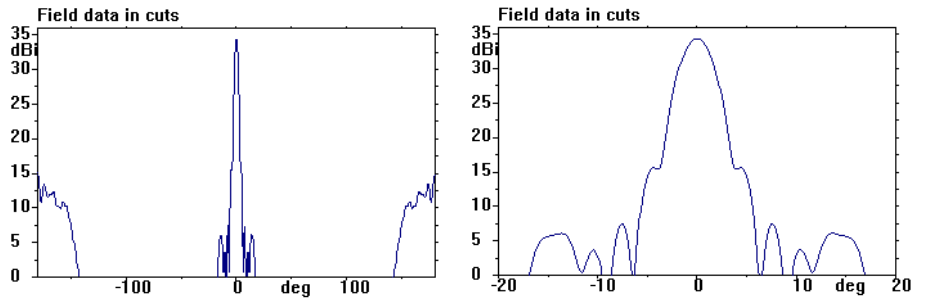

Fig. 79: Simulated radiation pattern of single parabolic reflector fed by conical horn, with 12 ribs and no pillowing (E-field)

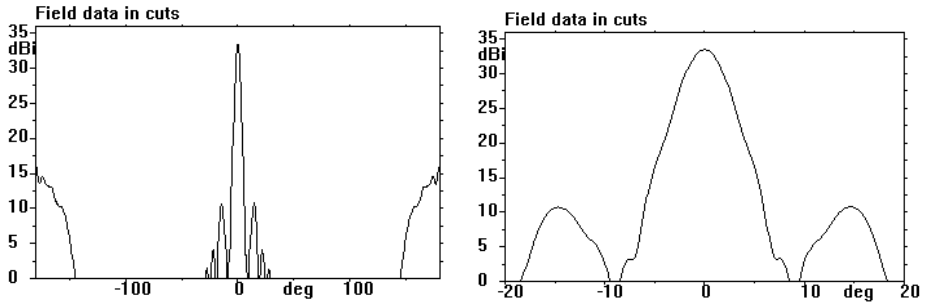

Fig. 80: Simulated radiation pattern of single parabolic reflector fed by point source, with 12 ribs and pillowing (E-field)

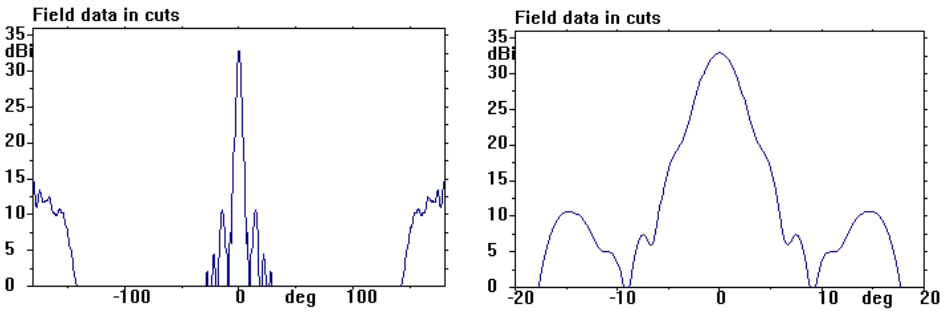

Fig. 81: Simulated radiation pattern of single parabolic reflector fed by conical horn, with 12 ribs and pillowing (E-field)

4.1.4.7 Impact of pillowing in an antenna with 16 ribs

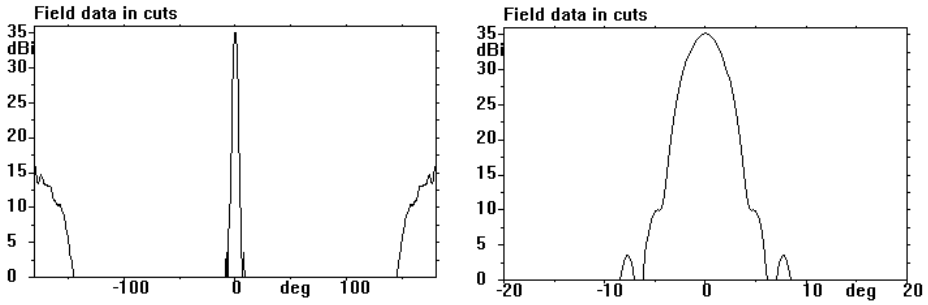

Fig. 82: Simulated radiation pattern of single parabolic reflector fed by point source, with 16 ribs and no pillowing (E-field)

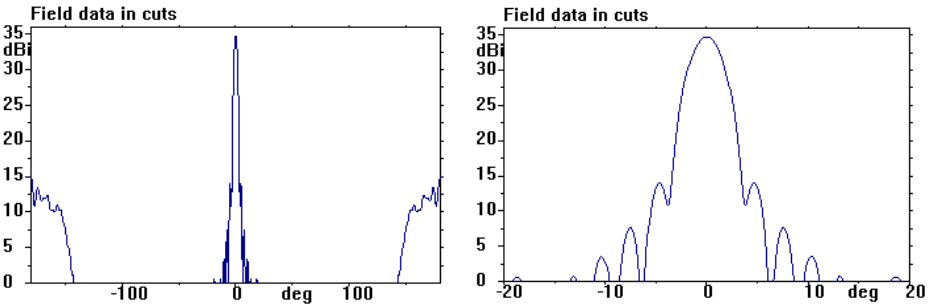

Fig. 83: Simulated radiation pattern of single parabolic reflector fed by conical horn, with 16 ribs and no pillowing (E-field)

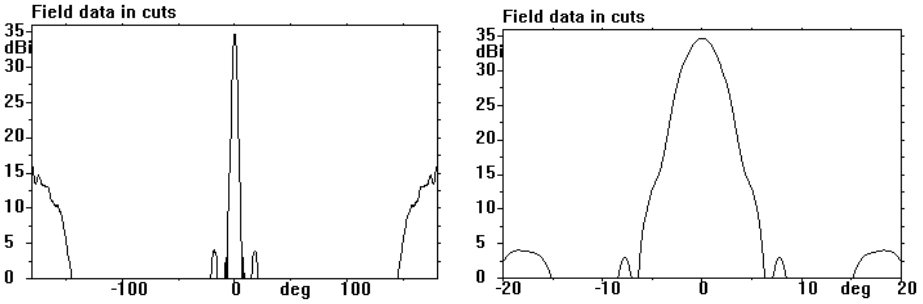

Fig. 84: Simulated radiation pattern of single parabolic reflector fed by point source, with 16 ribs and pillowing (E-field)

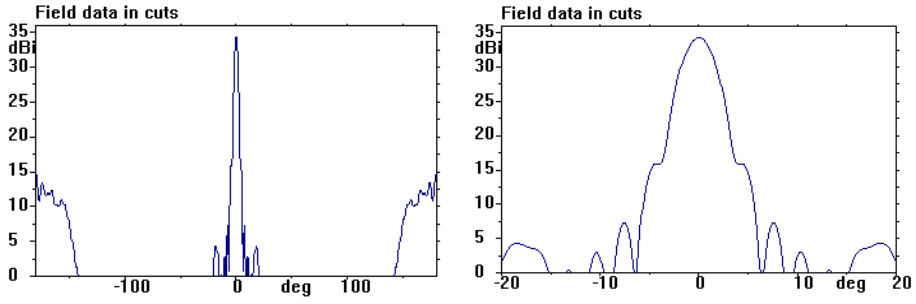

Fig. 85: Simulated radiation pattern of single parabolic reflector fed by conical horn, with 16 ribs and pillowing (E-field)

4.2 Material Testing

4.2.1 Structural properties

Property	Units	Clear thin film	Metalized thin film
Thickness	μm	24	50
Yield	m^2/kg	60	31.25
Unit Weight	g/m^2	68.23	79.44
Tensile Strength (Ultimate)	MPa, MD TD	97	106
Elongation at Break	%, MD TD	122	130

Table 3: Measured structural properties of clear thin film and metalized thin film

4.2.2 Electromagnetic properties

Property	Units	Clear thin film	Metalized thin film
Return loss	dB	-43.611	0

Table 4: Measured electromagnetic properties of clear thin film and metalized thin film

The transmission properties of the clear thin film and the metalized thin film were tested as detailed in *section 3.3.2*. Measurements were taken at 0.5 GHz increments between 12 GHz and 13 GHz. It was observed that the clear thin film had a minimum return loss of -43.611 dB and the metalized thin film fully reflected the signal at all frequencies within the range.

4.3 Microstrip patch

The microstrip was tested with the intention of using it to feed a gossamer horn. This was explored to reduce the overall weight of the antenna, improve the balance of the structure and achieve a higher gain and directivity than would be achieved by using a patch alone to feed the antenna. The use of a patch to feed a conical horn is an entirely novel approach and one that could have many applications. The interaction of the patch with the horn and the optimisation of a patch for this purpose offer a whole new area of research which was not explored as part of this investigation. This investigation focused on the impact of using a gossamer material to construct an antenna and feed horn. As such the patch was tested and defined but the comparison of the gossamer horn fed by the microstrip patch with the rigid horn fed with the microstrip patch was of greatest interest.

Before any testing was undertaken a conical horn fed by a microstrip patch and a conical horn fed by a TE11 waveguide were simulated and the results compared. The simulated results are presented in Section 4.1.2. From *Fig. 62* and *Fig. 64* it can be seen that, for the design under consideration, using a microstrip patch to feed the horn has little impact on the performance of the horn.

The impedance characteristics of the patch were tested and the results are shown in *Fig. 90*. It can be seen that the patch has a resonant frequency of 12.59 GHz and a maximum return loss of -18 dB. The patch has a bandwidth of 480 MHz. From these results it can be seen that the patch will operate at the design frequency of 12.5 GHz.

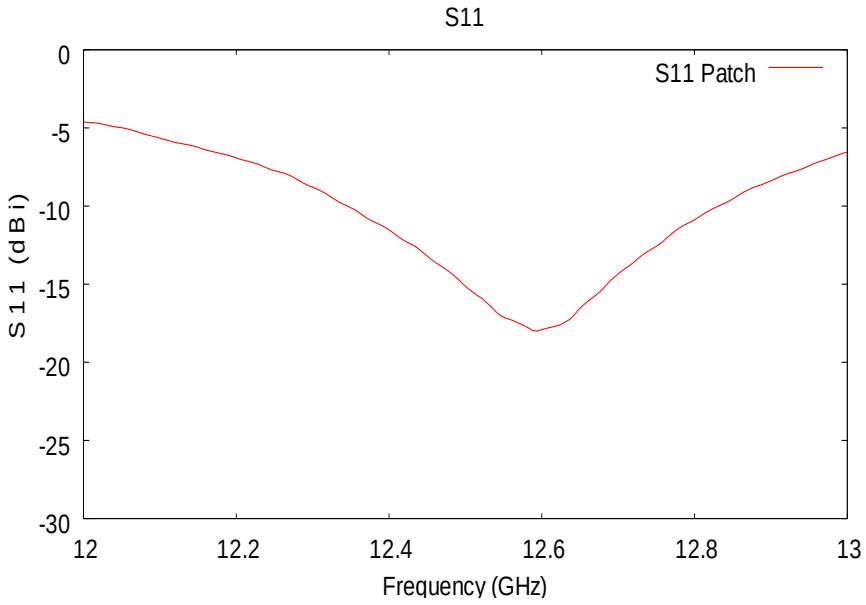

Fig. 86: Impedance characteristics of microstrip patch

The radiation characteristics of the patch were tested in the anechoic chamber at RMIT. To understand the interaction between the patch and the feed horn the near field radiation pattern should be measured. As this investigation is interested in the impact of using an inflatable structure on the performance of the feed horn and the antenna the performance of the assembled feed horn is of more interest. To demonstrate the increase in gain and directivity achieved by using a patch fed horn as opposed to a patch on its own the radiation characteristics of the patch were measured and presented below.

These results are shown in *Fig. 87*. The results showed that the patch had a maximum gain of 7 dB at 28°. The results also showed that the radiation patterns were not symmetrical and that there was a dip in gain in the forward direction. In future development the patch would be optimized for improved performance. In this investigation the important thing is to define the performance of the patch to differentiate between a loss in performance due to the patch as distinct from a loss in performance due to the use of an inflatable structure.

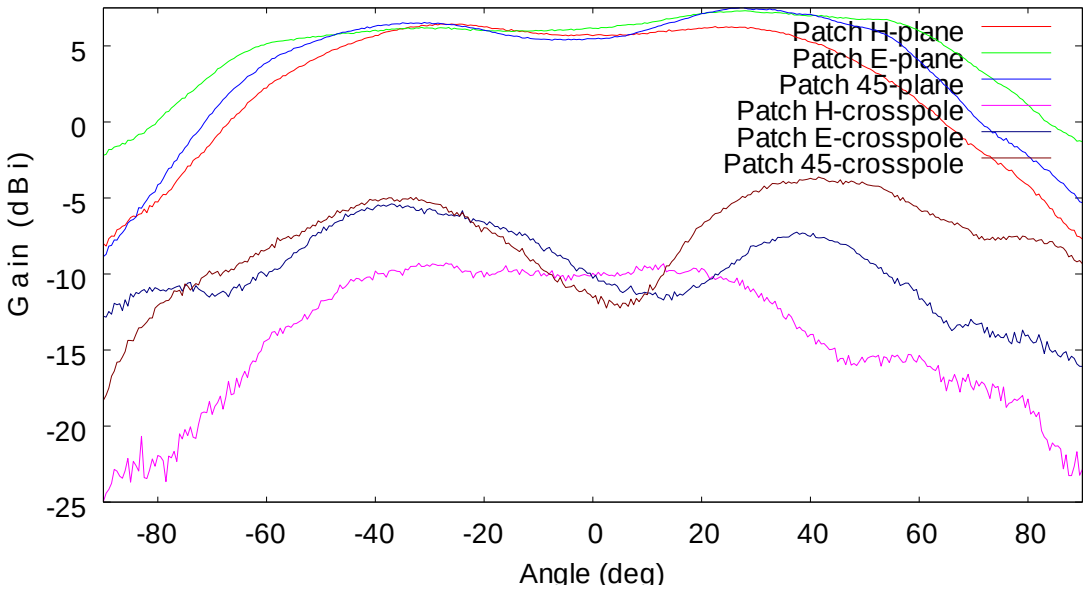

Fig. 87: Radiation patterns of microstrip patch

4.4 Gossamer horn

The impedance characteristics of the gossamer horn fed by the microstrip patch were tested and the results are shown in *Fig. 88*. The results showed that the horn patch combination has a resonant frequency of 12.576 GHz with a return loss of -29.91 dB and a bandwidth of 390 MHz.

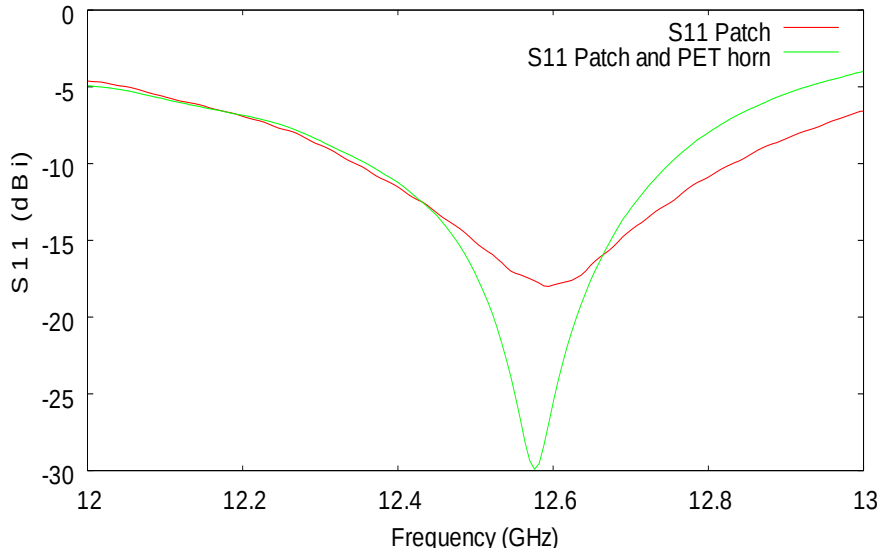

Fig. 88: Impedance characteristics of microstrip patch and gossamer horn fed by microstrip patch

Testing conducted using an earlier patch design compared the impedance characteristics of a rigid Aluminium horn fed by a microstrip patch, a gossamer horn fed by the same patch

and a gossamer horn that had been crushed and then returned to its original shape, also fed by the same patch, to simulate a horn that had been stowed and then deployed. The results are shown in *Fig. 89*.

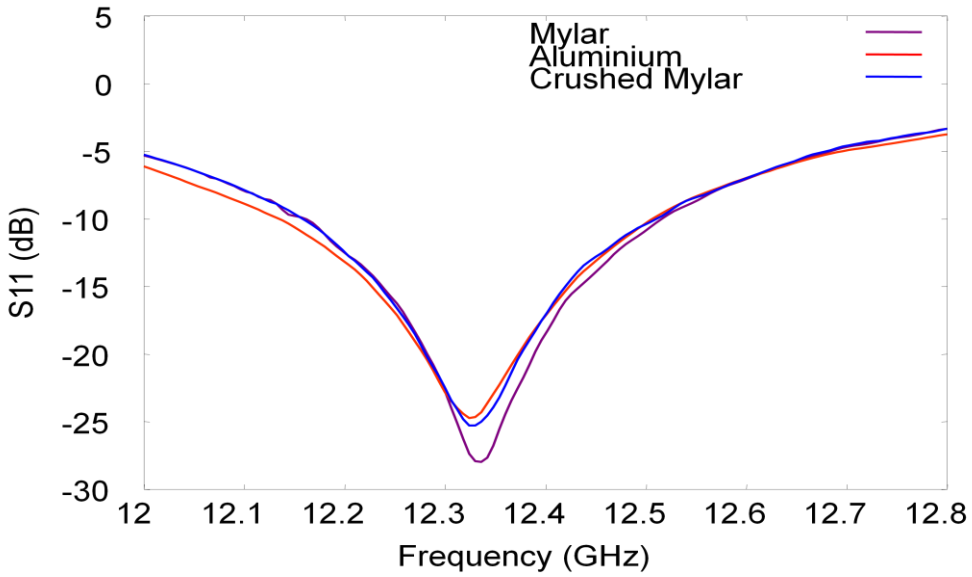

Fig. 89: Impedance characteristics of an Aluminium horn fed by a microstrip patch, a gossamer horn fed by a microstrip patch and a crushed gossamer horn fed by a microstrip patch

The radiation characteristics of the rigid and gossamer horns fed by the microstrip patch were tested in the anechoic chamber at RMIT at 12.576 GHz and the results normalized with respect to a standard gain horn.

Fig. 90 shows the radiation patterns for the Aluminium horn fed by the microstrip patch. These results showed that the horn produced a symmetrical radiation pattern with a maximum gain of 13.23 dBi and a beamwidth of 47°. It can be seen from *Fig. 90* that the Aluminium horn produces a 10 dB beamwidth of 83°. The cross polar characteristics of the system are good with the only significant cross polar radiation being seen in the E-plane with a front to back ratio of 10 dB.

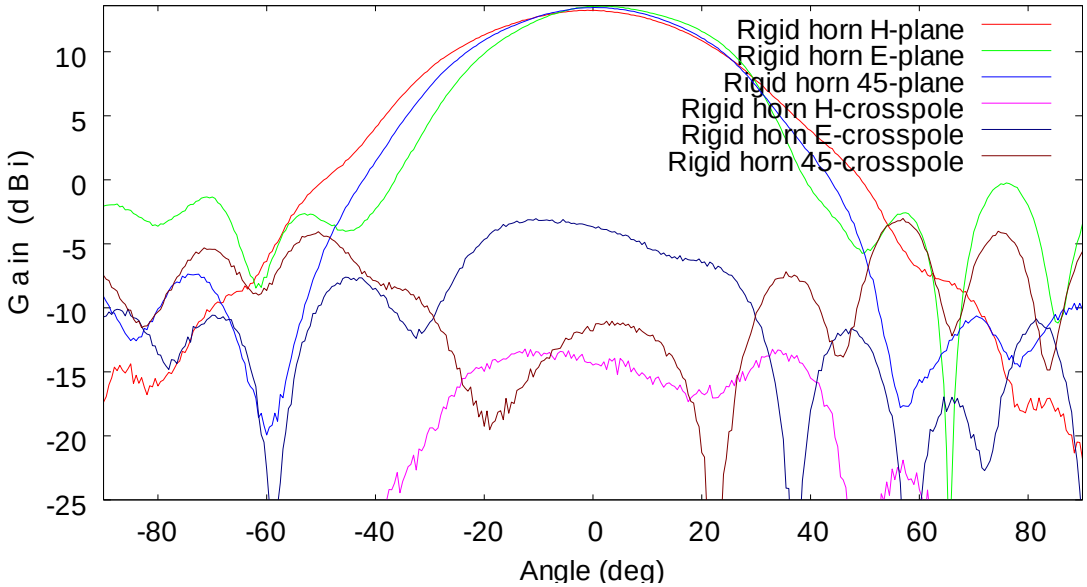

Fig. 90: Radiation patterns of rigid conical horn fed by microstrip patch operating at 12.576 GHz

Fig. 91 shows the radiation patterns for the gossamer horn fed by the microstrip patch. These results showed that the horn produced a symmetrical radiation pattern with a maximum gain of 12.1 dBi and a beamwidth of 40.5°. It can be seen from *Fig. 91* that the gossamer horn produces a 10 dB beamwidth of 77°. The cross polar characteristics of the system are good with the most significant cross polar radiation being seen in the 45-plane with a front to back ratio of 9 dB.

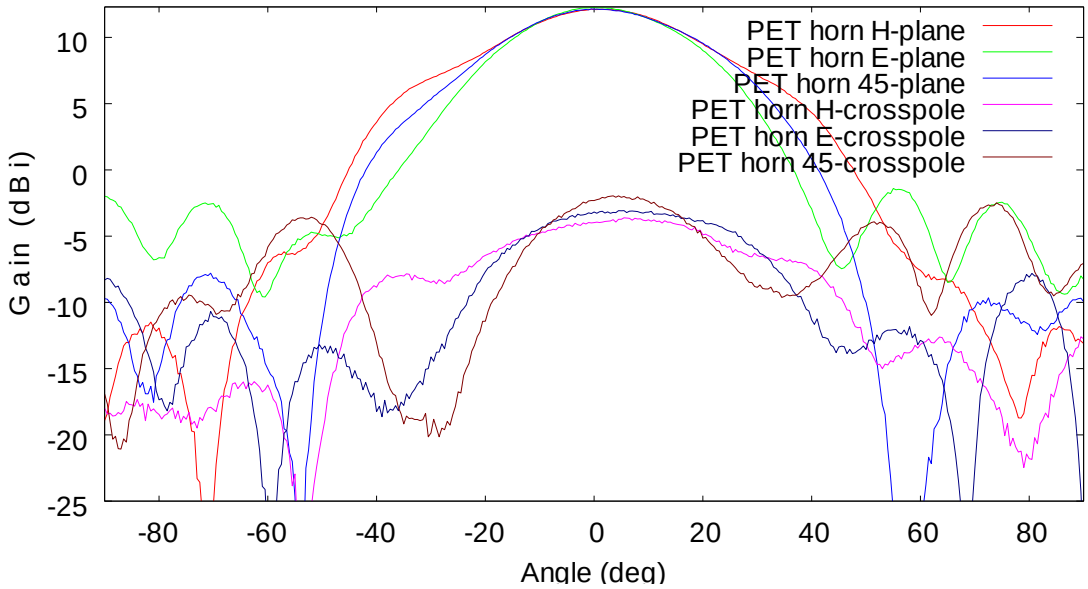

Fig. 91: Radiation patterns of gossamer conical horn fed by microstrip patch operating at 12.576 GHz

Fig. 92 shows a comparison between the E and H-plane radiation patterns of the rigid and gossamer horns.

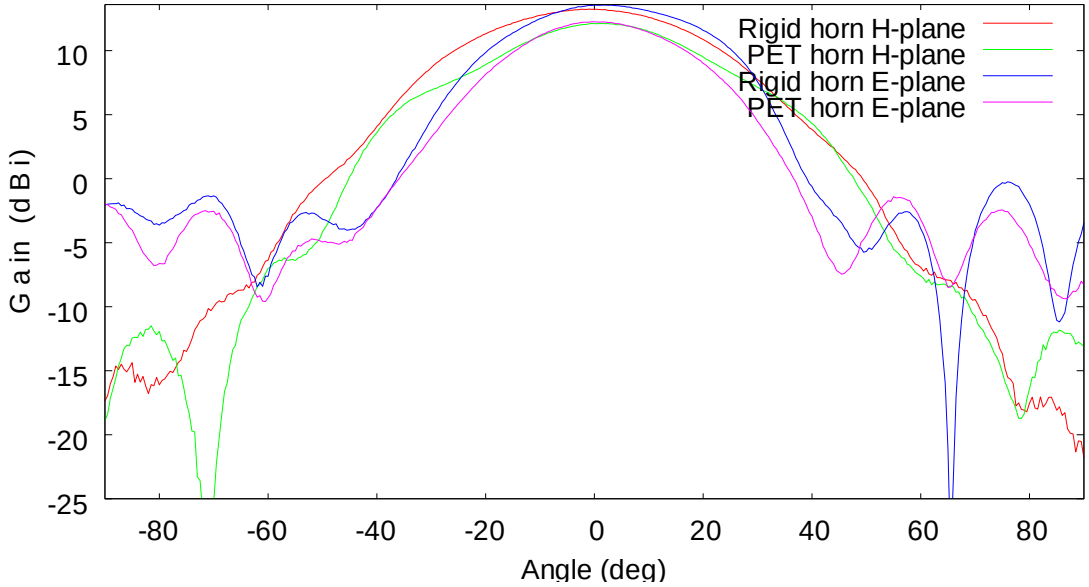

Fig. 92: Comparison between rigid and inflatable conical horns fed by microstrip patch operating at 12.5GHz

The two horns with the microstrip patch feed were weighed. The rigid Aluminium horn and patch weighed 124.6g and the gossamer horn and patch weighed 1.5g.

4.5 Parabolic reflector

The radiation characteristics of the rigid and gossamer parabolic reflectors fed by the gossamer horn were tested in the anechoic chamber at RMIT at 12.576 GHz and the results normalized with respect to a standard gain horn.

Fig. 93 shows the radiation patterns for the rigid parabolic antenna fed by the gossamer horn. These results showed that the antenna produced a maximum gain of 24 dBi and a beamwidth of 4.3°. The maximum side lobe level is in the H-plane at 20 dB down.

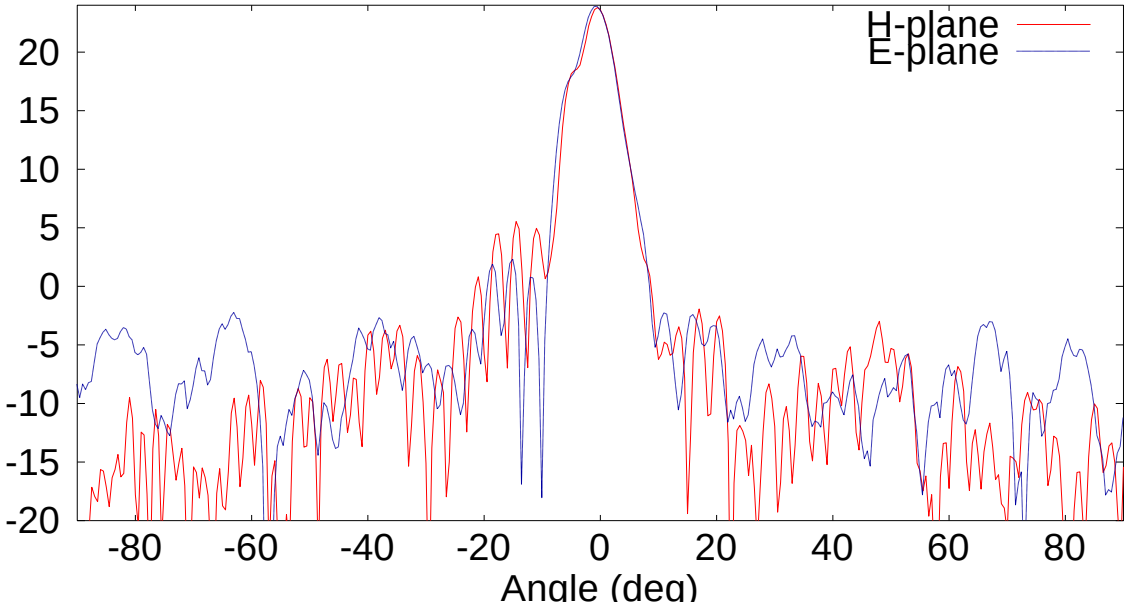

Fig. 93: Radiation pattern of rigid prime focus parabolic dish antenna fed by gossamer feed horn operating at 12.576GHz

Fig. 94 shows the radiation patterns for the inflatable antenna fed by the gossamer horn. These results showed that the antenna produced a maximum gain of 27 dBi and a beamwidth of 3.5°. The maximum side lobe level is in the H-plane at 17 dB down.

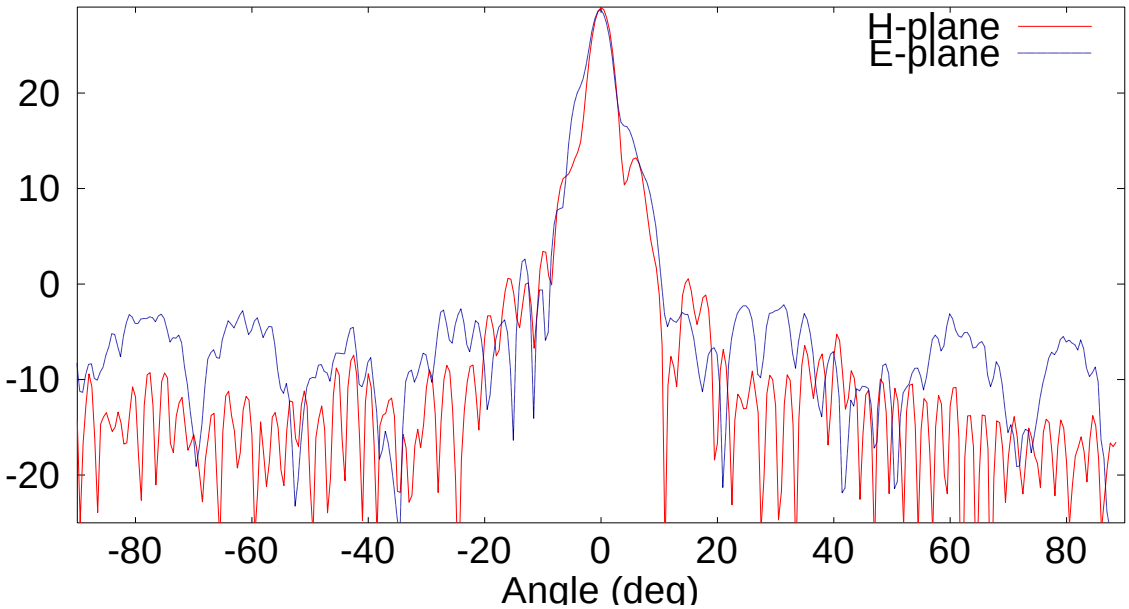

Fig. 94: Radiation pattern of inflatable prime focus parabolic dish antenna fed by gossamer feed horn operating at 12.5GHz

Fig. 95 shows the co-polar and cross-polar radiation patterns for the inflatable antenna fed by the gossamer horn. These results showed that the antenna produced had a front to back ratio of 16.55 dB.

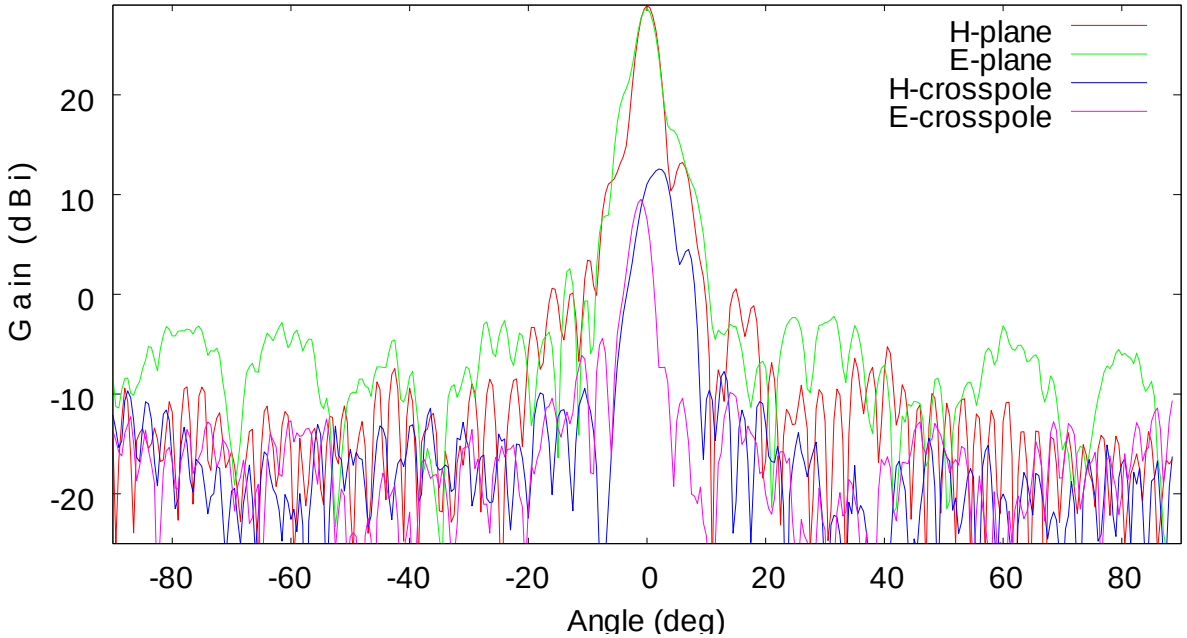

Fig. 95: Co-polar and cross-polar radiation patterns of inflatable prime focus parabolic dish antenna fed by gossamer feed horn operating at 12.5GHz

The two antennas were weighed without the rigid rim support. The rigid parabolic dish and gossamer feed horn weighed 150 g and the inflatable antenna weighed 12.2g.

The ability to reduce the stowed volume of a rigid parabolic dish antenna is limited by the diameter of the reflector. Assuming the feed horn and support strut could be folded and stowed within the dish, the rigid parabolic reflector under consideration has a stowed volume of 825 x 10^{-6} m^3. When folded and stowed the inflatable antenna has a stowed volume of 80.75 x 10^{-6} m^3. *Fig. 96* shows the stowed inflatable antenna.

Fig. 96: Inflatable antenna folded and stowed

Section 5 presents an evaluation of the simulated and measured results. Based on these results recommendations for further work are then presented in *section 6*.

5 Evaluation

This thesis presents a design for a Cassegrain antenna constructed entirely from polyester thin film. To further reduce the weight and stowed volume of the antenna the conical horn is fed by a microstrip patch. The enclosed environment is formed between the parabolic reflector and a clear conical canopy. This canopy supports the sub reflector at its apex and the gossamer horn is positioned at the centre of the parabolic reflector. The connection between the parabolic reflector and the canopy is supported by an inflatable torus. The performance of the antenna is related to the shape and surface accuracy of the components and the ability to maintain the dimensional relationship between them.

The aim of this investigation is to evaluate the performance of the components and assess their ability to operate under terrestrial conditions.

The performance of a parabolic dish antenna is related to the shape and surface accuracy of the dish and the ability to maintain the dimensional relationship between the feed and the reflector(s). Any deviation from the design will result in a reduction in gain, an increase in side lobe level, an increase in cross-polar level and an increase in beamwidth. In an inflatable antenna the shape and surface accuracy, and the relationship between the elements is achieved through material selection, structural design and internal pressure.

The flexible nature of inflatable structures eliminates the possibility of validating the shape accuracy via contact methods. The contact methods commonly used are invalid as the application of anything to the surface will change the local stiffness and load bearing properties of the skin and the structure will conform to a template placed in contact with the surface. Scanning methods such as photogrammetry can be employed but the use of both transparent and highly reflective materials impact on the accuracy of these methods. Reference dots would normally be used to overcome the reflective nature of the material but as previously mentioned contact methods change both the local stiffness of the material and the shape of the structure.

As the shape and surface accuracy of the dish and the ability to maintain the dimensional relationship between the feed and the reflector(s) has a direct impact on the performance,

the radiation pattern of the gossamer structure can be compared to that of a rigid structure to indirectly assess the shape accuracy. This method is not definitive but it is acceptable for evaluating the potential of inflatable structures to be used for land-based direct satellite communication. The accuracy of the gossamer structures were evaluated by comparing the input impedance, gain, beamwidth and peak cross polar level. Any deviation from the design will result in an increase in return loss, a reduction in gain, an increase in side lobe level, an increase in cross-polar level and an increase in beamwidth.

The flexible nature of the various components and the large number of new techniques being introduced made it important to test each component individually before combining them to help isolate the impact of the various new techniques and identify the limitations in the system. A literature review showed that there was no evidence of anyone replacing the waveguide with a microstrip patch to feed a horn. The use of a microstrip patch further reduces the weight and stowed volume of the feed assembly and reduces the loading on the inflatable antenna. Before testing commenced simulations were performed to assess if it was theoretically possible to feed a horn with a microstrip patch and to help identify the impact of varying parameters such as aperture blockage and pillowing. These simulations were then used to assist the interpretation of the measured results.

5.1 Simulation

A microstrip patch was investigated as an alternative to a traditional waveguide. If it could be demonstrated that a horn fed by a patch performed as required the weight of the feed assembly could be reduced considerably which would also reduce the loading on the inflatable antenna. Using a microstrip patch to feed the horn would have the additional benefits of reducing the stowed volume of the feed and the manufacturing cost.

Before testing commenced a simulation was generated to compare the performance of a conical horn fed by a microstrip patch and a conical horn fed by a standard TE11 circular-waveguide mode. This mode was selected as it is the best theoretical feeding mechanism. To facilitate comparison at a later stage, the conical horn used in the simulation is the design that will be manufactured and tested. A comparison of the simulated radiation patterns of the patch fed horn and the waveguide fed horn are presented in *Fig. 97, 98 and 99*.

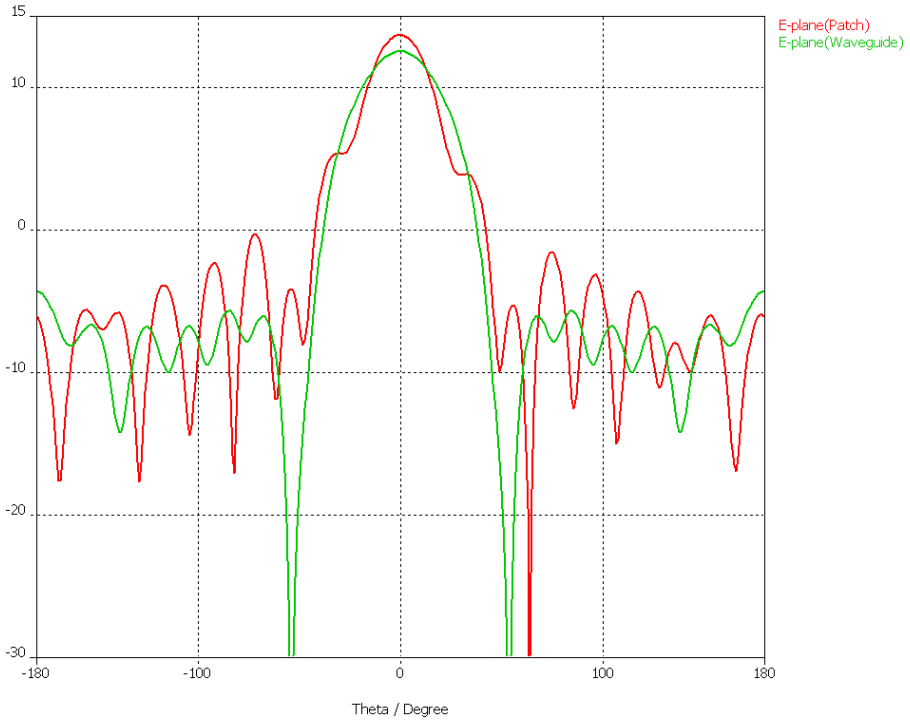

Fig. 97: Comparison of E-plane simulations for patch fed horn and TE11 waveguide fed horn (conical horn for prime focus antenna)

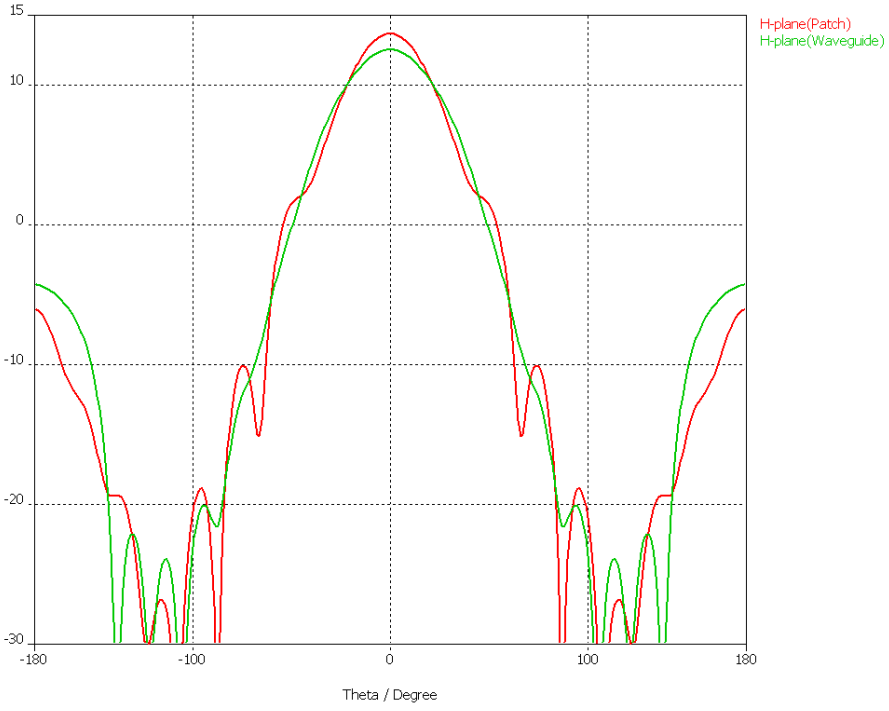

Fig. 98: Comparison of H-plane simulations for patch fed horn and TE11 waveguide fed horn (conical horn for prime focus antenna)

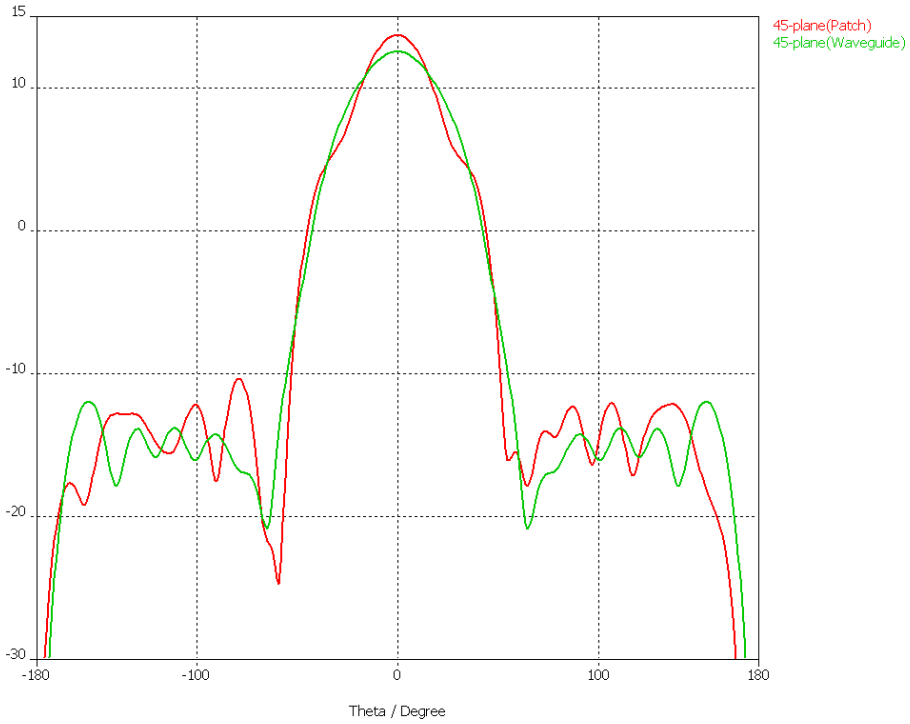

Fig. 99: Comparison of 45-plane simulations for patch fed horn and TE11 waveguide fed horn (conical horn for prime focus antenna)

The simulation indicated that the conical horn fed by the microstrip patch was well matched with a return loss of -27 dB. The radiation patterns were generated in the E-plane, H-plane and 45-plane and showed that the horn fed by the microstrip patch performed well when compared to the horn fed by the TE11 circular-waveguide mode. The horn fed by the microstrip patch generates a slightly higher gain (approx. 1 dB) than the horn fed by the TE11 circular-waveguide mode; it also has a slightly narrower half power beamwidth. In all three planes the side lobe levels of the patch fed horn were higher than the TE11 circular-waveguide fed horn but all were at least -15 dB relative to the main beam.

The cross polar radiation levels are another measure of the efficiency of the horn and the effectiveness of using a microstrip patch to feed the conical horn. The simulated cross polar radiation patterns for the prime focus horn fed by a microstrip patch are shown in *Fig. 100*. The cross polar radiation in the E-plane is too low to show on the plot.

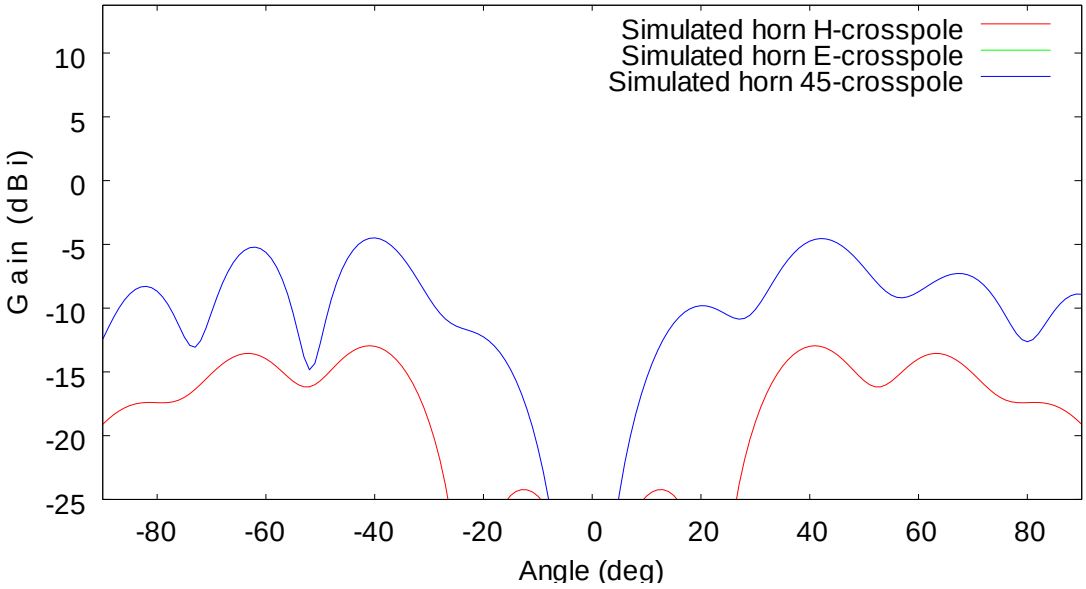

Fig. 100: Simulated cross polar radiation patterns for prime focus horn fed with patch.

The simulated results for the patch fed horn show excellent cross polar performance in the forward direction and compare well to the simulated cross polar radiation results presented in *Fig. 64* for the waveguide fed horn. The use of a microstrip patch increased the peak 45° plane cross polar level by approx. 3 dB. The overall cross polar performance can be improved through the optimization of the horn and patch designs but this is outside the scope of this thesis. These results indicated that it was theoretically possible to feed a solid conical horn with a microstrip patch and that testing should proceed.

To examine if the shape of the feed horn influenced the effectiveness of using a microstrip patch, simulations were also generated of a conical horn for a dual reflector antenna with both a microstrip patch feed and a TE11 waveguide feed. The results are presented in *section 4.1.4* and the most significant comparisons are presented in *Fig. 101, 102 and 103*.

The simulation indicated that the Cassegrain conical horn fed by the microstrip patch was well matched with a return loss of -31 dB. The radiation patterns were generated in the E-plane, H-plane and 45-plane and showed that the horn fed by the microstrip patch

performed well when compared to the horn fed by the TE11 circular waveguide mode. The maximum gain and the half power beamwidth for the two horns were identical. In all three planes the side lobe levels of the patch fed horn were minimally higher than the TE11 circular waveguide fed horn but all were at least -15 dB relative to the main beam. These results cannot conclusively prove that all conical horns can be effectively fed by a microstrip patch but the results do indicate that it was theoretically possible to feed the two conical horns used in this investigation and that testing should proceed.

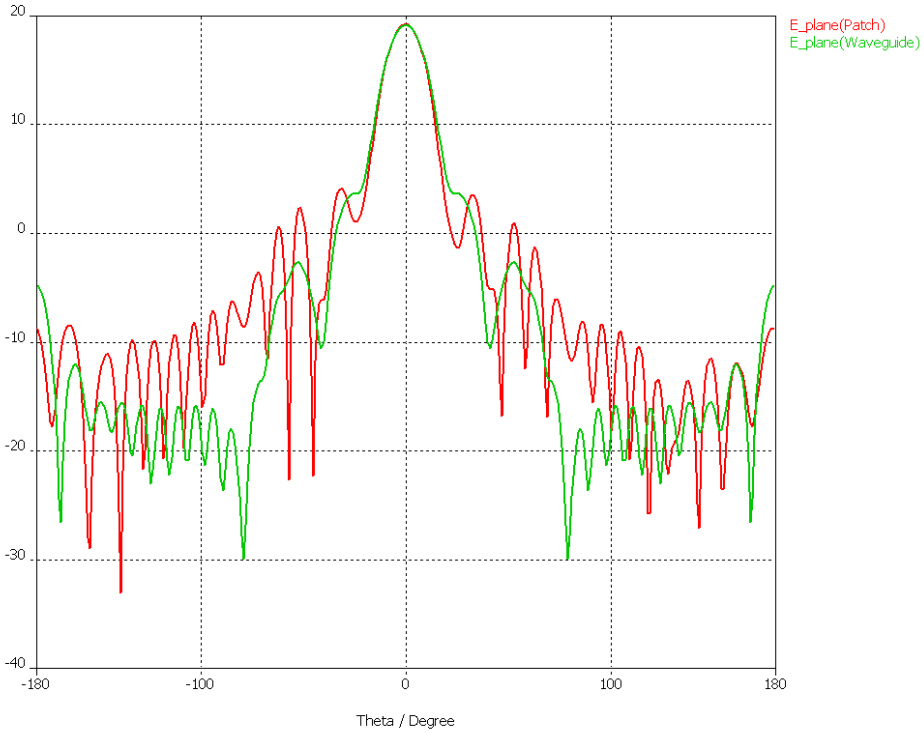

Fig. 101: Simulated comparison of E-plane radiation pattern for Cassegrain antenna fed by conical horn with patch and conical horn with waveguide

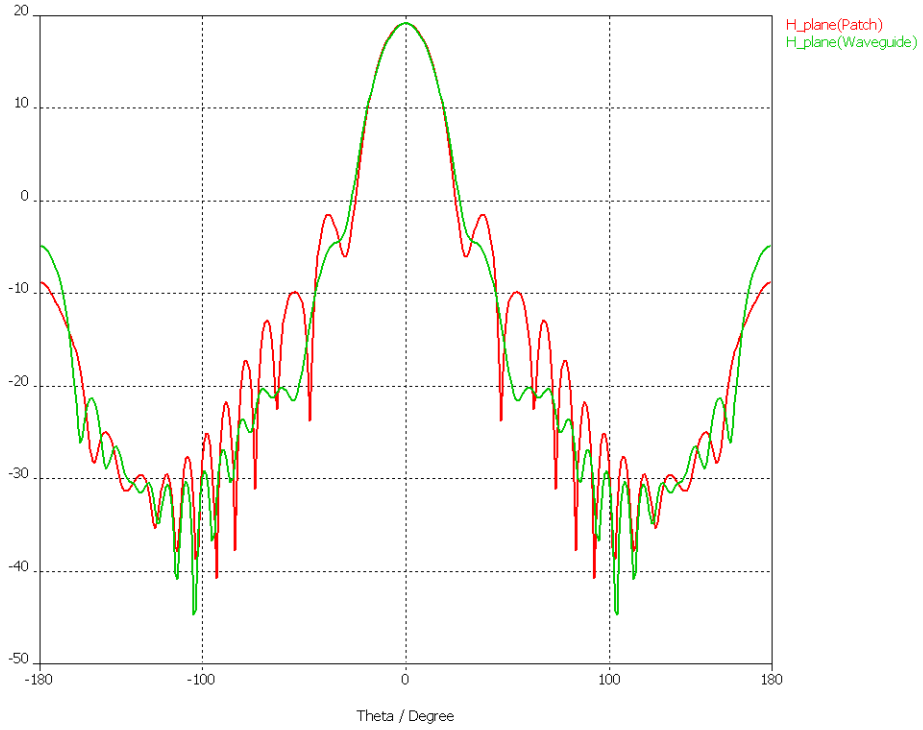

Fig. 102: Simulated comparison of H-plane radiation pattern for prime focus antenna fed by conical horn with patch and conical horn with waveguide

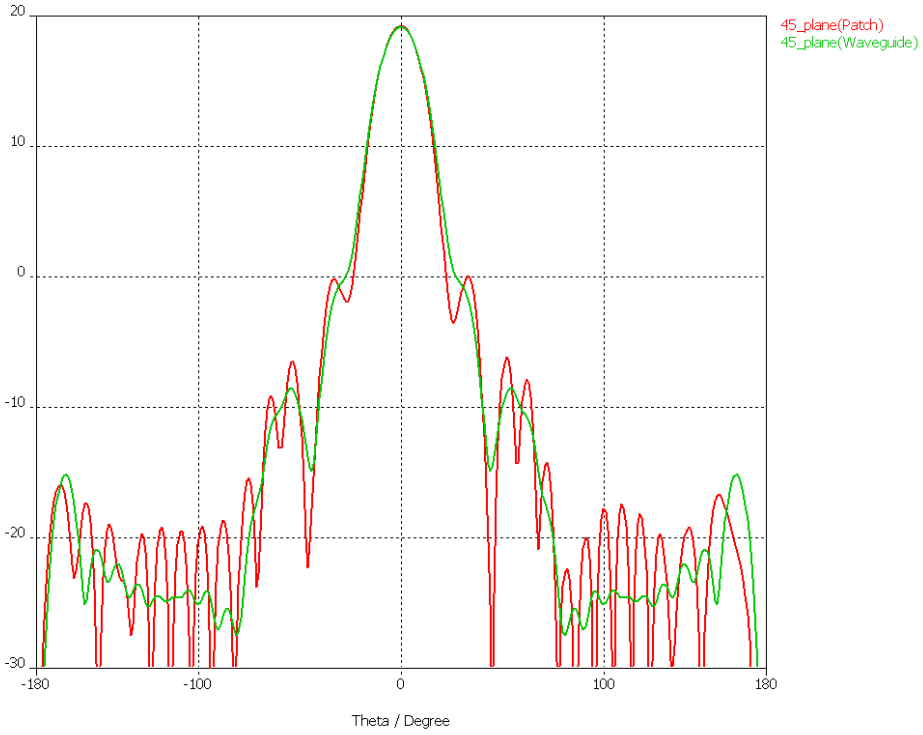

Fig. 103: Simulated comparison of 45-plane radiation pattern for prime focus antenna fed by conical horn with patch and conical horn with waveguide

These simulations will aid the interpretation of the measured results and held distinguish the effects of the feed as distinct from the impact of using a gossamer material to construct the horn.

Further simulations were performed to help differentiate the impact of various factors in the measured radiation patterns for the antenna. It is known that aperture blockage from the feed and support struts adversely affects antenna performance, as does the deformation of the parabolic reflector due to the use of ribs and the effects of pillowing. The simulations presented in *section 4.1.6* show varying degrees of these impacts and will be used in the evaluation of the shape accuracy of the antennas dish and the ability of an inflatable antenna to perform under terrestrial conditions.

The simulations investigating the impact of struts were performed using a perfect paraboloid reflector. The results showed that the aperture blockage caused by the feed horn increased the side lobe levels and the use of struts to support the feed assembly caused aperture blockage as well as scattering of the signal. The scattering of the signal was observed as an increase in the number of side lobes and their intensity, and an increase in cross polar levels.

The simulations investigating the impact of ribs and pillowing were generated with both a point source and a conical horn but no support struts. The elimination of the support struts reflects the use of a clear canopy to support the feed assembly. Pillowing is a common problem in articulated antenna dishes where the local stiffness of the ribs, compared to the flexibility and weight of the mesh, imparts a distortion and the performance is reduced [13]. When working with membrane structures the seams are commonly either taped or heat welded, giving some flexibility. This reduces the localized stiffness and the pillowing effect but does not eliminate it. The series of simulations helped extrapolate the level of pillowing in the measured radiation patterns for the inflatable antenna.

From the simulations it can be seen that the introduction of ribs reduces the overall gain, increases the beamwidth and increases the side lobe level. These effects are exacerbated when the effects of pillowing are included. The simulations showed that the impact of the ribs and pillowing were reduced when the number of ribs was increased from eight to

twelve to sixteen. As the number of ribs is increased the reflector surface approaches a perfect paraboloid. However, continuing to increase the number of ribs to improve performance counteracts any weight and stowed volume advantage gained through the use of a deployable structure. It is suggested that the use of a gossamer material can achieve both good performance and a reduction in weight and stowed volume.

5.2 Material

The material is an integral part of the design of any inflatable structure. For the structure to be stowed and then inflated the material must be foldable and have low gas permeation to sustain the inflation. The material when stowed must not become permanently deformed and to maintain inflation it must be durable, and tear and puncture resistant. The materials that best fulfil these requirements are polymer thin films, including polyesters, ploymides and polyamides. These thin films are often referred to as membrane or gossamer materials as they have a small thickness, which allow them to be folded for storage, but are incapable of carrying a compressive load. It is therefore necessary to use the design of the structure combined with internal pressure to give the inflated structure its desired shape.
If the gossamer material is to be used to construct a non-precision structure, high packing efficiency and durability are the key factors for material selection. If the final product is to be a precision structure then the dimensional stability of the material becomes important, and if the structure is intended for a communications application then the electromagnetic properties of the material must also be considered. Any components which will act as a canopy must be radio frequency (RF) transparent at the operating frequency and any components acting as a reflector must be metalized such that the signal is reflected without loss. To maintain antenna performance the inflatable structure must maintain the shape accuracy of the individual components and maintain the relationship between the antenna components whilst under the influence of the operating environment.

There is an extensive range of polymer thin films with varying material properties and this range continues to expand. The material properties of thin films can be manipulated at a polymer level and by varying the conditions during extrusion to significantly vary the physical and mechanical properties of the film. Thin films can also be combined in layers to form a laminate to further control their properties. The design of the material that best

satisfies the requirements of the inflatable antenna is an area of research in itself. This level of design was beyond the scope of this investigation.

Off the shelf materials that provide the basic material properties required to demonstrate the concept of an inflatable antenna are readily available. It is therefore more important to test and define the properties of the material used to allow the limitations of the material to be differentiated from the limitations of the antenna.

The material used to demonstrate the inflatable antenna concept was Polyethylene Terephthalate (PET) thin film. PET is a polymer that has been commercially available for some time under various trade names including Mylar, Melinex and Diafoil [41]. To form a thin film the bulk material is extruded in two directions producing an orthotropic film. This means the material properties will be different in the two directions, the material direction (MD) and the thickness direction (TD). This difference is not significant but must be taken into consideration. PET thin film is used successfully in a wide range of applications, due to its excellent combination of optical, physical, mechanical, thermal, and chemical properties, as well as its unique versatility and low cost.

The PET thin films used for the inflatable antenna prototype were donated by VISIPAK and only limited material properties were defined. A range of structural and electromagnetic tests were conducted to confirm the properties specified and define the unknown properties. The results of these tests are presented in *section 4.2* and a comparison to typical properties for three typical gages of Mylar as given by Du Pont [41] are shown in *Table 5*.

Property	Test	Units	48 Gauge	75 Gauge	92 Gauge	Clear PET thin film	Metalized PET thin film
Thickness	ASTM-D374	μm	12	19	32	24	50
Yield		m^2/kg	59.35	38.02	31.25	60	31.25
Unit Weight	ASTM-E252	g/m^2	16.85	26.30	32.00	68.23	79.44
Tensile Strength (Ultimate)	ASTM-D882	MPa, MD TD	 186 234	 200 242	 187 276	97	106
Elongation at Break	ASTM-D882	%, MD TD	 110 80	 130 100	 140 80	122	130
Modulus	ASTM-D882	Mpa	3790	3790	3790		
Tear (Graves)	ASTM-D1004	G	300	400	500		
Haze	ASTM-D1003	%	4.5	6.5	9.0		
Clarity	ASTM-D1746	%	76	73	70		
Gloss (20°)	ASTM-D2457		200	180	150		
Shrinkage	30min in 150°C oven	%, MD TD	 2.2 1.3	 2.2 1.1	 1.6 1.6		
Oxygen Permeability	ASTM-D3985 22°C	cc/ m^2.day.atm	140	110	75		

Table 5: Typical Properties of Mylar MBP as specified by Du Pont [33]

It is known that the clear PET thin film has an additional layer of Linear Low Density Polyester (LLDPE) and that the metalized thin film was produced by evaporating a thin layer of Aluminium onto the PET core and laminating it on both sides with LLDPE. Comparing the measured results to the stated properties it is most likely that the clear film has a core of 48 Gauge Mylar MBP and the metalized film has a core of 75 Gauge Mylar MBP.

It can be seen that the clear PET has comparable yield strength to the material properties as stated by DuPont but the metalized PET yields at a much lower value. Combined with the higher elongation at break it is possible that the metalized PET has been co-polymerized to reduce the crystallinity of the film and increase the bond between the metal deposit and the PET layer.

5.2.1 Material physical properties

Tensile strength: The tensile strength of a material quantifies how much stress the material will endure before failing. This helps to assess a polymer's physical strength and durability. Although the strength and durability of the material is important its dimensional stability has greater implications for the performance of the antenna.

Young's modulus of elasticity: Young's Modulus quantifies the elasticity of the polymer. It is defined, for small strains, as the ratio of rate of change of stress to strain. The modulus is dependent on temperature.

As the intended application is a precision inflatable structure dimensional stability is critical. The dimensional stability of the material impacts the ability of the structure to maintain the relationship between the elements so the material must neither shrink nor creep due to the environmental conditions or the applied loads. As such it is not sufficient for the skin to carry the load due to the internal pressure and wind loading without failing, it must also carry the load without creeping.

The tests showed that both the clear and metalized thin films had a higher elongation at break than that stated by Du Pont. It is known that the clear PET thin film has an additional layer of LLDPE and the metalized thin film has two additional layers of LLDPE. LLDPE has a Young’s modulus of 0.2 GPa compared with PET which has a Young’s modulus of between 2 - 3.8 GPa [41]. When evaluating the results the elasticity of the material will be considered however it is not expected to have an adverse effect on the performance of the antenna as the load carried by the material due to inflation of the antenna is much lower than the loads applied during the material tests.

The inflatable antenna will operate at a pressure just above atmospheric. As the skin is the primary load bearer it must carry the stress due to the internal pressure. Referring to *section 2.2* the metalized thin film can withstand an internal pressure of 12.5 kPa without yielding. Beyond this pressure the dimensional stability of the structure cannot be maintained and the performance of the antenna will be reduced. In future tests it is recommended that a material with lower modulus of elasticity is tested.

5.2.2 Material electromagnetic properties

To verify that the polyester thin film selected can be used for communications applications it must be demonstrated that it satisfies electromagnetic as well as structural requirements. For the material to be used as a canopy it must be RF transparent at the operating frequency and if it is to be used as a reflector it must be metalized such that an RF signal is reflected without loss. From the equation for skin depth it was calculated that at least 0.24 μm of Aluminium must be deposited for a 12.5 GHz signal to be reflected without loss. The temptation is to deposit an Aluminium layer well in excess of the calculated minimum to ensure that the signal is fully reflected. The drawback with this is that a thicker metal layer is more likely to bend or fracture when it is stowed, creating permanent deformations or voids in the reflector surface and reducing the performance of the antenna.

The electromagnetic properties of the clear PET thin film and the metalized PET thin film were tested and the results presented in *section 4.2.2*. It was shown that between 12 - 13 GHz the clear thin film transmitted the signal without loss and the metalized thin film reflected the signal with a return loss of -43.6 dB. From these tests it was shown that at 12.5 GHz the electromagnetic properties of the material will have no impact on the performance of the inflatable antenna.

5.3 Testing of the inflatable antenna

Once it was shown that the material had both the structural and electromagnetic properties required to construct an antenna, it must then be demonstrated that an antenna can be manufactured from this material such that it matches the performance of a rigid antenna. As shape accuracy has a direct impact on the radiation patterns produced by an antenna, the radiation patterns of the gossamer structure will be compared to those of a rigid structure to indirectly assess the shape accuracy.

The flexible nature of the various components and the large number on new techniques being introduced made it important to test each component individually before combining them to help isolate the impact of the various new techniques and identify the limitations in the system. The first thin film component to be tested is the conical horn. The design of

the conical horn is presented in *section 2.4.3* and the manufacturing techniques are discussed in *section 3.5*. The horn is constructed from thin film and fed by a microstrip patch to further reduce the weight and stowed volume of the feed assembly and reduce the loading on the inflatable antenna. Before the gossamer horn can be tested it is important to understand the performance of the microstrip patch.

5.3.1 Microstrip patch

The use of a microstrip patch to feed a conical horn reduces the weight and stowed volume of the feed assembly and reduces the loading on the inflatable antenna it will be used to feed. The use of a microstrip patch instead of a waveguide also significantly reduces the manufacturing cost of the antenna. A literature review was conducted and no evidence was found of a microstrip patch being used to feed a horn.

The design of the microstrip patch is outside the scope of this investigation. Dr Kamran Ghorbani at RMIT University was approached to design a microstrip patch that would resonate at 12.5 GHz with low cross polar levels. The resulting patch design is presented in *section 2.4.6*. Further optimization of the patch design is required, but as this is a proof of concept it is sufficient to understand the performance of the patch so that its limitations can be differentiated from the limitations of the feed horn and the inflatable antenna.

The impedance characteristics of the patch were tested and the results are presented in *section 4.3*. It can be seen that the patch has a resonant frequency of 12.59 GHz and a maximum return loss of -18.00 dB which is within the acceptable limits. The microstrip patch has a bandwidth of 480 MHz. Patch antennas are not broadband devices, and the bandwidth characteristics of the patch will limit the bandwidth of the feed horn. From these results it was shown that the patch will operate at the design frequency of 12.5 GHz.

The radiation characteristics of the patch were then tested in the anechoic chamber at RMIT. These results are presented in *section 4.3*. Fig. 91 shows that the patch has a maximum gain of 7 dB at 20° and a gain of 5.5 dB in the forward direction. This decrease in gain in the forward direction will be considered when evaluating the radiation patterns for the conical feed horn fed by the microstrip patch, although the microstrip patch will be used as the feed in all future tests so the impact will be sustained uniformly throughout

testing. Once the characteristics of the microstrip patch were understood it was possible to use it as the feed for a conical horn.

5.3.2 Gossamer horn

A feed horn operates as a radiating body in the same way as an antenna. It is therefore suggested that the conical horn can be used to test the premise that a gossamer material can be used to construct an antenna that matches the performance of a rigid antenna under terrestrial conditions. Before this testing began it was necessary to demonstrate that using a microstrip patch was a viable method for feeding a conical horn.

A conical horn was chosen, as opposed to a rectangular horn, because the curved components of a conical horn distribute the load applied by the internal pressure evenly throughout the skin with a minimum of shape distortion. If a rectangular feed was used the natural tendency of a pressure vessel to evenly distribute the stress through the skin would cause the straight sides of the horn to pillow and the corners of the horn to round out, thus reducing the performance of the horn.

The design of the conical horn is presented in *section 2.4.3* and the manufacturing process is presented in *section 3.5*. The manufacturing processes used to construct the gossamer horn have implications for its performance. The method of construction must produce the desired shape and surface accuracy and then maintain it. The theoretical acceptable limit for surface inaccuracies is $\lambda/8$, where λ is the operating wavelength of the antenna. It can be seen that at lower frequencies where the wavelength is longer the seams present no problem but when the antenna is operating at higher frequencies the surface imperfection caused by the seams will reduce the performance. In *section 2.4.2* it was shown that at an operating frequency of 12.5 GHz the surface roughness must not exceed 3mm.

5.3.2.1 Pattern making

As the horn is being constructed from a flat, dimensionally stable gossamer material, the shape is established using pattern making techniques and seaming the panels together to form an enclosed structure which can then be inflated. A conical feed horn is a combination of a tubular section and a conical section. As both these geometric shapes

have curvature in only one direction, a flat pattern can be easily produced. Despite the simplicity of the geometry, care must be given to the accuracy of the seam allowance calculation and the cutting precision. Any deviation from the pattern will result in a variation in the final dimensions of the horn which in turn impacts on its performance. The individual pieces of the horn constructed to test the hypothesis were cut by hand using scissors. In a commercial context the pieces would be either laser cut or punched to increase the accuracy.

5.3.2.2 Assembly

Once the individual pieces were cut the horn was assembled. The flexible nature of the material made it difficult to assemble the components with accuracy. It was found that using a plug simplified this process whilst confirming the shape accuracy of the individual components as a plug is a rigid representation of the desired shape. Two plugs were machined to assist in the assembly of the horn, one for the conical section and one for the tubular section. *Fig. 104* shows the plug used to assemble the conical section of the feed horn.

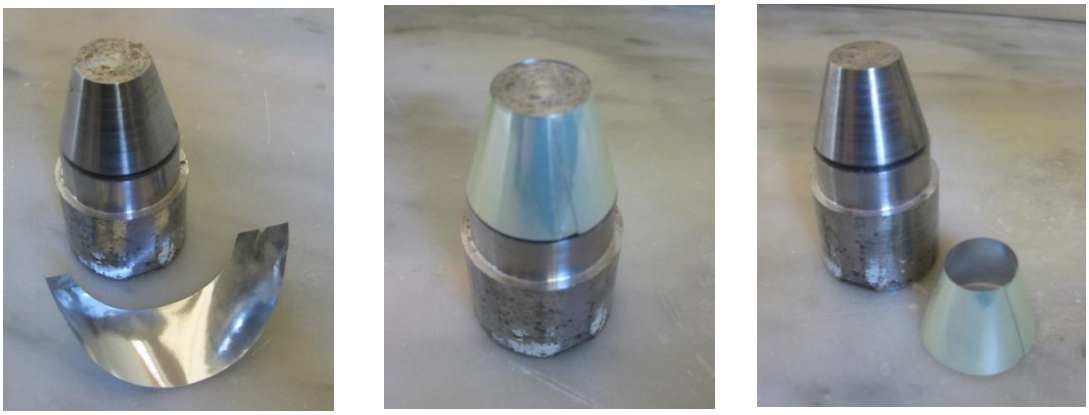

Fig. 104: Assembly of conical section of feed horn using a plug

As discussed in *section 2.4.2*, to maintain performance any surface discontinuity must be less than $\lambda/8$. The use of flat gores to construct the horn introduces a single seam on each component and a seam at the joint of the components. The challenge is to minimize the surface discontinuity due to the seams whilst ensuring the seams are strong enough to carry the load distributed through the skin. Ideally, the strength of the bond should

approach that of the material to prevent rupture; the seam should have the same flexibility as the material to prevent pillowing; and should introduce no surface discontinuity.

5.3.2.3 Tape

To reduce the stiffness of the seams and minimize pillowing a highly adhesive transfer tape was used to assemble the cone and the tube of the feed horn. Transfer tape is a pressure sensitive tape pre-applied to a special release liner. As the tape is applied to the first surface the release liner is removed ready for the second surface to be connected and pressure applied. As it has no backing it is highly flexible and can bond gossamer materials without causing localized stiffening. Transfer tapes are available with a variety of adhesive properties including high tack, high temperature resistance, exceptional moisture or solvent resistance and adhesion to low surface energy plastic. The tape used to construct the horn was adequate for testing in the laboratory, for field use the choice of tape would need to be revised.

Tape is strongest in plane or shear mode and weakest in tensile mode. *Fig. 105* shows the technique used for taping the gores together to form the components of the conical horn. It can be seen that each of the components are connected using lap joints and so all of these seams are loaded in shear.

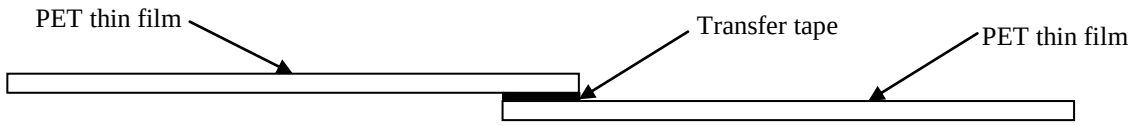

Fig. 105: Lap joint used to assemble conical canopy and feed horn

The seams have minimal impact on the flexibility of the surface, making it possible to achieve the desired shape with inflation. Taped lap joints are an effective assembly method for surfaces under low pressure, if the pressure is increased the loading on the seam is increased and the tape will fail. The inflatable horn operates at a very low pressure; in fact once deployed the horn is able to maintain its shape without internal pressure, so the use of taped seams is acceptable.

Transfer tape was also used to attach the feed horn to the microstrip patch. It is important to make sure that there is a cohesive connection between the horn and the patch to prevent the signal leaking. Transfer tape has a low profile and provides a strong bond and even coverage.

5.3.2.4 Heat welding

Transfer tape was used to assemble the cone and tube for the feed horn but the sharp joint between these components made the use of tape to connect them impractical. To maintain the performance of the horn the components must be connected with precision. Care must be taken to ensure there are no gaps between the components to prevent the signal leaking. Care must also be taken to ensure there are no sharp edges inside the horn that can scatter the signal.

Heat welding is a seaming technique widely used in the film packaging industry to produce complex shapes with high precision. It can be used to produce bonded joints with mechanical properties that approach those of the base material. Heat welding uses a combination of temperature and pressure to, melt two thermoplastic layers, force them to combine, and then allow the combined layer to harden to an extremely strong bond. Heat welding can be divided into two main groups:

1. Processes involving mechanical movement – ultrasonic welding, friction welding, vibration welding.
2. Processes involving external heating – hot plate welding, hot gas welding and resistive and implant welding.

If the correct material was available, and a technique such as ultrasonic welding was used, it would be possible to assemble the entire antenna using heat welding. Ultrasonic welding was not available. The assembly of the gossamer feed horn was achieved using a crude form of heat welding. A hot glue gun was used to apply a line of hot glue to the connection between the individual components of the feed horn. The hot glue melted the LLDPE layer and as the glue and the LLDPE cooled they combined to form an adequate bond. This technique would not be suitable for commercial use as it is neither strong enough nor accurate enough but is acceptable to demonstrate the concept.

5.3.2.5 Testing

To test the ability of a microstrip patch to feed a conical horn a rigid Aluminium horn was tested using a microstrip patch. Testing conducted using an earlier patch design compared the impedance characteristics of a rigid Aluminium horn fed by a microstrip patch, a gossamer horn fed by the same patch and a gossamer horn that had been crushed and then returned to its original shape, also fed by the same patch. The crushed horn was tested to investigate the impact of stowing a horn and then deploying it. From *Fig. 89* it can be seen that the system of horn fed by microstrip patch was well matched and that the gossamer material had no impact on the impedance characteristics of the system. It can also be seen that even when the gossamer horn is crushed excessively, generating more creases than normal stowage would cause, the impedance characteristics are not adversely affected.

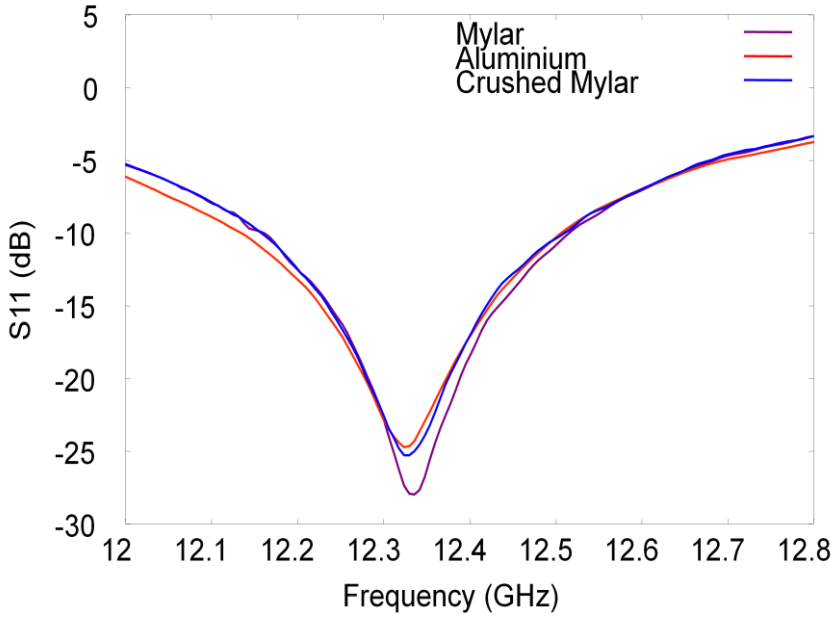

Fig. 89: Impedance characteristics of an Aluminium horn fed by a microstrip patch, a gossamer horn fed by a microstrip patch and a crushed gossamer horn fed by a microstrip patch (reproduced from section 4.4)

Once it was confirmed that a microstrip patch could be used to feed a conical horn without sacrificing performance the ability to manufacture a radiating structure from gossamer materials could be tested. The conical feed horn was tested first because of its structural simplicity. Structures with straight sided components such as the conical horn can be manufactured using flat panels or gores. The shape accuracy of the inflated structure is

then largely dependent on the accuracy of the pattern and the manufacturing technique, and the dimensional stability of the material.

The impedance characteristics of the horn fed by the microstrip patch were tested and the results presented in *section 4.4*. *Fig. 88* is reproduced below and shows that the combination of the patch and the gossamer horn has better impedance characteristics that the patch alone, showing that the system is well matched. The combination of the patch and gossamer horn has a slightly narrower bandwidth of 390 MHz than the patch alone at 500 MHz, but the impedance graph confirms that the horn will operate at the design frequency of 12.5 GHz. The test showed that the horn patch combination has a resonant frequency of 12.576 GHz with a return loss of -29.91 dB so all radiation testing will be conducted at this frequency.

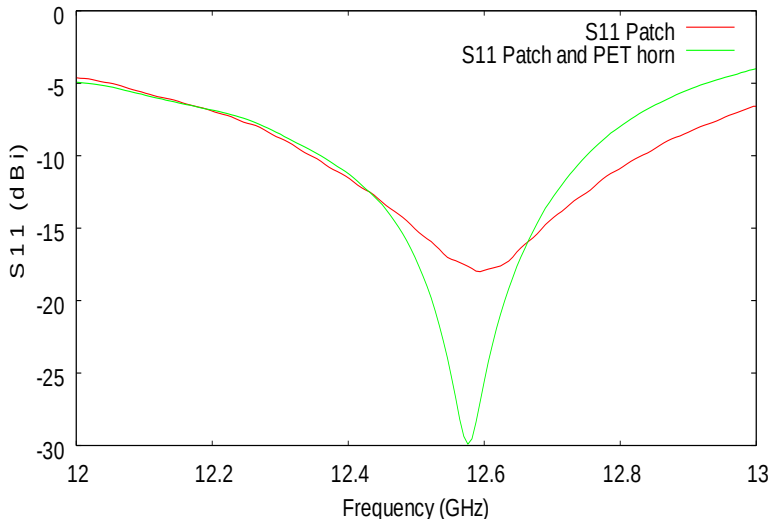

Fig. 88: Impedance characteristics of microstrip patch and gossamer horn fed by microstrip patch (reproduced from section 4.4)

These results confirmed the results generated in the simulation although the resonant frequency is a little higher than that predicted by the simulation. For simulated results refer to *section 4.1.2*.

Once it was confirmed that a microstrip patch can be used to feed a conical horn without affecting the impedance characteristics it was then possible to consider the radiation patterns. The impedance testing identified 12.576 GHz as the resonant frequency. The rigid Aluminium horn and the gossamer horn fed by the same microstrip patch were tested

in the anechoic chamber at RMIT at 12.576 GHz and the results normalized with respect to a standard gain horn. The tests were conducted in an anechoic chamber to eliminate the impact of wind. The antenna system is ultimately required to operate reliably under all environmental conditions; however before the impact of environmental conditions such as wind and rain can be considered the impact of the material and the structural design must be fully understood.

The radiation patterns for the Aluminium horn fed by the microstrip patch are presented in *section 4.4 Fig. 90* shows that the horn produced a symmetrical radiation pattern with a maximum gain of 13.23 dBi, a beamwidth of 47° and a 10 dB beamwidth of 83°. Referring to *section 2.4.3* the horn was designed to have a 10 dB beamwidth of 73.6° which would produce a theoretical maximum gain of 12.55 dB.

It is not proposed that the measured horn is performing better than theoretical; the discrepancy in gain is within the margin of error. The results do show that it is possible to use a microstrip patch to feed a conical horn without sacrificing gain. The 10 dB beamwidth of the Aluminium horn is broader than desired so if this horn were used as the feed for the design antenna the parabolic reflector would be slightly overfed, producing some spillover. The cross polar characteristics of the system have been defined with a front to back ratio of 10 dB. Once the cross polar characteristics of the system are understood any additional cross polar radiation generated by using a gossamer structure can be identified.

A gossamer horn of the same dimensions and fed by the same microstrip patch was then tested at the same operating frequency. The radiation patterns for the Aluminium horn fed by the microstrip patch are presented in *section 4.4.*

From *Fig. 91* it can be seen that the horn produced a symmetrical radiation pattern with a maximum gain of 12.1 dBi, a beamwidth of 40.5° and a 10 dB beamwidth of 88° in the H-plane and 79° in the E-plane. Referring to *section 2.4.3* the horn was designed to have a 10 dB beamwidth of 73.6° which would produce a theoretical maximum gain of 12.55 dB.

The simulation indicated that a rigid conical horn fed by a microstrip patch would produce a maximum gain of 13.72 dB and a half power beamwidth of 38°. The 10 db beamwidth of

the simulation was 77 dB. The measured gain of the gossamer horn compares well with the theoretical value of 12.55 dB and the simulated gain of 13.78 dB. It also compares well with the measured gain of the Aluminium horn of 13.23 dBi. The beamwidth of the gossamer horn was slightly narrower than the Aluminium horn at 40.5°. The results show that it is possible to use a metalized gossamer material to construct a conical horn with a small sacrifice in gain. The 10 dB beamwidth of the gossamer horn is broader than desired in both the E-plane and H-plane, so if this horn were used as the feed for the design antenna the parabolic reflector would be slightly overfed, producing some spillover. The variation in the two planes means the antenna will experience greater spillover in the H-plane than in the E-plane.

As expected the cross polar characteristics of the gossamer horn are not as good as the rigid horn with cross polar radiation being observed in all planes. An increase in cross polar radiation was expected due to the flexible nature of the structure. The question is whether the increase in cross polar radiation is workable and whether the increase in achievable gain and portability outweigh any increase in cross polar radiation. The highest cross polar radiation was observed in the 45-plane with a front to back ratio of 9 dB. This is high for a rigid horn when the weight and stowed volume of the patch fed horn are considered it is acceptable.

A comparison between the E and H-plane radiation patterns of the rigid and gossamer horns is presented in *section 4.4 Fig. 92* shows that the use of gossamer materials produced nearly a 2 dB decrease in gain and an increase in the side lobe level.

It has been shown that the use of a gossamer structure produces a small loss in the gain of the horn. Next the impact of using a gossamer structure on the shape of the radiation pattern will be examined. To compare the shape of the radiation patterns more closely the simulated and measured radiation patterns from the rigid and gossamer horns were normalised and compared. *Fig. 106* shows a comparison of the shape of the radiation patterns in the E, H and 45-planes.

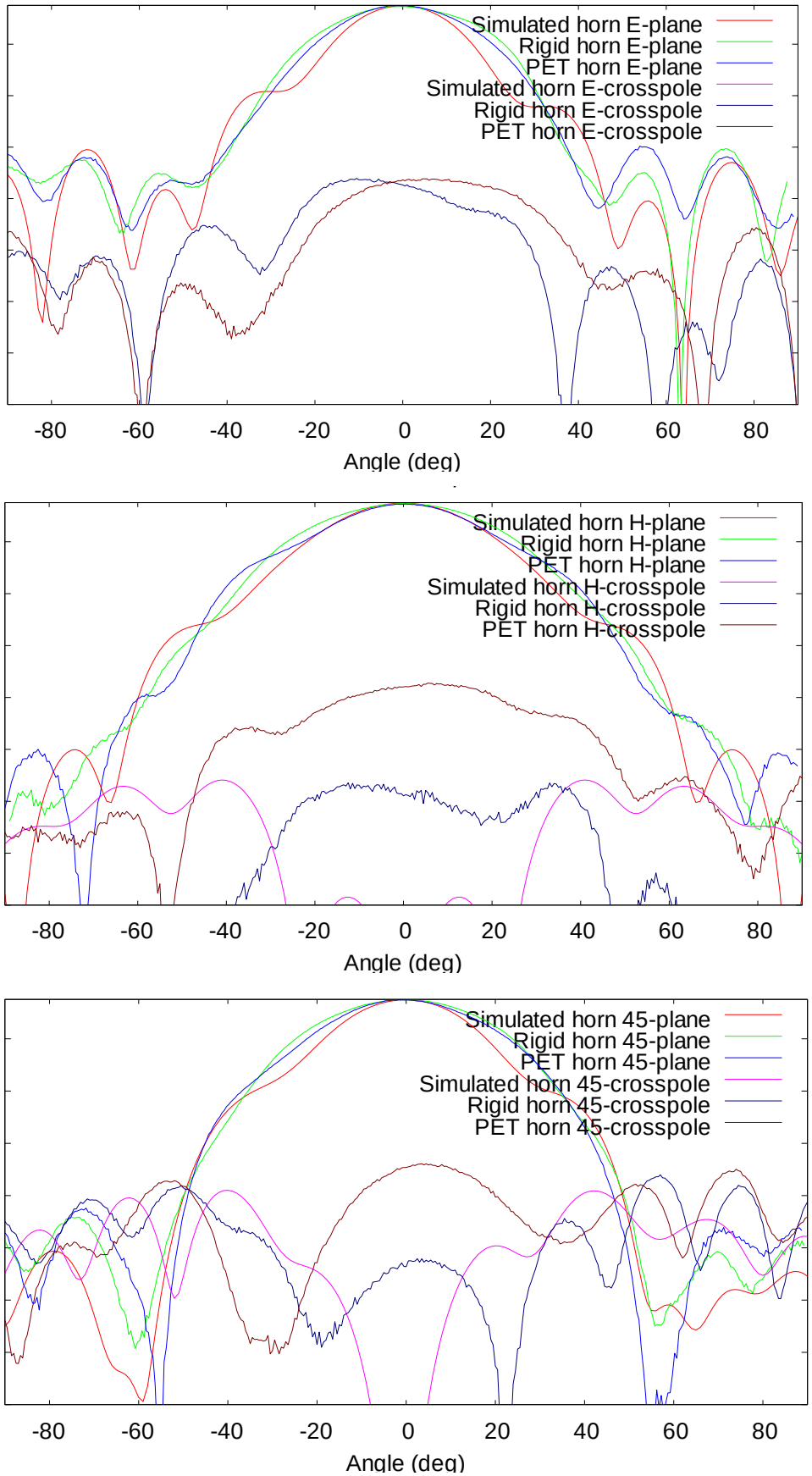

Fig. 106: Comparison of normalized radiation patterns for a simulated, rigid and gossamer conical horn fed by a microstrip patch operating at 12.576 GHz

From these results it can be seen that the use of a gossamer structure has minimal impact on the shape of the radiation pattern indicating that the shape accuracy of the conical horn was good and that it was maintained under the effects of gravity. It can therefore be concluded that as long as the metalized layer is of sufficient thickness [40] it is possible to use a polymer thin film to construct a conical feed horn that provides the dimensional accuracy and structural stability required for communication under the influence of gravity.

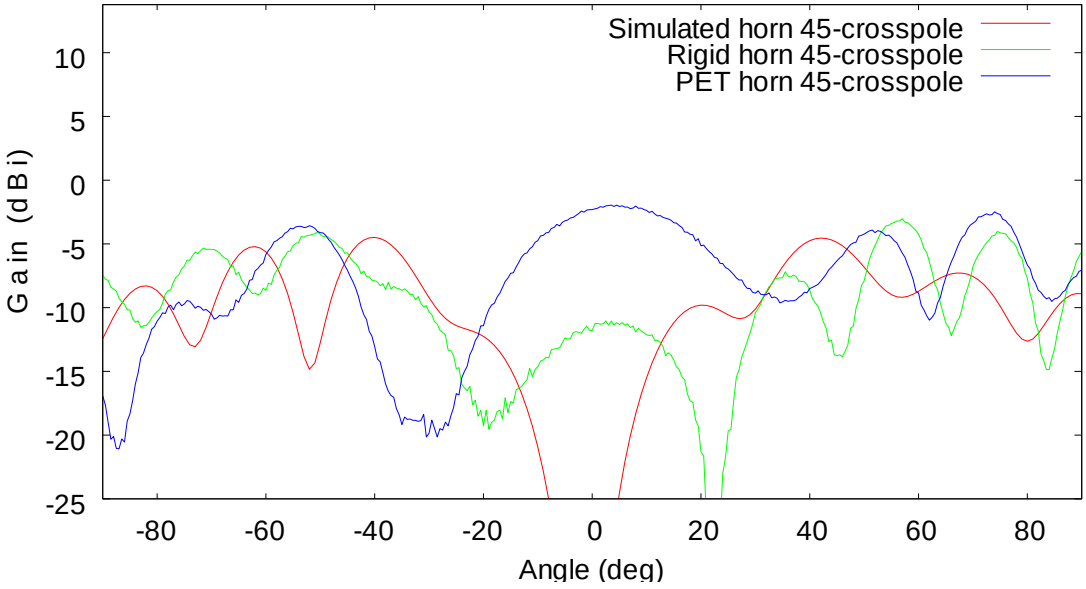

Fig. 107: Comparison of cross polar performance of simulated, rigid and gossamer horns

It can further be concluded that a microstrip patch can be used to feed such a horn to produce an ultra lightweight, low cost feed system. The rigid Aluminium horn and patch weighed 124.6g whilst the gossamer horn and patch weighed 1.5g. The loss in gain due to the use of a thin film could be easily compensated for by increasing the aperture of the horn with little or no additional weight.

These results demonstrate that it is possible to manufacture an antenna from gossamer materials that matches the performance of an identical rigid antenna. At this point the results are limited to an antenna with curvature in one dimension. The next step is to construct and test an inflatable parabolic dish antenna which has curvature in two dimensions. Now that the performance of the feed system is defined it can be incorporated in the inflatable antenna to further reduce the overall weight and stowed volume.

5.3.3 Inflatable antenna

The success of the gossamer horn as a radiating body demonstrated that it is possible to construct an antenna with curvature in one dimension, such as a conical feed horn, from thin film material that matches the performance of an identical rigid antenna. The next step is to demonstrate that an antenna with curvature in two dimensions can be manufactured from thin film material that matches the performance of an identical rigid antenna.

A parabolic reflector constructed from polyester thin film was tested and compared to an identical rigid parabolic reflector. As the performance of the gossamer horn was now defined it was used to feed both the inflatable and rigid antennas.

In the ultimate Cassegrain configuration the canopy will support the sub-reflector at its apex. To test the shape accuracy of the parabolic reflector it was initially tested as a prime focus antenna with the clear canopy supporting the gossamer feed horn. With the behavior of the feed horn and the canopy understood and the rim of the antenna constrained the performance of the parabolic reflector was investigated.

As with the gossamer horn the radiation patterns were used to indirectly assess the shape and surface accuracy. The radiation patterns were measured and compared to those of an identical rigid reflector. Simulations were generated to help differentiate the impact of various factors such as aperture blockage, pillowing and struts in the measured radiation patterns for the antenna. These simulated results are presented in *section 4.1.6*.

5.3.3.1 Pattern making

To manufacture a gossamer parabolic dish, a surface with curvature in two directions must be constructed from a flat, dimensionally stable material. This requires either a gored construction or forming the dish as a single entity. As the antenna is being constructed from a flat, dimensionally stable gossamer material, the shape is established using pattern making techniques and seaming the panels together to form an enclosed structure which can then be pressurized. To construct a parabolic reflector, the curvature is generated using shaped gores which are then seamed together. The pattern for the parabolic reflector was

created by producing a CAD model and then using a feature of the software to unwrap the surface and generate a flat pattern.

The shape accuracy is restricted by the number of gores, as the number of gores is increased the shape approaches the design. However, as the number of seams is increased surface discontinuities are introduced and the potential for seams to rupture is increased. This becomes compromise between more gores offering better shape accuracy and less gores offering better surface accuracy. For the 0.5m dish constructed for testing, 6 gores were chosen as the best compromise. The introduction of seams also introduces the same pillowing effect experienced in articulated antenna dishes however the flexibility of the seams reduces the localized stiffness, which minimizes this effect.

The acceptable limit for surface inaccuracies is $\lambda/8$, where λ is the operating wavelength of the antenna. It can be seen that at lower frequencies where the wavelength is longer the seams present no problem but when the antenna is operating at higher frequencies the surface imperfection caused by the seams will reduce the performance. In *section 2.3* it was shown that at an operating frequency of 12.5 GHz the surface roughness must not exceed 3mm.

5.3.3.2 Forming the parabolic reflector

The inflatable antenna design presented is constructed using individual gores which are then assembled using transfer tape. These seams produced surface and shape inaccuracies and degrade the performance of the antenna. To maximize the performance of the antenna forming the dish as a single entity was explored. Forming the dish as a single entity has the added advantage of reducing the number of seams that can rupture and cause the structure to deflate.

To successfully produce a reflector as a single entity requires the ability to accurately shape the material without sacrificing any of the physical or electromagnetic properties. Mackenzie et al [42] attempted to cast a self-metalizing polyamide film. This approach achieved some success but demonstrated that it was difficult to control the distribution of the metal particles, which limited their ability to produce a uniform reflective surface.

Using the thermal properties of Polyester films makes it possible to thermoform a dish under temperature and pressure. When the film is re-heated beyond its glass transition temperature T_g the crystal structure relaxes and the material becomes ductile. In this state the film can be formed. It is necessary to then rapidly cool the material to prevent crystallization. Should the material crystallize it becomes brittle and is no longer foldable. Crystallization can also be reduced with the addition of co-polymers. However with the addition of co-polymers dimensional stability of the film is sacrificed and the material becomes more ductile.

The success of this process with a pre-metalized film relies on the strength of the bond between the base film and the metal layer. The inert nature of PET can cause the bond between the polymer and the metal coating to be quite weak. The difference in the coefficient of thermal expansion between the film and the coating can cause the coating to delaminate. Should the metal layer delaminate and fracture the reflective characteristics of the surface are compromised and any improvement gained through increased shape accuracy is lost. As the material is orthotropic the material properties vary in the longitudinal and transverse directions and forming a uniform paraboloid becomes difficult. The other alternative is to metalize the film after it has been formed. This increases the complexity of the metal deposition and makes it hard to achieve a uniform reflective layer.

When the antenna is intended for use at lower temperatures metalized Orientated Polypropylene (OPP) can be substituted for PET. The bond between the metal layer and the OPP is much stronger, causing the metal to draw rather than fracture, and thus maintaining the integrity of the reflective surface.

Some initial experiments were conducted using the metalized PET but the metalized layer fractured. This is suggested as an area for further investigation but for the purpose of this investigation the manufacturing method will be limited to a gored construction.

5.3.3.3 Assembly

As with the horn a plug was used to facilitate the assembly of the parabolic reflector. The plug was produced from the CAD model using a CNC machine and provided an accurate representation of the parabolic reflector. Guidelines were marked on the plug as shown in

Fig. 108 to help position the gores, and transfer tape with an additional strip of PET film was used to connect the gores as presented in *Fig. 109*. A butt join with a reinforced strip on the back was used to minimize any discontinuities on the surface of the reflector whilst providing a strong join that won't rupture. The use of the metalized PET for the strip on the back of the reflector ensures that there is no gap in the reflector surface where the signal will not be fully reflected.

Fig. 108: Assembly of parabolic reflector from thin film gores using a plug.

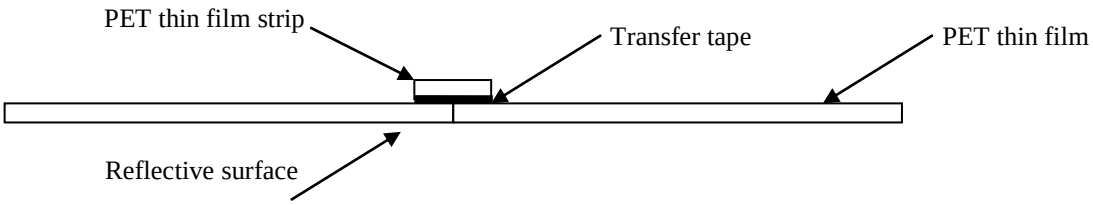

Fig. 109: Lap joint used to assemble gores in parabolic dish reflector

This procedure can be replicated for antennas of any size and curvature but the greater the curvature the more gores that are required. This method of construction is adequate for surfaces under low pressure; the strength of the tape limits the pressure the seams can carry without rupturing. The antenna operates at very low pressure and so this method of construction is suitable for testing purposes. It is recommended that the use of heat welded seams be investigated. Heat welding would provide a stronger seam but it would need to be demonstrated that the required shape and surface accuracy could be achieved.

5.3.3.4 Testing

The premise that it is possible to manufacture a gossamer parabolic reflector that matches the performance of a rigid parabolic reflector under terrestrial conditions was tested by integrating the two reflectors into separate prime focus antennas of identical design and measuring their performance. These results can then be compared to evaluate the shape accuracy and stability of the gossamer reflector. The performance of a parabolic dish antenna is related to the shape and surface accuracy of the dish and the ability to maintain the dimensional relationship between the feed and the reflector. Any deviation from the design will result in a reduction in gain, an increase in side lobe level, an increase in cross polar level and an increase in beamwidth. These are the factors that are used to assess the shape accuracy of the gossamer dish and the ability of the conical canopy to accurately position the feed horn. The radiation patterns of the gossamer antenna will be compared to the radiation patterns of a rigid antenna of the same design and the simulated results.

Both antennas were tested using the same support stand and both used the gossamer horn as the feed. The tests were conducted in an anechoic chamber to eliminate the impact of wind and other environmental factors. It will be necessary for the final antenna system to operate reliably under all environmental conditions however initially it is important to understand the impact of gravity alone.

All rigid prime focus antennas require the feed assembly to be supported at the focal point of the reflector. The feed assembly and the support strut, or struts, cause aperture blockage and scattering of the signal which reduces gain and increases side lobe level. When testing the rigid parabolic reflector the feed horn was positioned at the focal point using an adjustable stand. When testing the inflatable antenna the feed horn was supported by the clear canopy. The clear canopy is also used to create an enclosed environment which can be pressurized to generate the curvature of the gossamer reflector.

Radiation patterns were measured for both the inflatable and rigid parabolic antennas in the E-plane and H-plane. The results of these tests are presented in *section 4.5*.

Fig. 93 shows the measured radiation patterns for the rigid prime focus antenna fed by the gossamer horn. It can be seen that the rigid antenna produced a maximum gain of 23.8 dBi,

and a beamwidth of 4.4°. Referring to *section 2.4.3* the theoretical gain of the antenna is 35.35 dB and the beamwidth is 3.36°.

The aperture blockage due to the horn is consistent between the rigid and inflatable antennas but the horn support stand introduces additional aperture blockage in the rigid antenna. To understand the impact of the stand on the radiation patterns a series of simulations were generated with different feed support configurations. These results can be reviewed in *section 4.1.6* and a summary is presented in *Fig. 110*.

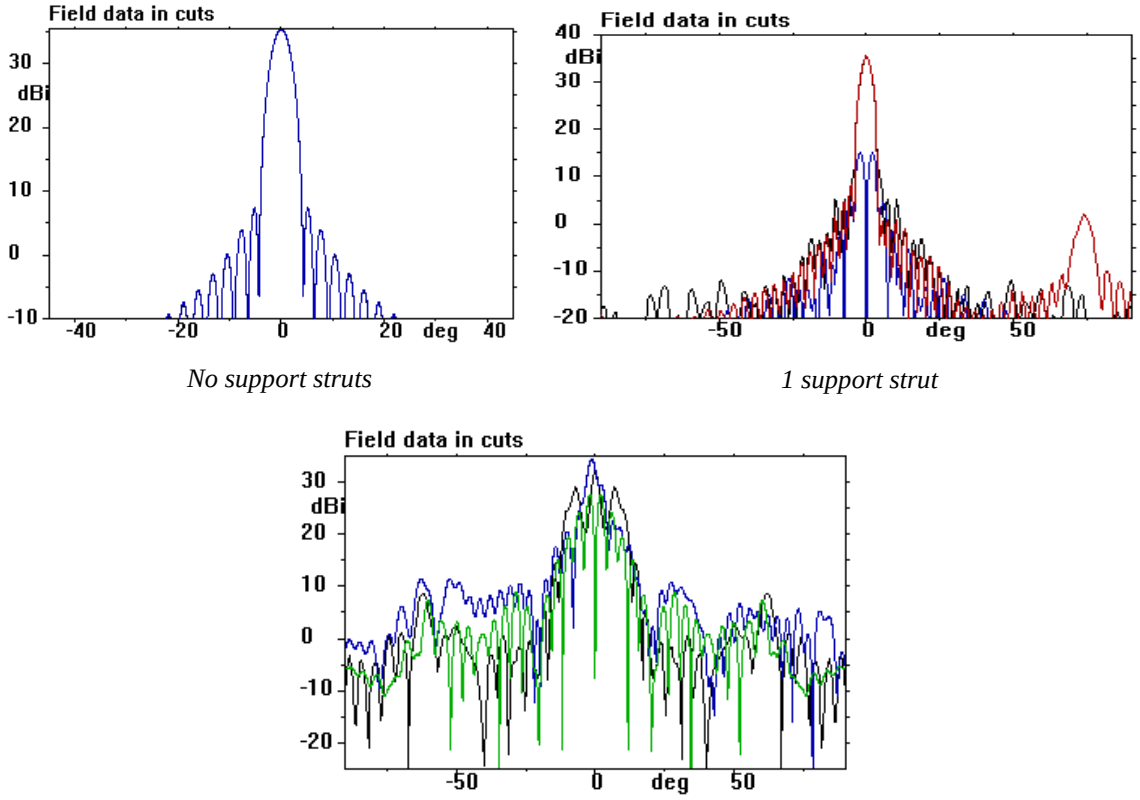

No support struts

1 support strut

3 support struts

Fig. 110: Summary of simulated results showing the impact of feed support struts on the radiation pattern of a prime focus antenna

From the simulations in *Fig. 110* it can be seen that the introduction of a feed support introduces aperture blockage and scattering of the signal, reducing the gain of the antenna and increasing the number of side lobes and the side lobe level. This is consistent with what is observed in the radiation patterns. In the rigid antenna radiation pattern, the very

high side lobe observed at -4.5°, which is merging with the main beam, can be attributed the feed support.

From the tests conducted on the gossamer horn it is known that the 10 dB beamwidth of the horn is broader than desired in both the E-plane and H-plane. It is therefore expected that both the rigid antenna and the inflatable antenna will be overfed and the radiation patterns will show signs of spillover. The 10 dB beamwidth of the horn is broader in the H-plane than the E-plane and so it is expected that the antenna will experience greater spillover in the H-plane than in the E-plane. The higher side lobe levels in H-plane plots support this. Other factors that contribute to a loss in gain and an increase in side lobe level are misalignment of the feed and the reflector, and distortions in the main reflector due to gravity.

Fig. 94 shows the measured radiation patterns for the inflatable prime focus antenna fed by the gossamer horn. It can be seen that the inflatable antenna produced a maximum gain of 28.9 dBi, and a beamwidth of 3.04°. Referring to *section 2.4.3* the theoretical gain of the antenna is 35.35 dB and the beamwidth is 3.36°. From *Fig. 93* it can be seen that the rigid prime focus antenna had a measured gain of 23.8 dBi and a beamwidth of 4.4°.

It is not surprising that the gain of the inflatable antenna did not match the theoretical value. What was unexpected is that the inflatable antenna produced a gain 5 dB higher than the rigid antenna. Any loss in shape accuracy or misalignment of the feed with respect to the reflector results in a decrease in gain. Comparing the gain of the rigid and inflatable antennas indicates that the inflatable antenna experienced minimal loss in gain due to shape accuracy or misalignment. The cross polar radiation produced by the gossamer horn will contribute to a reduction in gain but as the horn is being used to feed both antennas any reduction in gain due to the horn will be consistent between the two antennas.

Fig. 111 presents a comparison of the radiation patterns for the rigid antenna and the inflatable antenna. This comparison clearly shows the reduction in gain for the rigid antenna. It also shows that the overall shape of the radiation patterns for the two antennas compare well. Both main beams are positioned at 0° and both antennas have a narrow beamwidth that is close to design. The side lobe level in both planes of both antennas is at

least 15 dB down from the maximum gain, and so will have little impact on the performance of the antenna.

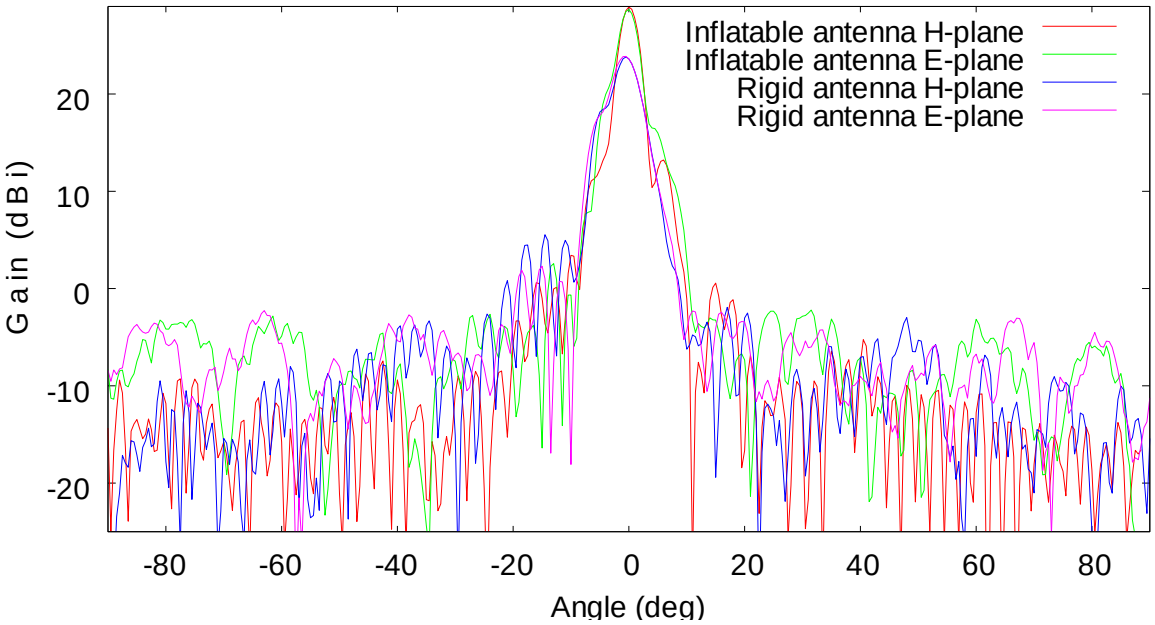

Fig. 111: Comparison of the radiation patterns of the inflatable prime focus parabolic dish antenna fed by gossamer feed horn and the rigid prime focus parabolic dish antenna fed by gossamer feed horn both operating at 12.5GHz

The next step is to use the radiation patterns to identify if the inflatable antenna has experienced a loss in performance due to misalignment of the feed and reflector, loss of shape accuracy or surface accuracy on the radiation patterns. To facilitate this comparison *Fig. 112* shows the H-plane radiation plots for the rigid and inflatable antennas and *Fig. 113* shows the E-plane radiation plots for the rigid and inflatable antennas.

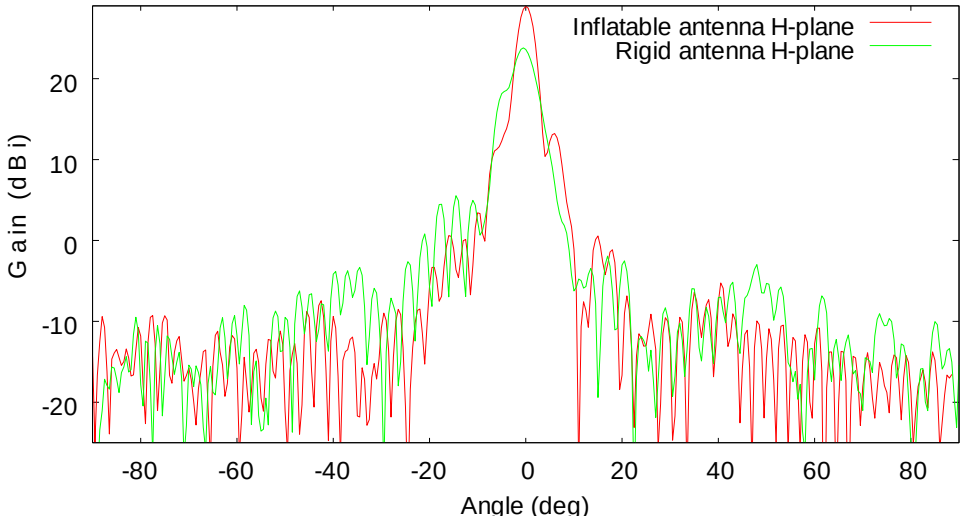

Fig. 112: Comparison of the H-plane radiation patterns of the inflatable prime focus parabolic dish antenna fed by gossamer feed horn and the rigid prime focus parabolic dish antenna fed by gossamer feed horn both operating at 12.5GHz

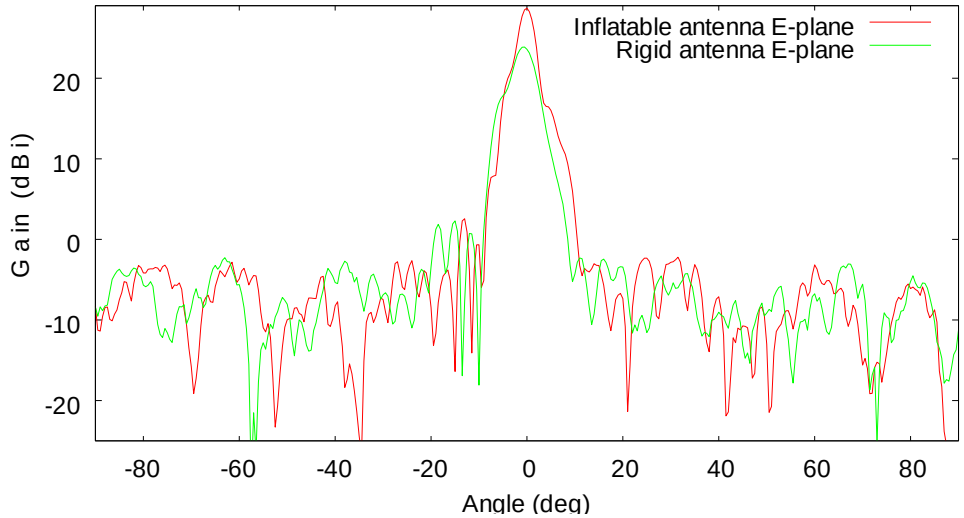

Fig. 113: Comparison of the E-plane radiation patterns of the inflatable prime focus parabolic dish antenna fed by gossamer feed horn and the rigid prime focus parabolic dish antenna fed by gossamer feed horn both operating at 12.5GHz

The inflatable antenna uses a clear conical canopy to create an enclosed environment which can then be pressurized to give the whole structure rigidity and shape the parabolic reflector. If this antenna deforms under the influence of gravity the parabolic dish will suffer shape deformation and the feed and reflector will become misaligned. The positioning of the feed at the apex of the canopy places an extra load on the canopy which will be eliminated in the Cassegrain configuration. This additional loading increases the impact of gravity on the inflatable antenna. Misalignment of the feed and reflector would

be observed as a reduction in gain, broadening of the main beam and increase in side lobe level. From the radiation patterns these effects were more obvious in the rigid antenna.

The results suggest that the inflatable antenna experienced little reduction in performance due to the impact of gravity. The results also suggest that the conical cone maintained the alignment of the reflector and the feed.

The greatest concern with respect to the shape and surface accuracy of the gossamer parabolic reflector was the gored construction. The gossamer parabolic reflector was constructed from individual gores that were taped together. The seams between the gores have the potential to reduce the surface accuracy as well as reduce the shape accuracy due to pillowing. Pillowing is a common problem in articulated antenna dishes where the local stiffness of the ribs, compared to the flexibility and weight of the mesh, imparts a distortion [13]. When working with membrane structures the seams are commonly either taped or heat welded, giving some flexibility. This reduces the localized stiffness and the effect of pillowing but does not eliminate it. To understand the effects of both ribs and pillowing on the performance of the antenna a series of simulations were performed. Full results are presented in *section 4.1.6* and a summary is presented in *Fig. 114*.

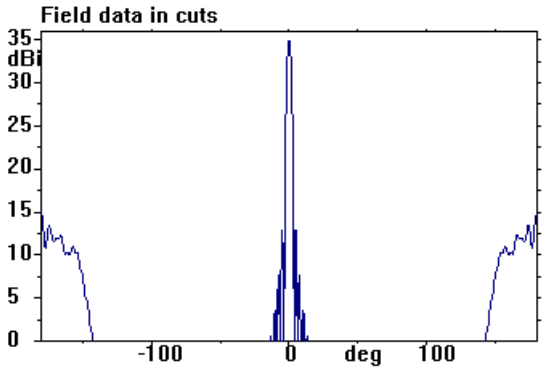

No ribs, no pillowing

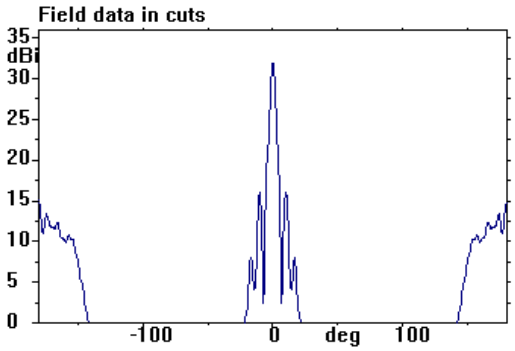

8 ribs, with pillowing

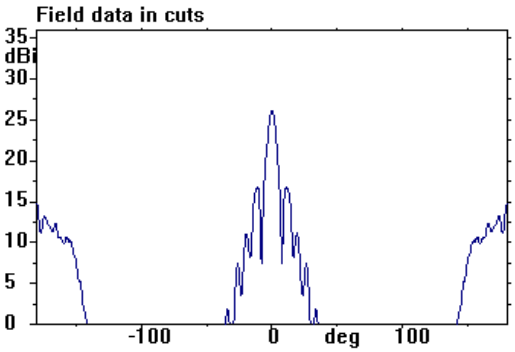

8 ribs, no pillowing

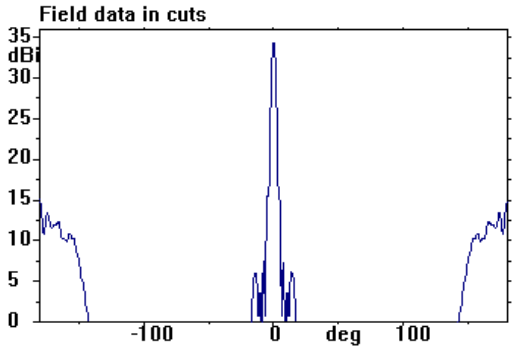

12 ribs, no pillowing

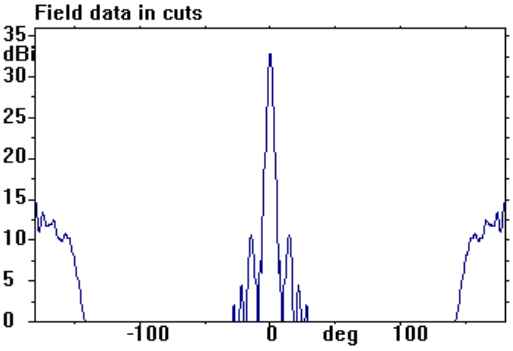

12 ribs, with pillowing

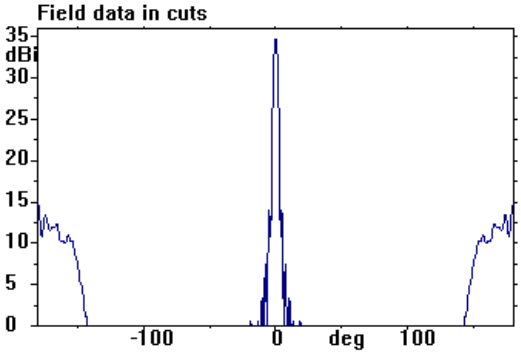

16 ribs, no pillowing

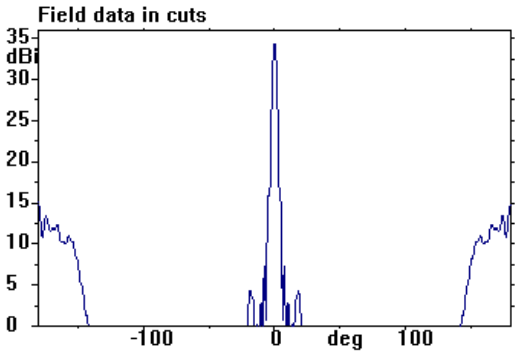

16 ribs, with pillowing

Fig. 114: Summary of simulated results showing the impact of ribs and pillowing on the radiation pattern of a prime focus antenna

The simulated results showed that the introduction of ribs has a measurable impact on the performance of the antenna but the introduction of pillowing had a significant impact. The simulated results showed that when ribs are used in an antenna but there is no pillowing it is better to minimize the number of ribs in order to maximize performance. When pillowing is introduced the effects are reduced when the number of ribs is increased. The increase in the number of ribs reduces the distance between them and hence the deformation of the reflector surface between them.

The radiation patterns in *Fig. 112* and *Fig. 113* show that the impact of pillowing on the gossamer dish is minimal. Some reduction in gain, increase in beamwidth, increase in side lobe number and level could be attributed to pillowing but it is suggested that when comparing the inflatable antenna radiation patterns to those of the rigid antenna the common factors of aperture blockage and spillover far outweigh the impact of pillowing.

The last factor to consider is cross polar radiation. The cross polar radiation is a good measure of the alignment of the antenna and its shape and surface accuracy. *Fig. 115* shows the measured co-polar and cross polar radiation patterns for the inflatable antenna. The results show that the antenna experience high cross polar radiation levels but that the antenna had a front to back ratio of 16.55 dB. Some of the cross polar radiation measured in the antenna can be attributed to the horn and subsequently to the microstrip patch.

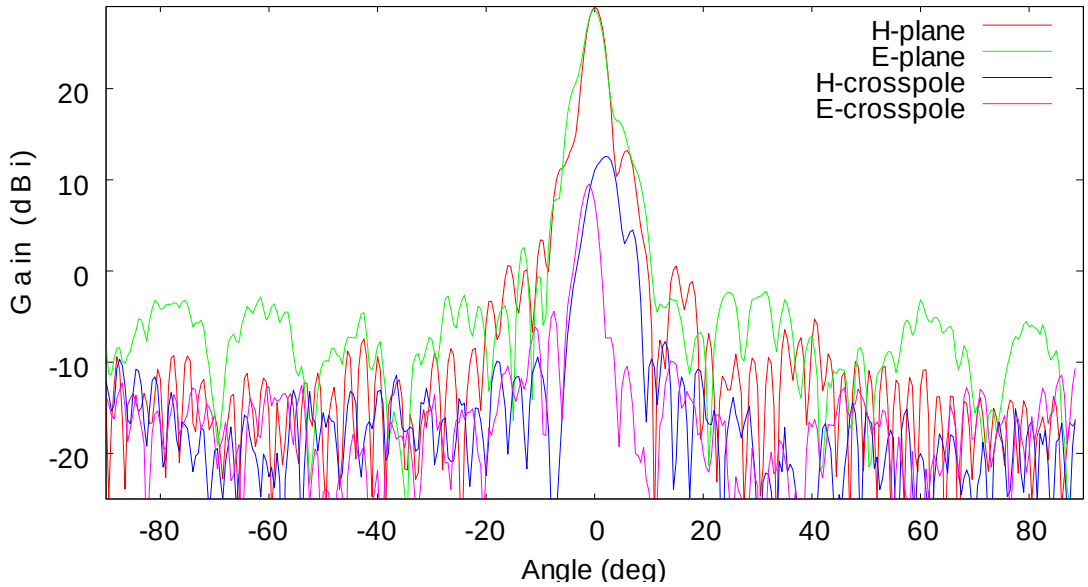

Fig. 115: Co-polar and cross-polar radiation patterns of inflatable prime focus parabolic dish antenna fed by gossamer feed horn operating at 12.5GHz

The results obtained from these tests were very encouraging and although they showed that there are many areas that need to be further developed and refined, they also showed that it was possible to construct a reflector with curvature in two directions from gossamer material that could match the performance of a rigid dish under the influence of gravity.

The prime focus antenna is not the intended design for operation as a direct satellite antenna but it has successfully demonstrated that it is possible to manufacture an inflatable antenna that matches the performance of a rigid antenna of the same design. In the case of the rigid antenna used for comparison the inflatable antenna performed better than the rigid antenna.

The light weight and high packing efficiency of inflatable structures facilitates the construction of larger structures that can then be stowed for transportation. As antenna gain is directly related to the diameter of the dish any loss in performance due to shape distortion can be compensated for by an increase in size without sacrificing portability. *Table 4* shows the comparison of weight and stowed volume for a variety of parabolic reflectors.

Type of Dish	**Weight**	**Stowed Volume**
Rigid Aluminium	5kg	$0.05m^3$
Grid Aluminium	3kg	$0.05m^3$
Mesh	1.9kg	$0.0125\ m^3$
Inflatable	12g	$80 \times 10^{-6}\ m^3$

Table 6: Comparison of weight and stowed volume for a variety of 0.5m diameter parabolic dish reflectors

Before progressing to the manufacture of a Cassegrain antenna and the appropriate conical horn to feed this antenna it is suggested that further refinement and testing be performed on the microstrip patch, the gossamer horn fed by the microstrip patch and the manufacturing techniques used to produce the gossamer reflector.

Although the final Cassegrain configuration wasn't tested the results from the inflatable prime focus antenna showed that it is possible to manufacture an inflatable antenna fed by

a gossamer horn, which in turn is fed by a microstrip patch, that produces the shape and surface accuracy and maintains the dimensional stability required to match the performance of an identical rigid antenna under terrestrial conditions. Most importantly this was achieved with an antenna that weighed a little over 12g that can be stowed in a package the size of a CD case, thus providing the potential of truly portable direct satellite communication.

6 Future Work

The objective of this investigation is to investigate the possibility of using an inflatable antenna for portable direct satellite communication under terrestrial conditions. The tests conducted on the gossamer horn and inflatable prime focus antenna demonstrated that it is possible to construct an inflatable structure from gossamer materials that maintains the shape and surface accuracy, as well as the dimensional stability required to operate as an antenna under terrestrial conditions.

Although it was demonstrated that the concept was possible there remains a number of investigations that must be completed to move from a proof of concept antenna to a commercial prototype.

Inflatable torus

The ability of an inflatable torus to provide the necessary rim support for the antenna must be tested and the results compared to the rigid support. It is possible that depending on the operational circumstances and the tracking system used both types of rim support could be viable.

Dual reflector configuration

It was demonstrated that the inflatable structure could maintain the dimensional relationship between the feed horn and the primary reflector under the influence of gravity. For the design presented to be realized, the ability of the inflatable structure to maintain the dimensional relationship between the feed horn, a sub-reflector and the primary reflector must be tested. Further testing could then be undertaken to compare the performance of inflatable Cassegrain and Gregorian antennas as well as inflatable offset antennas.

Environmental conditions

The inflatable antenna performed well under the influence of gravity. It must then be demonstrated that the antenna can operate reliably under the influence of the full range of environmental conditions. This includes both the performance of the overall structure and the material.

The impact of environmental factors on the physical and electromagnetic properties of polymers is best addressed during the material selection process. The impact of environmental conditions on the shape accuracy and the relative dimensional stability of the antenna components can be influenced directly by environmental conditions like wind or indirectly by the operating temperature increasing the internal pressure.

The impact on performance of all conceivable environmental conditions must be tested individually and then in combination to understand the limitations of the antenna. It is not expected that this type of antenna will operate reliable under extreme weather conditions but its limitations should be well defined.

Optimizing performance

The antenna design presented demonstrated the concept of an inflatable antenna for terrestrial use but there are many aspects of the design that require further investigation and optimization.

It was demonstrated that it is possible to use a microstrip patch to feed a gossamer feed horn. The performance of two conical horns was simulated but only a single horn design was tested and no optimization was performed on the microstrip patch design. To characterize the performance and limitations of this combination, further testing should be conducted on various microstrip patch designs, with particular emphasis on cross polar reduction, and various conical horn designs.

It is recommended that further investigation of the antenna operating pressure be conducted, including the impact of pillowing on each component as well as on the overall

performance of the antenna. This investigation should be conducted in conjunction with an investigation into adjusting the antenna pattern and construction technique.

It is known that increasing the effective area of the antenna and increasing the operating frequency will both increase the gain of the antenna. The use of an inflatable antenna makes it possible to increase the dish diameter beyond any existing portable antenna. However, there is a limit to the physical size that can be achieved before the structure becomes unstable under environmental conditions and a limit to the shape and surface accuracy that can be achieved, placing a limit on the operating frequency. It is recommended that these limits be established.

Material

The material used to construct the prototype performed as required. However, as the material was donated there was no possibility of selecting and testing the materials based on their physical and electromagnetic qualities. It is recommended that further investigation be conducted into the material selection as well as the possibility of forming the reflector as a single entity.

Forming thin films

The inflatable antenna design presented is constructed using individual gores which are then assembled using either tape or heat welding. The seams produced as a result of these construction methods create localized stiffening which exaggerates a condition known as pillowing. To eliminate pillowing and any interference caused by the seams, as well as guarantee the shape accuracy of the reflector dish, the ideal would be to mould the dish as a single entity. This approach has the added advantage of reducing the number of seams that can rupture and cause the structure to deflate.

To successfully produce a reflector as a single entity requires the ability to accurately shape the material without sacrificing any of the physical or electromagnetic properties. Mackenzie et al [42] attempted to cast a self-metalizing polyamide film. This approach achieved some success but demonstrated that it was difficult to control the distribution of the metal particles, which limited their ability to produce a uniform reflective surface.

The thermal properties of Polyester films make it possible to thermoform a dish under temperature and pressure. This requires careful manipulation of temperature and pressure to prevent the material crystallizing and becoming brittle. Crystallization can also be reduced with the addition of co-polymers. However with the addition of co-polymers dimensional stability of the film is sacrificed and the material becomes more ductile.

In addition to the structural properties of the material the electromagnetic properties must also be maintained. The success of this process with a pre-metalized film relies on the strength of the bond between the base film and the metal layer. The inert nature of PET can cause the bond between the polymer and the metal coating to be quite weak. The difference in the coefficient of thermal expansion between the film and the coating can cause the coating to delaminate. Should the metal layer delaminate and fracture the reflective characteristics of the surface are compromised and any improvement gained through increased shape accuracy is lost. PET thin film is orthotropic so the material properties vary in the longitudinal and transverse directions making forming a uniform paraboloid very challenging. The other alternative is to metalize the film after it has been formed. This increases the complexity of the metal deposition and makes it hard to achieve a uniform reflective layer. Developing a technique for forming a metalized material will enhance the performance of the inflatable antenna presented.

Dichroic surfaces

As well as manipulating the shape of the film the differing electromagnetic properties of films make it possible to construct a laminate such that the different RF characteristics are used to the advantage of the designer. Films with different attenuation properties can be laminated to produce the desired electromagnetic properties. This is the principle used for frequency selective surfaces (FSS), known as dichroic surfaces. Dichroic surfaces can be used to manipulate the radiation characteristic of the antenna or the use of a polarizing layer can control the skin temperature of the antenna. In this way the material becomes an integral and important part of both the structural and RF design process.

Rigidizing

The inflatable antenna design presented can maintain its structural integrity without relying on rigidization and so the decision was made not to sacrifice the vibrational damping characteristics of inflatable structures by rigidizing the antenna. It is recommended that further investigation be conducted into both alternatives and the wide range of rigidizing techniques available [36], including:

- stretched Aluminium laminate
- hydro-gel
- heat-cured thermoset composite laminate
- thermoplastic composite laminate
- UV curable composite laminate
- Inflation gas reaction laminates
- Cold Hibernation Elastic Memory (CHEM) materials

Of all the techniques available the most promising is CHEM materials as the process is reversible. CHEM materials have a fully cured elastic memory. When heated above the glass transition temperature T_g, the material becomes pliable enough to be stowed. The material is then cooled below T_g "setting" it in its stowed form. Reheating the material above T_g returns the material to its cured shape. CHEM materials can undergo this process repeatedly without degradation to either physical or mechanical properties.

Packaging and Deployment

One of the most attractive features of an inflatable structure is its ability to be folded down to a fraction of its final size. To successfully deploy the structure to its intended shape the packing method and deployment mechanism is critical. Much can be learned from the use of deployable structures in the space environment including the deployment of the Inflatable Antenna Experiment [43].

One attractive feature of a monocoque structure is that it eliminates any possibility of the structure tangling during deployment. Therefore, the emphasis of any packaging technique is minimizing permanent creasing, minimizing stowed volume and ensuring the safety of the feed assembly. There are many inflation techniques available. The inflatable antenna

requires a large volume of gas but the operating pressure is low and if the antenna is well sealed constant inflation should not be required.

It is recommended that different folding techniques be tested for ease of deployment and the amount and permanence of creasing. It is also recommended that the impact of stowing the antenna for increasing lengths of time on the permanence of creasing be tested. It is recommended that various inflation techniques be tested for practicality and effectiveness. In particular it is recommended that the possibility of inflating the antenna by mouth be explored for emergency situations. It is known that this inflation technique will add moisture to the enclosed environment which could attenuate the signal at particular operating frequencies. It is recommended that this be quantified.

As this is a new area of investigation there are a number of aspects that need to be evaluated and optimized. However, the results obtained from this initial investigation are very promising and indicate that further development would result in an ultra light antenna capable of providing portable direct satellite communication.

7 Other Applications

After demonstrating the performance of the inflatable antenna under terrestrial conditions it is proposed that the structural approach presented can also be used to overcome the limitations the launch vehicle places on the size of communications antennas for space-based use. Limiting the size of a parabolic reflector limits the gain of the antenna and restricts the scientific information that can be returned to Earth.

When unmanned spacecraft or humans travel beyond Earth the Deep Space Network (DSN) provides the two-way communications link that guides and controls the mission and receives the images and scientific data they send back. The amount, quality and regularity of the data sent back is dependent on the capabilities of both the Earth-based and space-based systems. On Earth the three communications complexes of the DSN are equipped with a range of large, rigid, high precision, high gain antennas supported by ultra sensitive receiving and processing systems. In space the restrictions placed on the size, weight and power supply of the communications equipment by the cargo area and weight lifting capacity of the launch vehicle limit the gain of the antenna and result in extremely weak signals being received by the DSN.

These restrictions place limits on the scientific information that can be returned to Earth for analysis. To increase the scientific return, the gain and bandwidth of the space-based antennas must be increased to transmit video, high definition still images and hyperspectral imaging. To increase the gain of the antenna the size of parabolic dish must be increased whilst minimizing launch weight and volume. An increase in the gain of the antenna has the added advantage of narrowing the beamwidth resulting in an improved signal-to-noise ratio and higher resolution.

7.1 Portable direct satellite communication on the moon

It is proposed that the inflatable antenna developed for portable terrestrial communication could be applied to the lunar environment to provide high gain, light weight, portable direct satellite communication. The use of an inflatable antenna gain would also reduce the launch weight and hence the launch cost as well as making it possible to carry multiple

antennas for redundancy. The articulated antenna used during the Apollo program suffered from lunar dust settling on the dish and distorting its shape [44]. The enclosed design used for the inflatable antenna prevents moon dust settling in the dish and applying additional loading. The reduced gravity environment and absence of wind on the moon further reduces the loading on the structure.

To adapt the structural design to the lunar environment the selection of a suitable material is the greatest obstacle. The material used for the inflatable antenna prototype, Polyethylene Terephthalate (PET), was initially developed for the space environment to provide radiation shielding for space structures. Its low gas permeability, structural stability, durability, tear and puncture resistance, low cost, chemical inertness, high packing efficiency, RF transparency and reflectivity when metalized make it perfect for use in inflatable antennas in the terrestrial environment. Despite being developed for the space environment, it has been shown that prolonged exposure to the space environment degrades PET due to particulate radiation, Atomic Oxygen (AO), UV radiation and thermal cycling [45].

Specialist films such as Kapton, and the polyimides CP1 and CP2 have been developed specifically for long duration exposure to the space environment, making them suitable for use in inflatable antennas on the lunar surface [45]. The development of these new materials is also concentrating on optical transparency, low solar absorptivity and high thermal emissivity to avoid overheating and allow for thermal energy dissipation, allowing the power levels of the antenna to be increased. Solar winds contribute to antenna noise but they also carry elements such as Hydrogen, Helium, Nitrogen, Carbon and the Noble gases Krypton, Xenon and Argon, which are volatile to many materials. The thin films proposed are not degraded under the influence of these elements.

7.2 Radio astronomy from the moon

In addition to providing portable high gain communications on the lunar surface inflatable antennas could enable astronomers to access the low frequency window between 50 kHz and 30 MHz to make observations related to the early universe. These frequencies are not accessible from the Earth's surface due to attenuation of the ionosphere and radio interference. The two weeks of Lunar night on the far side of the moon provides an

environment free from solar radiation and radio noise from the Earth, and the lack of seismic activity and wind provide a stable environment.

Concept studies from the 1960's to present [46] have explored what might be possible by establishing an array of antennas on the far side of the moon, including a Very Low Frequency Lunar Array proposed by ESA in 1997. *Fig. 116* presents an artist's concept of an array of radio telescopes on the moon. The disadvantage of all proposals to date has been the cost and logistics of placing an array of antenna having an estimated weight of 100kg over an area of 20km to 30 km on the far side of the Moon.

Fig. 116: Radio Astronomy on the lunar surface. (image courtesy of ESA)

The use of inflatable antennas would reduce the launch costs associated with transporting the antennas to the moon and also increase the achievable diameter of each antenna thus increasing their gain. The use of lightweight, inexpensive infrastructure also reduces establishment, maintenance and replacement costs.

There are many applications that could benefit from the low weight and high packing efficiency offered by inflatable structures. The inflatable antenna concept presented can be replicated in various sizes and operated at different frequencies. The availability of thin films that can withstand both terrestrial and space conditions makes it possible to apply this approach in both environments.

Conclusions

Technology is constantly being transferred between the terrestrial and space environments. In this case a concept that addressed the limitations placed on the size of space structures by the launch vehicle has been used to inspire a design for increasing the portability of terrestrial-based communication antennas. This thesis demonstrates that an inflatable structure manufactured from polyester thin film can maintain the shape accuracy and dimensional stability required for satellite communication under the influence of gravity. It has also been shown that a microstrip patch can be used to feed a gossamer horn and further reduce the weight and stowed volume of the system. The resulting product is an antenna with a fraction of the weight and stowed volume of a rigid or articulated dish which is suitable for portable, re-usable, low-cost, land-based direct satellite communication.

This concept requires further development but the performance of the inflatable antenna compared to the rigid antenna demonstrated that the concept is viable. This concept can be replicated in various sizes to operate at a range of frequencies making it suitable for multiple applications such as mobile military communication, emergency response communication, tele-medicine, tele-education and media broadcasting in remote areas. With the use of existing materials developed for the space environment it has also been shown how this concept could be applied to the lunar environment.

References

1. Meissner, A., Risse, T., Kirste, T. and Kirchner, H., *"Design Challenges for an Integrated Disaster Management Communication and Information System"* IEEE DIREN, New York, June 2002.
2. Jameson, H. *"COTM: A Top Priority for the Military"*, Global Military Communications, Sept. /Oct. 2008, pp 48-52.
3. Mahoney, T., Kerr, P., Felstead, B., Wagner, L., Wells, P., Cunningham, M., Ryden, K., Baumgartner, G., Demers, H., Dayton, W.L., Jeromin, L., Spink, B., *"An Investigation of the Military Applications of Commercial Personal Satellite Communications Systems"* IEEE MILCOM, Atlantic City, Oct. 1999.
4. Ingerson, P. and Wong, W., *"The Analysis of Deployable Umbrella Parabolic Reflectors"*, Antennas and Propagation, IEEE Transactions, July 1972, Issue 4, Vol. 20, pp. 409-414.
5. Guest, S. D. and Pellegrino, S., *"A New Concept for Solid Surface Deployable Antennas",* Acta Astronautica, Vol. 38, Issue 2, Jan. 1996, pp 103-113.
6. Jenkins, C.H., Freeland, R.E., Bishop, J.A., Sadeh, W.Z., *"An Up-to-Date Review of Inflatable Structures Technology for Space-Based Applications,"* Space 98 Conference, Albuquerque, April 1998.
7. Freeland R., Bard S., Veal G., Bilyeu G., Cassapakis C., Campbell T., and Bailey M.C., *"Inflatable Antenna Technology with Preliminary Shuttle Experiment Results and Potential Applications",* AMTA96, Seattle, Oct. 1996.
8. Skinnemoen, H., Hansen, S. K., Jahn, A., and Beriolo, M., *"Satellite Based Infrastructure for Emergency Communication"*, AIAA ICSSC, Seoul, April 2007.
9. Skinnemoen, H., Johansen, T. V. and Eriksen, E., *"Ultra-portable Multimedia Satellite Terminals for the BGAN Satellite System"* IEEE VTC, Orlando, Oct. 2003.
10. Loiselle, J., Tarleton, R. and Ingerski, J., *"The Next Generation Mobile User Objective Scheme (MUOS)"*, IEEE MILCOM, Atlantic City, Oct. 1999.
11. Goldberg, H., Sullivan, W. F. and Yin D. H. L., *"A Man-portable X-band Terminal System"* IEEE MILCOM, Boston, Oct. 1989.
12. Rusch, W. and Wanselow, R. *"Boresight-gain Loss and Gore-related Sidelobes of an Umbrella Reflector"*, Antennas and Propagation, IEEE Transactions, Jan. 1982, Issue 1, Vol. 3, pp. 153-157.

13. Prata, A., Rusch, W. V. T., Miller, R. K., (1989), *"Mesh Pillowing in Deployable Front-Fed Umbrella Parabolic Reflectors"* Antenna and Propagation Society International Symposium, 1989. AP-S Digest 26-30, Vol 1 pages 254-257.
14. Darooka, D. K. and Jensen, D. W, *"Advanced Space Structure Concepts and their Development",* AIAA/ASME/ASCE/AHSA/ASC Structures, Structural Dynamics and Materials Conference and Exhibit, Seattle, April 2001.
15. Johnson, M.R., *"The Galileo High Gain Antenna Anomaly",* 28th Aerospace Mechanisms Symposium, NASA Lewis Research Center, May 1994, NASA CP-3260, Accession number N94-33291, pages 359-377.
16. Freeland R. E. *"Survey of Deployable Antenna Concepts",* NASA Technical Report 19850041512, Jan. 1983.
17. Russell, R. A., Campbell, T. G. and Freeland, R. E., *"NASA Technology for Large Space Antennas",* NASA Technical Report 19790068661, Oct. 1979.
18. Cassapakis, C. and Thomas, M., *"Inflatable Structures Technology Development Overview"*, AIAA Space Programs and Technologies Conference, Huntsville, Sept 1995.
19. Cadogan, D., Sandy, C. and Grahne, M., *"Development and Evaluation of the Mars Pathfinder Inflatable Airbag Landing System"*, Acta Astronautica, Vol. 50, Issue 10, May 2002, pp 633-640.
20. de la Fuente, H., Raboin, J. L., Valle, G. D. and Spexarth, G. R., *"TransHab-NASA's Large-scale Inflatable Spacecraft"*, AIAA/ASME/ASCE/AHSA/ASC Structures, Structural Dynamics and Materials Conference and Exhibit, Atlanta, April 2000.
21. Freeland R. E. and Bilyeu G, *"In-Step Inflatable Antenna Experiment"*, International Astronautical Congress, Washington DC, Aug. 1992.
22. Chemielewski, A. B. and Freeland, R. *"Low Cost Large Space Antennas"*, NASA Technical Report 19980137515, 1997.
23. Jenkins, C., *"Gossamer Spacecraft: Membrane and Inflatable Structures Technology for Space Applications"* AIAA, 2001, ISBN 1-56347-403-4ck
24. Palisoc, A. L., *"Inflatable Reflector Development Program, Task 3 Report"*, L'Garde Technical Report, LTR-94-AP-008, May 1994
25. Pappa, R. S., Lassiter, J. O. and Ross, B. P., *"Structural Dynamics Experimental Activities in Ultra-Lightweight and Inflatable Space Structures"*, AIAA Gossamer Spacecraft Forum, Seattle, April 2001.

26. Itanami, T., Misawa, M. and Kumazawa, H., *"Highly Accurate Fan Rib Type Mesh Deployable Reflector with Precise Surface Adjuster and Link Deployment System*", 22nd European Microwave Conference, Helsinki 1992.
27. Takano, T., Miura, K., Natori, M., Hanayama, E. Inoue, T., Noguchi, T., Miyahara, N. and Nakaguro, H., *"Deployable Antenna With 10-m Maximum Diameter for Space Use"*, IEEE Transactions on Antennas and Propagation, Vol. 52, No. 1, January 2004.
28. Tsujihata, M. A. and Hamamoto, A. N., *"The 13 m aperture space antenna reflectors for Engineering Test Satellite VIII"*, IEEE Antennas and Propagation Society International Symposium, Orlando, Florida, July 1999.
29. Van 't Klooster, K., Scialino, L., Cherniavski, A., Medzmariashvili, E., Korneev, V., Kravchenko, Y., Gulyayev, V., Magjanov, R., Santiago-Prowald, J., Scolamiero, L., Lubrano, V., Silvestrucci, F., Fei, E. and Raboso, D., *"Large Deployable Antenna for Various Space Applications"*, 5th International Conference on Antenna Theory and Techniques, Kyiv, Ukraine, May 2005.
30. Zheng, F., Chen, M., Li, W. and Yang, P., *"Conceptual Design of a New Huge Deployable Antenna Structure for Space Application"*, IEEE Aerospace Conference 2008, Big Sky, MT, March 2008.
31. Ruggiero, E. J. and Inman, D. J., "*Gossamer Spacecraft: Recent Trends in Design, Analysis Experimentation, and Contro*l", Journal of Spacecraft and Rockets Vol. 43, No. 1, January–February 2006.
32. Di, J., Duan, B. and Zheng, F., "*The Reflector Shape Adjusting Methods for Cable Mesh Deployable Antenna*" 1st International Symposium on Systems and Control in Aerospace and Astronautics, Harbin, Jan 2006.
33. Salama, M., Lou, M. and Fang, H., *"Deployment of Inflatable Space Structures",* AIAA Structures, Structural Dynamics & Materials Conference, Atlanta, April 2000.
34. Cadogan, D. P. and Grahne, M. S., *"Deployment Control Mechanisms for Inflatable Space Structures"*, Aerospace Mechanisms Conference, Pasadena, May 1999.
35. Lou, M. C. and Feria, V. A., *"Development of Space Inflatable/Rigidizable Structures Technology"*, Symposium on Deployable Structures, Cambridge, Sept. 1998.
36. Cadogan, D. P., "*Rigidizable Materials for Use in Gossamer Space Inflatable Structures",* AIAA/ASME/ASCE/AHSA/ASC Structures, Structural Dynamics and Materials Conference and Exhibit, Seattle, April 2001.
37. Lowe, L. T. and Hackett, R. D., *"Terrestrial Based Inflatable Dish Antennas"*, IEEE Radar Conference, Huntsville, May 2003.

38. Lowe, L. T., Gierow, P. and Danis, A. *"Terrestrial Based Inflatable Dish Antenna Performance Characterization",* IEEE Antennas and Propagation Society International Symposium, Washington DC, July 2005.
39. Park, G., Ruggiero, E., Sausse, M. and Inman, D. J., *"Vibration Testing and Analysis of Inflatable Structures Using Smart Materials"*, ASME International Mechanical Engineering Congress and Exhibit, New York, Nov. 2001.
40. Hwang L., Turlik I., *"A Review of the Skin Effect as Applied to Thin Film Interconnections"*. IEEE Transactions on Components, Hybrids, and Manufacturing Technology, Vol. 15, No. 1, Feb 1992.
41. Du Pont Product Database: http://www.dupont.com/cgi-bin/corp/proddbx.cgi
42. Mackenzie A., Cravey R., Miner G., Dudley K., Stoakley D. and Fralick D., *"Fabrication and Electromagnetic Characterization of Novel Self-Metallized Thin Films"*, IEEE Aerospace Conference, Big Sky, Montana, March, 2004.
43. Cadogan, D. P. and Grahne, M. S., *"Deployment Control Mechanisms for Inflatable Space Structures"*, Aerospace Mechanisms Conference, Pasadena, May 1999.
44. Compton, W. D., *"Where No Man Has Gone Before: A History of Apollo Lunar Exploration Missions",* The NASA History Series SP-4214, 1989.
45. Dever, J. A., Messer, R., Powers, C., Townsend, J. and Wooldridge, E., *"Effects of Vacuum Ultraviolet Radiation on Thin Polyimide Films"*, High Performance Polymers, 2001, Vol. 13, pp. S391 - S399.
46. Takahashi, Y. D., *"Radio Astronomy from the Lunar Far Side: Precursor Studies of Radio Wave Propagation around the Moon"* In New Views of the Moon, Europe: Future Lunar Exploration, Science Objectives, and Integration of Datasets, Noordwijk, Jan 2002.

Bibliography

- Antenna Engineering Handbook (2nd Edition)
  Johnson R.C. and Jasik H.
  McGraw-Hill
  1984
- Antenna Theory: Analysis and Design (2nd Edition)
  Constantine A. Balanis
  John Wiley & Sons
  1997
- Antenna Theory and Design (2nd Edition)
  Warren L. Stutzman and Gary A. Thiele
  John Wiley & Sons
  1997
- Gossamer Spacecraft: Membrane and Inflatable Structures Technology for Space Applications
  Edited by Christopher H. M. Jenkins
  Progress in Astronautics and Aeronautics Volume 191
  American Institute of Aeronautics and Astronautics
  2001
- Microwave Horns and Feeds
  A. D. Olver, P. J. B. Clarricoats, A. A. Kishk and L. Shafai
  IEE Electromagnetic Wave Series 39
  IEEE Press
  1994
- Practical Antenna Handbook (3rd Edition)
  Joseph J. Carr
  McGraw-Hill International
  2001

- Recent Advances in Gossamer Spacecraft
  Edited by Christopher H. M. Jenkins
  Progress in Astronautics and Aeronautics Volume 212
  American Institute of Aeronautics and Astronautics
  2006
- Roark's Formulas for Stress and Strain (6th Edition)
  Warren C. Young
  McGraw-Hill Book Company
  1989
- Satellite Communication Systems: Design Principles (2nd Edition)
  M. Richharia
  MacMillan Press
  1999
- Solid Dielectric Horn Antennas
  Carlos Salema, Carlos Fernandes and Rama Kant Jha
  Artech House
  1998
- Theory of Elastic Stability (2nd Edition)
  Stephen P. Timoshenko and James M. Gere
  McGraw-Hill Book Company
  1961
- Theory of Plates and Shells (2nd Edition)
  Stephen P. Timoshenko and S. Woinowsky-Krieger
  McGraw-Hill Book Company
  1959

List of Publications

Book chapter

Mathers, N., *"Using Inflatable Antennas for Portable Satellite-Based Personal Communications Systems",* Space Technologies for the Benefit of Human Society and Earth, Phillip Olla (Ed). pp 233 -253

Journal article

Mathers, N. and Thompson, L., *"Using Inflatable Antennas for Portable Satellite-based Personal Communications Systems"*, ACTA Astronautica, Vol. 61 No., 7-8 October 2007

Conference papers

1. Mathers, N. and Thompson, L., *"Inflatable Antennas: Deployable Communications Systems for Earth, Moon and Beyond"*, Australian International Aerospace Congress, Melbourne, Australia, March 2006
2. Mathers, N. and Thompson, L., *"Inflatable Antennas in Terrestrial and Extraterrestrial Environments"*, International Astronautical Congress, Valencia, Spain, October 2006
3. Mathers, N. and Thompson, L., *"Using Inflatable Antennas for Portable Satellite-based Personal Communications Systems"*, International Astronautical Congress, Fukuoka, Japan, October 2005
4. Mathers, N. and Thompson, L., *"Applications for Inflatable Antennas in Terrestrial and Space Environments"*, Australian Space Science Conference, Melbourne, Australia, September 2005
5. Mathers, N., Ghorbani, K. and Thompson, L. *"Using Inflatable Structures Technology for Portable Land-based Communication"* Australian International Aerospace Congress, Melbourne, Australia, March 2005
6. Mathers, N., Ghorbani, K. and Thompson, L., *"Inflatable Antennas for Satellite-based Personal Communications Systems"*, Australian Symposium on Antennas, Sydney, Australia, February 2005

7. Mathers, N., Ghorbani, K. and Thompson, L., *"Development of a Gossamer Parabolic Dish Reflector"*, International Symposium on Antennas, Nice, France, November 2004
8. Mathers, N., Thompson, L. and Ghorbani, K., *"Inflatable feed horn for inflatable parabolic dish antenna"*, Australian Space Science Workshop, Sydney, Australia, July 2003.
9. Thompson, L., Mathers, N., Kanchanakpan, T. and Bil, C., *"Reinventing the wheel a novel approach to long duration space habitat"*, AIAA International Air and Space Symposium and Exposition, Dayton, USA, July 2003
10. Mathers, N., Thompson, L. and Ghorbani, K., *"Development of inflatable feed horn for parabolic dish antenna"* Australian Symposium on Antennas, Sydney, Australia, February 2003